



Analysis of various techniques for ECG signal in healthcare, past, present, and future



Thivya Anbalagan^{a,*}, Malaya Kumar Nath^a, D. Vijayalakshmi^b, Archana Anbalagan^c

^a Department of ECE, NIT Puducherry, Karaikal, India

^b Department of ECE, Vignan's Institute of Engineering for Women Visakhapatnam, India

^c Sri Lakshmi Narayana Institute of Medical Sciences Puducherry, India

ARTICLE INFO

Keywords:

ECG
QRS complex
Arrhythmia
Machine learning
Heart disorder from fundus image

ABSTRACT

Cardiovascular diseases are the primary reason for mortality worldwide. As per WHO survey report in 2019, 17.9 million people died due to CVDs, accounting for 32% of all global deaths. Among these, heart attacks and strokes were responsible for 85%, whereas CVDs caused 38% of the premature deaths (under age of 70) affected by non-communicable diseases. The rate of death can be delayed and may be prevented by efficiently analyzing the ECG signals (i.e., captured by a non-invasive method) at the early stage of the disease. QRS complex in ECG provides pivotal information about the heart diseases. Many researchers have analyzed the ECG signal by traditional approach and machine learning methods for identifying the heart disorders. Performance of these techniques depend on accurate detection of different parameters (such as: P-, Q-, R-, S-, T-waveforms, QRS complex duration, R-peak, PR-interval, and RR-interval) from the ECG signals. This review paper provides a detail discussion and comparison of various ECG analysis techniques along with their pros and cons. It summarizes the ECG capturing method, databases available for disease detection & classification, and performance measures used by the researchers. Based on these, a future road map is suggested for real time ECG analysis (for identifying the heart related conditions) captured from the wearable devices and suggested the precautionary steps by the artificial system and experts. This method will help in identifying the co-relation of heart disorders with other body organs (such as: retina and brain parts) by analyzing ECG, fundus image, and magnetic resonance imaging (MRI) of human brain.

Abbreviations: ADT, Adaptive dual threshold; AMD, Age-related macular degeneration; AF, Atrial fibrillation; AFL, Atrial flutter; APB, Atrial premature beat; ASPP, Atrous spatial pyramid pooling; AVR, Ateriole to venule ratio; BNN, Binarized neural networks; CAC, Coronary artery calcium; CHB, Complete heart block; CAD, Computer aided diagnostic; CHD, Coronary heart diseases; CMUH, China medical university hospital; CNN, Convolutional neural network; CRT, Cardiac resynchronization therapy; CRAE, Central retinal artery occlusion eye condition; CRVE, Central retinal vein occlusion eye condition; CWT, Continuous wavelet transform; DAE, Denoising auto encoder; DLP, Deep learning platform; DHR, Difference of heart rate; DR, Diabetic retinopathy; DWT, Discrete wavelet transform; EAR, Ectopic atrial rhythm; EDSS, ECG diagnostic support system; EMD, Empirical mode decomposition; EMI, Electromagnetic interference; FCN, Fully convolutional network; FRAV, First degree atrioventricular block; GAP, Global average pooling; GUI, Graphical user interface; HOS, Higher order statistics; HMM, Hidden Markov model; ICA, Independent component analysis; IMFs, Intrinsic mode functions; KNN, K nearest neighbors; LBBB, Left bundle branch block; LDA, Linear discriminant analysis; LSTM, Long short term memory; MBGD, Mini batch gradient descent; MI, Myocardial ischemia; MIn, Myocardial infarction; MLP, Multilayer perceptron; NCA, Neighborhood component analysis; NSR, Normal sinus rhythm; NST, Noise stress test; OPF, Optimum path forest; PCA, Principal component analysis; PAC, Premature atrial contractions; PLI, Powerline interference; PRD, Percentage root mean square difference; PSG, Polysomnography; PSVT, Paroxysmal supra ventricular tachycardia; PTB, Physikalisch technische bundesanstalt; PVC, Premature ventricular contractions; QDA, Quadratic discriminant analysis; RBBB, Right bundle branch block; ReLU, Rectified linear activation unit; RF, Random forest; RMSE, Root mean square error; REWARD, Relative energy based wearable R-peak detection; SAV, AV block; SBR, Sinus bradycardia; SCM, Structural co-occurrence matrix; SSCAV, simultaneous segmentation and classification of the retinal arteries and veins; ST, Sinus tachycardia; STD, ST segment depression; STE, ST segment elevation; STFT, Short time fourier transform; SVD, Singular value decomposition; SVE, Supraventricular ectopic beats; SVM, Support vector machine; VEB, Ventricular ectopic beats; VPB, Ventricular premature beats.

* Corresponding author.

E-mail addresses: thivyaanbu@gmail.com (T. Anbalagan), malaya.nath@gmail.com (M.K. Nath), vijaya1183@gmail.com (D. Vijayalakshmi), anbuarchana6@gmail.com (A. Anbalagan).

<https://doi.org/10.1016/j.bea.2023.100089>

Received 7 January 2023; Received in revised form 27 April 2023; Accepted 9 May 2023

Available online 29 May 2023

2667-0992/© 2023 The Author(s). Published by Elsevier Inc. This is an open access article under the CC BY-NC-ND license (<http://creativecommons.org/licenses/by-nd/4.0/>).

1. Introduction

Due to the exponential development of technologies and the modern living style (such as: addicted to alcohol, consumption of junk foods, stress, and chair bound conditions etc.) people affected by numerous health related problems, among which the heart/cardiovascular diseases draw the attention of Governments in many countries due to its higher rate of fatalities [1–3]. As per the WHO 2019 report, 32% deaths happened globally due to cardiac diseases. This disease becomes severe due to past medical history, obesity, and diabetics etc. The death rate can be controlled by continuous medication, monitoring, treatment, and diagnosis at the early stage. Structure of the heart and its electrical functionality can be analyzed from the electrocardiogram (ECG), which is treated as a golden standard for clinical diagnosis (such as: analysis of heartbeats, biometric identification, and emotion recognition etc.) [4, 5]. Continuous analysis of ECG is time consuming, cumbersome, boring, and expensive for handling the data manually. Analysis of ECG sometimes create outliers due to the variation of expert opinions. Researchers have developed various techniques for ECG analysis, delimiter extraction, classification, and disease identification etc. These approaches are broadly divided into three categories, conventional/traditional, machine learning (ML), and deep learning (DL) approaches. In traditional methods various ECG features are extracted and analyzed. They consist of time [6], frequency [7,8] and wavelet [9–18] based approaches. ML methods used the extracted features by hidden Markov model (HMM), support vector machine (SVM) [11,14,19,20], principal component analysis (PCA) [21–27], linear discriminant analysis (LDA) [12,25,28, 29] independent component analysis (ICA) [14], k-nearest neighbor classifier (KNN) [20], vector quantization [30], and random forest (RF) [31] etc. DL models used CNN [32–35] and LSTM [36,37] for automatic classification. These above methods can be further grouped into patient-dependent and patient-independent. Depending on heart diseases the ECG signal morphology is altered that help the cardiologist for diagnosis. Each of these methods/techniques has their own advantages and disadvantages, which are outlined/listed in later part of this paper. ECG signal analysis, detection, recognition, and classification proceeds through numerous processes/stages (such as: ECG acquisition by standard leads & wearable sensors, filtration from embedded & external noise, extraction of fiducial features, and classification). These stages are discussed in Section 3. The manuscript will help in understanding the ECG acquisition, early analysis of diseases, and motivate the readers to develop an efficient & robust ECG analysis & classification method. The main contributions of the manuscripts related to ECG and cardiovascular diseases are:

- * Overview of human heart and its relation with the electrical impulses, acquisition of ECG & its morphology, and heart conditions for cardiovascular diseases & its effect of ECG signal.
- * Discussion of heart diseases (such as: arrhythmias, myocardial infarction, atrial fibrillation, atrial flutter, heart failure, and myocardial ischemia).
- * Overview about ECG databases used for various studies and wearable devices for real time analysis. Performance measures used for analyzing the effectiveness of various methods/models.
- * Discussion and encapsulation are made at various stages of ECG analyzing techniques. This include preprocessing (denoising, data augmentation, peak detection, signal segmentation, and temporal feature extraction etc.), analysis, and classification (by traditional, ML, and DL approaches).
- * Highlight the limitations for various methods and suggesting a road map for an efficient analysis of diagnostic information from the ECG signal.

The rest part of the article is organized as follows. Section 2 explained about electrocardiography, which further subdivided into six subsections. These subsections discussed about different ECG leads for

Table 1
ECG leads and its positions.

Sl. No.	Leads	Position	Heart view
1	6-Limb	Lead-I	Left arm & right arm
		Lead-II	Left leg & right arm
		Lead-III	Inferior left view
	3-Unipolar/ Augmented	aVR	Inferior right view
		aVL	Upper right side
		aVF	Upper left side
		V1	Inferior wall of heart
		V2	2-Oriented to right ventricle
		V3	2-Face inter ventricular septum
		V4	2-Lateral wall
		V5	2-Face left ventricle anterolaterally
		V6	

acquisition, artifacts in ECG, morphology & rhythm information about the ECG, heart related diseases and noises in ECG. Literature review about identification of various pivotal waveforms along with the diseases are discussed in Section 3. This Section discusses about the various ECG databases available publicly along with the performance measures for disease classification techniques (various ML and DL approaches). This Section investigates the types of noises that occur during ECG collection, as well as the techniques for removing them. Section 4 discusses various developing technologies to identify fetus abnormalities, obstructive sleep apnea (OSA), real-time analysis of heart conditions, and structural changes in retina due to heart related diseases. Abdominal ECG (AECG) from the pregnant woman is used to identify the fetus ECG (FECG). Study of FECG, provides structural development of fetus heart along with its abnormalities. The study of RR-interval helps in diagnosing sleeping disorders due to inappropriate breathing. Real-time ECG data analysis methods are discussed in this Section to identify the heart conditions for delaying heart related fatalities. The heart diseases can also be identified from the study of retina. Section 5 highlights and explores the challenges and research gaps in diagnosing heart illnesses by various ML and DL algorithms. Section 6 proposed a road map for identifying heart related abnormalities and diseases from ECG signal. Conclusions of this paper are summarized in Section 7.

2. Electrocardiography

ECG precisely record the electrical activity of heart rhythm over a period using electrodes/leads, which captures the electrical changes caused by depolarization and re-polarization of heart muscles during heartbeat [38]. This section includes recording of ECG signal by standard 12-conventional leads, noises associated during ECG acquisition, morphology (structural & physiological), and identification of heart related diseases from ECG.

2.1. ECG leads

Spatial information about the electrical activity of heart can be captured by standard 12 conventional leads (equally divided into limb- and pre-cordial/chest-leads) placed in three orthogonal directions (i.e., right to left, superior to inferior, and anterior to posterior) on human

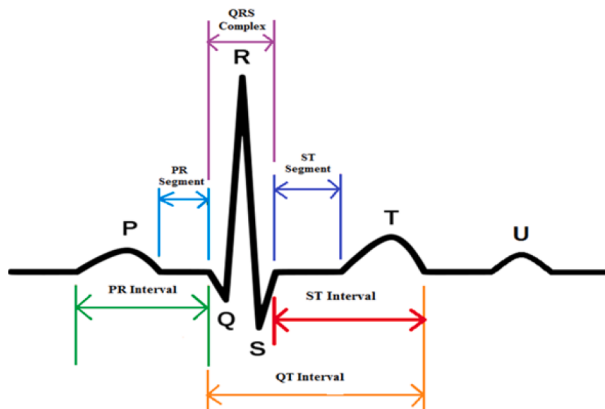


Fig. 1. ECG morphology: different segments of ECG signal for normal person [39].

Table 2
Specification of morphological features in normal ECG.

Sl. No.	Waveform	Duration (in seconds)	Amplitude (in mV)	Remarks
1	P-wave [40]	0.08–0.12	0.25	Depolarization of LA & RA
2	Q-wave [41]	0.03	0.2–0.4	Initial ventricular depolarization
3	R-wave [42, 43]	–	1.60	Depolarization of the ventricles
4	S-wave [42]	–	1.8–3.0	Final ventricular depolarization
5	T-wave [44]	0.1–0.25	0.1–0.5	Ventricular re-polarization
6	U-wave	–	0.1–0.33	Purkinje fibers re-polarization
7	PR interval [45]	0.12–0.20	120	Atrial & ventricular depolarization
8	QRS duration [46,47]	0.06–0.12	2.5–3.0	Depolarization of ventricles
9	QT interval [48]	0.35–0.44	–	Reflect ventricular re-polarization
10	RR interval [49]	0.6–1.2	–	Measures heart rate variability
11	PP interval [40]	0.60–1.04	–	Interval between two P-waves
12	ST segment [50]	0.08	0.1–0.2	Early re-polarization

skin/body. Limb- and chest-leads help in recording the potential difference across the frontal- and horizontal-plane, respectively. The six limb leads are equally divided into bipolar/standard (such as: lead-I, lead-II, and lead-III) leads and uni-polar/augmented (aVR, aVL, and aVF) leads. The six uni-polar pre-cordial/chest leads are V1, V2, V3, V4, V5, and V6. The detail description, position, and purpose of the 12-leads are represented precisely in Table 1. This provides the relation of ECG with orientation of heart.

2.2. ECG signal morphology

Activity of heart and its condition can be known from the morphology (peaks and duration of various peaks) of ECG signal [28]. The main components are P-wave, QRS complex, T-wave, and the duration between them. P-wave occurs due to the sequential activation (i.e., depolarization) of the right and left atria. QRS complex is appeared by right and left ventricular depolarization (i.e., ventricles are activated simultaneously). T-wave arises by ventricular re-polarization, whereas U-wave is occurred after depolarization in the ventricles. Interval between different wave carries diagnostic information about the heart diseases. PR interval produced by time delay from onset of atrial

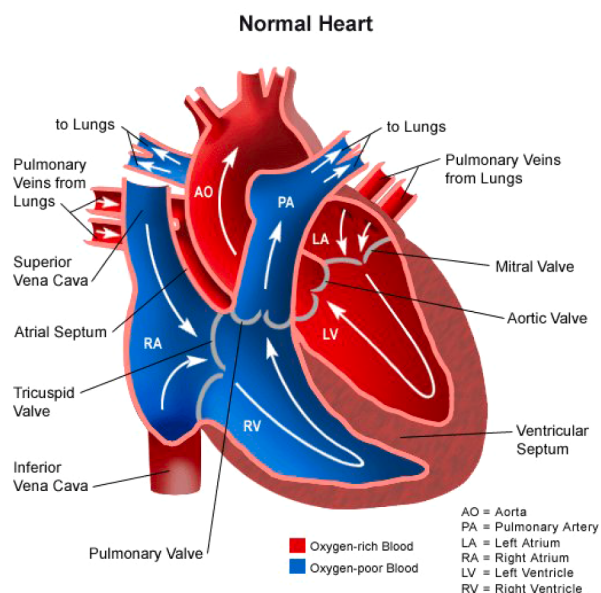


Fig. 2. Cross sectional view of human heart and corresponding labels [51].

depolarization (P-wave) to onset of ventricular depolarization (QRS complex). QRS period depends on ventricular muscle depolarization, whereas QT interval rely on the duration of ventricular depolarization and re-polarization. The RR- and PP-interval depend on ventricular-cycle and atrial-cycle duration (or rate), respectively. The morphological specification of an ECG signal of a normal person and the duration of different waveform are shown in Fig. 1 and Table 2 summarizes the duration, amplitude and the cause of various waveform in normal ECG signal.

2.3. Beat information

The sino atrial (SA) node is situated adjacent to the superior vena cava in right atrium. SA node spreads depolarization through the atria & results in P-wave. All heart beats are invited and regulated by SA node. Electrical impulses generated by the SA node travel through both atria and causing them to contract. Atrioventricular (AV) node is placed on the opposite side of the right atrium, near the AV valve. AV node acts as an electrical gateway to the ventricles, delaying electrical impulses to them. This delay ensures that the atria have evacuated all of the blood to the ventricles before its contraction. The AV node collects signals from the SA node and transmits them to the atrioventricular bundle. This bundle is separated into right and left bundle branches, which carry impulses to the heart's apex. The impulses are subsequently transmitted to purkinje fibres, which rise and spread across the ventricular myocardium.

When the atria are filled with blood, the SA node fires after the atria are filled with blood. This leads to the spreading of electrical signal throughout the atria and cause them to depolarize. Atrial contraction is also known as atrial systole, occurs roughly 100 ms after the P wave begins. The P-Q segment indicates the time required for a signal to travel from the SA node to the AV node. QRS complex shows ventricular depolarization and the firing of AV node. Q wave correlates to the interventricular septum. R wave is caused by the depolarization of the ventricle's major mass. The S wave signifies the final phase of ventricular depolarization at the base of the heart. During this time, atrial re-polarization occurs and the signal is hidden by the large QRS complex [47]. The S-T section reflects the cardiac action potential plateau. The ventricles contract and pump blood at this time. The T-wave shows ventricular re-polarization just prior to ventricular relaxation or diastole. The cycle is repeated with each heartbeat.

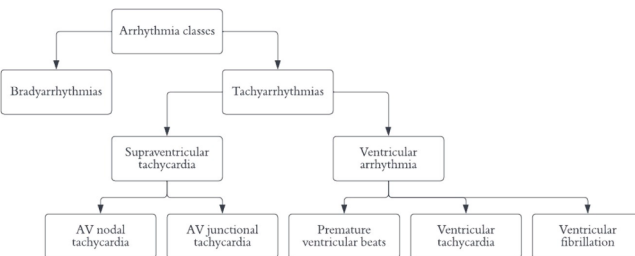


Fig. 3. Arrhythmia classes [53].

2.4. Healthcare

Heart is a 4-chamber organ, having two on the top (known as atrium) and two on the bottom (known as ventricle). Superior and inferior venacava carry oxygen-depleted blood from the upper and lower body parts, respectively. This blood is pumped from the right atrium to the right ventricle via the tricuspid valve, and it is sent to the lungs for purification via the pulmonary artery. The purified blood passes to left atrium through pulmonary veins. Left atrium pumps the blood to left ventricle through bicuspid valve. The oxygen-rich blood is circulated throughout the body from left ventricle through aorta. The cross sectional view of human heart and corresponding labels are shown in Fig. 2 [51].

Any variation in the electrical impulses stimulate heart contractions may result in arrhythmia, which causes problems with the electrical signals (that control the heartbeat, damage to heart tissue, an imbalance of fluids or electrolytes in the blood, and changes in hormone levels etc.). Arrhythmias, also known as dysrhythmias. It arises as a result of improper electrical signal transmission in the heart. An irregular heartbeat can feel like fluttering of heart. Many arrhythmias are completely harmless. But, few of them (i.e., highly irregular arrhythmias) cause severe, potentially fatal symptoms & complications, which may lead to death. Arrhythmias are classified into bradycardia (slower heart rate i.e., ≤ 60 beats/min) and tachycardia (faster heart rate i.e., ≥ 100 beats/min) [52]. Tachycardia can be further classified into supraventricular tachycardia (AV nodal and AV junctional) and ventricular arrhythmia (premature ventricular beats, ventricular tachycardia, and ventricular fibrillation). Figure 3 shows systematic representation for the classification of various arrhythmias.

From the analysis of ECG signal, 12 different types of heart rhythms can be identified for detecting heart related disorders (such as: arrhythmias, conduction abnormalities, myocardial ischemia, and myocardial infarction) [54]. The 12-types of heart rhythms represent various heart conditions, such as: atrial fibrillation (AFIB), ectopic atrial rhythm (EAR), atrial premature beat (APB), paroxysmal supraventricular tachycardia (PSVT), ventricular bigeminy (BIGEMINY), complete heart block (CHB), first-degree atrioventricular block (FRAV), normal sinus rhythm (NSR), atrial flutter (AFL), second-degree AV block (SAV), ventricular premature beat (VPB), and sinus tachycardia (ST) [55,56].

AFIB is the most familiar arrhythmia, which is caused due to abnormal heart rhythm starting from upper chambers of heart [59]. It depends on action of ventricle beats and causes symptoms such as fatigue, heart palpitations, difficulty breathing, and dizziness. It may lead to ischemia, blood clot, and heart failure [74]. It is classified into paroxysmal-, persistent-, and long-term-persistent-AFIB. Paroxysmal AFIB is not very serious. It lasts less than a week and usually resolves on its own without any therapies. Persistent AFIB lasts over a week and requires treatment. Long-term persistent AFIB causes serious heart condition and even death. It will last more than a year and might be hard to treat. AFL caused by abnormality inside the right atrium, or upper chamber of heart [60]. This occurs due to the rapid contraction of upper chamber, which latter transmits to the lower chamber of heart. During this condition, heart beats rapidly (nearly 250–400 beats/min). This

Table 3

Heart related diseases diagnosed from ECG signal.

Sl. No.	Disease	Symptoms	Abnormality in ECG	Causes
1	SVEB [57]	Shortness of breath and pounding sensation in neck	QRS complex >110 ms	Stress, caffeine, alcohol or certain cold medications
2	VEB [58]	Dizziness and fainting	QRS deflection	Emotional stressors
3	AFIB [59]	Sensations of a fast, fluttering or pounding heartbeat	Disorganized atrial electrical activity and contraction	Heart structure problem
4	AFL [60]	Lightheadedness & feeling faint	Narrow complex tachycardia	Abnormal electrical circuit
5	APB [61]	Fluttering	P-wave shape differs	Electrical activation of atria
6	BIGEMINY [62]	Breathing difficulty with chest pain	No P-wave	Failure of impulse generation or conduction
7	CHB [63]	Fatigue and chest pressure or pain	Narrow QRS complex	Inferior myocardial infection
8	EAR [64]	Pounding or fluttering in chest	Fast heartbeat	Stress, caffeine
9	FRAV [65]	Dyspnea	PR interval > 0.20 s	Prolonged conduction in the AV node
10	NSR [66]	Shortness of breath	* P-wave follows QRS, * QRS <100 ms, * Upright I, II, and inverted aVR.	Electrical impulses from the sinus node
11	PSVT [67]	Palpitations and chest pain	Fast heart rate (150–250 beats/min)	Abnormal electrical pathway of heart cells
12	SAV [68]	Trouble breathing or shortness of breath	P-wave refuse to follow QRS complex	Intermittent atrial to ventricle conduction
13	ST [69]	Faster heartbeat with breathing difficulty	Irregular heartbeat	Fear, exercise or not drinking enough fluids
14	VPB [58]	Skipped beats and fluttering	Retrograde P-wave occur after QRS wave	Alcohol or drug misuse
15	LBBB [70]	Presyncope	Wide QRS complex	Myocardial injury, strain or hypertrophy
16	RBBB [71]	Chest pain or shortness of breath	QRS >120 ms	Myocarditis
17	PAC [72]	Fluttering and missed heartbeats	QRS <120 ms	Coronary artery disease, heart attack
18	PVC [73]	Flip-flop in chest	Weird QRS	Cardiomyopathy, arrhythmia

heart condition is known as supraventricular tachycardia, as it is originated from atria. This condition surfaces the irregular pulse, shortness of breath, dizziness, and heart pounding symptoms. APB represents premature atrial depolarization takes place prior to the regular SA activation (i.e., outside the SA node) [60]. This is known as atrial or supraventricular extra-systoles. APB originates from AV node or bundle of His. Mostly, this occurs in adults of any age, with or without structural heart disease. It causes symptoms such as tingling in the legs, muscle weakness and stiffness.

Bigeminy rhythms occur as a result of conduction, ectopic activity, and failed impulse synthesis [62]. It is classified into atrial-, junctional-, and ventricular- bigeminy. In atrial bigeminy, each sinus beat is followed by an early atrial beat. Junctional bigeminy causes atrial fibrillation or sinus beats. Ventricular bigeminy is the most frequently occurred type of bigeminy, which is involved in ectopic firing. This can

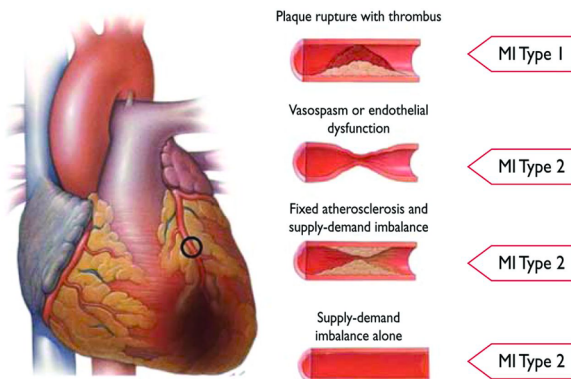


Fig. 4. Myocardial infarction [75].

be treated with medications. It may cause chest pain, lightheadedness, and heart palpitations. CHB happens when the electrical signal cannot transmit properly from atria to the ventricles [63]. Generally, it occurs due to injury of AV node during surgery. It leads to low blood pressure, causes harm to other internal organs, fainting, and cardiac arrest. Dizziness, palpitations, fatigue, chest pain, and shortness of breath are few observed symptoms during CHB. First-degree AV block (or First-degree heart block), is identified by observing PR interval [65]. In this case, duration of PR interval becomes longer than 200 ms and conduction through the AV node is slowed down. Time required between atrial and ventricular- depolarization lies from 120 to 200~ ms. It may causes dyspnea, malaise, and chest pain. During NSR (or normal heart rhythm) electrical signals from the heart's sinus node regulates the contraction and relaxation of heart sequentially, that leads to pump-in and pump-out of blood to heart in a controlled manner [66]. This causes normal heartbeat/rhythm. Irregular sinus rhythm leads to slower or faster pulse. This condition is known as sinus arrhythmia. It leads to chest pain, tightness, shortness of breath, fatigue, and fainting.

Second-degree heart block (or second-degree AV block) is occurred due to disruption or delaying of atrial impulse conduction to the

ventricles. This condition obstinate the AV node randomly. It arises due to coronary artery disease, cardiomyopathy, and congenital heart disease. This may cause heart block, syncope, dizziness, and chest pain. In sinus tachycardia (i.e., regular cardiac rhythm), heart beats hastily than usual. Tachycardia occurs due to exercise or stress. This leads to hazardous during rest. Symptoms visualized in ST are faster heartbeat, palpitations, fainting, chest pain, lightheadedness, difficulty breathing, and dizziness etc. [69]. Ventricular premature beats (VPB) are extremely common in both healthy and heart disease patients [58]. It is caused due to anxiety, stress, hypoxia, and electrolyte abnormalities. It can be identified by skipped or missed beats. Frequent occurrence of VPBs may cause mild hemodynamic symptoms, continuous hammering in neck, dizziness, and syncope etc. PSVT is the effect of abnormal electrical pathway in heart cells [67]. This causes bio-electricity to race in a circle and repeat the signal. This results rapid contraction of heart chambers and hinders heart function. This condition is a root cause of drowsiness and shortness of breath. In many situations, PSVT is misidentified as a panic attack. The description about various heart conditions, its cause & symptoms, and the morphological changes in ECG are represented in Table 3.

Myocardial infarction represents the heart condition for restricted or total discontinued blood flow in coronary artery. This causes damages to heart muscles and leads to heart attack. During this condition, person feels chest pain, shortness of breath, cold sweat, and tiredness. Most of this cases are caused due to coronary artery diseases. Myocardial infarction are classified into type-1, type-2, type-3, and type-4. Appearance of coronary artery during different infarction types are shown in Fig. 4.

Myocardial ischemia represents lack of oxygen and blood flow in heart, which leads to reduction of heart muscle's ability to pump blood and cause abnormal heart rhythms [76]. This kills heart muscle cells if it occurs for a prolonged period. This situation may cause heart attack or myocardial infarction [77]. Myocardial ischemia are classified into mesenteric ischemia, critical limb ischemia, and cutaneous ischemia. Mesenteric ischemia affects the intestine due to decreased blood flow. Critical limb ischemia is a complication of peripheral artery disease, which is caused by limited blood flow to legs and arms. Cutaneous

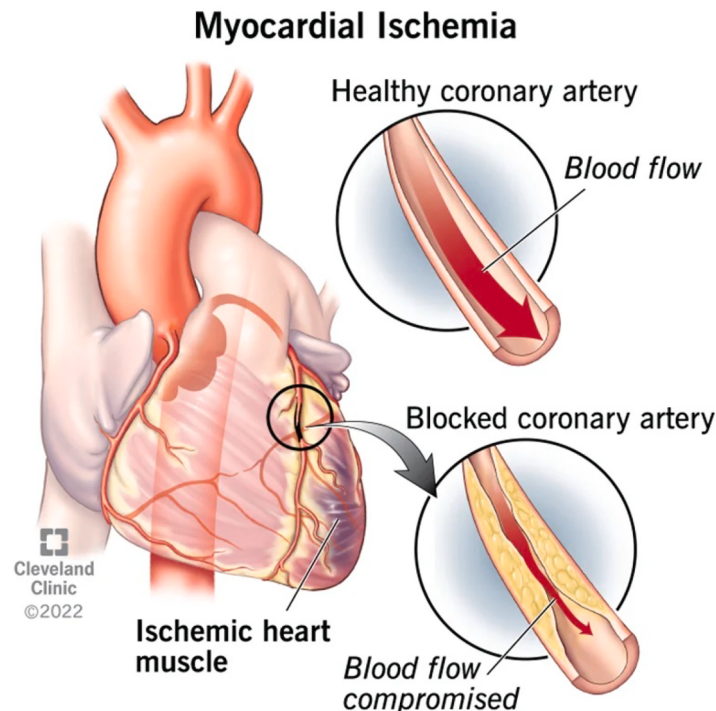


Fig. 5. Myocardial ischemia [79].

ischemia occurs due to decreased blood flow to the skin. So, early detection of ischemia is possible from ECG to avoid severity of CVDs [78]. Appearance of healthy-artery and blocked-coronary artery (in myocardial ischemia) are shown in the Fig. 5. Blocked coronary artery restricts the blood flow.

2.5. Disease identification from ECG

Analyses of various waveforms (P-, T-, and U-wave) along with QRS complex and their intervals from ECG waveform help in identifying the heart related diseases [80]. CVDs are identified from the analysis of ECG are supraventricular ectopic beat (S or SVEB) [57], AFIB [59], AFL [60], APB [61], ventricular ectopic beat (V or VEB) [58], Bigeminy [62], CHB [63], ectopic atrial rhythm (EAR) [64], left bundle branch block (LBBB) [70], first degree atrio ventricular block (FRAV) [65], NSR [66], PSVT [67], SAV [68], ST [69], VPB [58], right bundle branch block (RBBB) [71,81], premature atrial contractions (PAC) [72], and premature ventricular contractions (PVC) [73]. Among these diseases, AFIB, NSR, CHB, and Bigeminy lead to critical health conditions. PSVT, VPB, PVC, LBBB, RBBB, and FRAV are not very serious diseases. The emotional conditions of a person can be detected from the QRS deflection and irregular heartbeat. In VEB condition, an extra heartbeat that originates in the heart's lower chamber. This beat is known as PVC, occurs prior to the normal heartbeat. In SVEB condition, premature beats have shorter width and altered shape than normal beats. The origin of these beats can be sinus, atrial, or nodal.

By analyzing the above mentioned conditions, heart diseases can be identified at its earlier stage with the help of ECG signal. These conditions are detected by variation in the ECG signal compared to the normal one.

2.6. Misleading signals in ECG

During acquisition of the ECG signals, various noises are added that may lead to misdiagnosis. Mainly, ECG signals are affected by two forms of noise (high and low frequency). Baseline wander (BW) is coming under low frequency noise. Whereas, power-line interference (PLI), muscle artifact (MA), Gaussian noise, and electromagnetic interference (EMI) etc., lie in high frequency group. Description about these noises are mentioned below.

Baseline wander [82] It is a low frequency artifact in the ECG that caused due to loose contact of the electrodes, dried out electrolyte, body creams, and excessive movement of the chest wall during respiration. It can be reduced by sampling rate alteration method, which involves two steps (i.e., decimation and interpolation). Decimation removes the high-frequency content of the signal. High-pass filtering technique over BW is performed on a sampled signal at a much lower rate than the original ECG to reduce this noise.

Power-line interference (PLI) Its basic component is 50/60 Hz power line signal and its rhythms. It is one of the most distressing noise sources in bio-electrical recordings, preventing analysis of electrical signals produced by the human body. These noise have a very low frequency and mainly occurs between (0–0.7) Hz. PLI can be removed using adaptive filtering, while harmonic frequencies and ultrasonic noise in this can be eliminated using broad notch rejection filters.

Electromagnetic interference (EMI) This artifact is commonly caused by power lines, electrical equipment's, and mobile phones. In United States, this is known as 60 cycle interference. To reduce this interference, the diagnostic mode of 12-lead ECG monitor is set to 0.05–40 Hz. For accurate ST-segmentation, low frequency of high pass filter is set to 0.05 Hz.

Muscle artifact It is a type of motion artifact, which occurs when patient is suffering from cold and shivering. However, it can also occur when patients holdup themselves by their arms. These noise mainly occurs between the frequency range of 20–100 Hz.

3. Literature review: ECG signal analysis

Researchers analyzed the ECG signals for delineation of various wave-forms (P-wave, QRS complex, T-wave, and isoelectric line) for classification of arrhythmias and heart related diseases. Identification of CVDs from ECG is not a replacement of standard ECG, but help in reducing heart diseases, raising heart awareness, and saves time & cost for pre-diagnosis. These works can be grouped into removal of artifacts for improving the performance, extracting of delineations from ECG for identification of heart conditions, and classification of CVDs. These works are evaluated on publicly available ECG databases and locally collected ECG recording from hospitals and research organization. Researchers have used various subjective and objective measures to validate the efficiency of their model. The details about ECG databases, performance measures, and existing techniques for ECG analysis are discussed in below subsections.

3.1. ECG databases

MIT-BIH database consists of 48 ECG signals (sampled at 360 Hz, having 11 bit resolution) related to arrhythmia are collected from 47 subjects with lengths of 30 min duration [83]. MIT-BIH noise stress test database (NSTDB) consists of real noises (such as: BW, MA, and electrode motion (EM)). Each beat present in this database are labeled by two cardiologists independently.

FANTASIA ECG data is a part of MIT-BIH database, that consists of healthy persons ECG records collected at resting state in sinus rhythm during watching of the movie Fantasia (Disney, 1940) [83]. Here, ECG signal is sampled at a frequency of 360 Hz. Along with the ECG, respiration, and blood pressure signals were digitized at 250 Hz. An automated arrhythmia detection algorithm was used to annotate each heartbeat, which later verified visually. Records f1y01, f1y02, ..., & f1y10 and f2y01, f2y02, ..., & f2y10 came from the young cohort, while records f1o01, f1o02, ..., & f1o10 and f2o01, f2o02, ..., & f2o10 came from the elderly cohort. Each subject group has an equal number of men and women. Each record contains an ECG (with beat annotations) and respiration data. Half of the data in each group (i.e., f2 records) contain blood pressure waveform.

MIT-BIH normal sinus rhythm database (NSRDB) [83] includes 18 long-term ECG recordings of subjects referred to the Arrhythmia Laboratory at Boston's Beth Israel Hospital (now the Beth Israel Deaconess Medical Center). This database's subjects (five men aged 26 to 45 and thirteen women aged 20 to 50) were determined to have no major arrhythmias.

MIT-BIH atrial fibrillation database includes 25 long term ECG recordings of human subjects with atrial fibrillation (mostly paroxysmal). From these, 23 records include two ECG files (representing rhythm and annotation). Each recordings are of 10 h duration, having 250 samples per second, 12-bit resolution, and peak-to-peak amplitude ± 10 mV. These recordings were made at Boston's Beth Israel Hospital (now Beth Israel Deaconess Medical Center) using ambulatory ECG recorders with a typical recording bandwidth of 0.1–40 Hz.

European ST-T database (EDB) is a subset of MIT-BIH data having the ECG (sampled at 250 Hz) for ischemia affected persons [83]. This data developed for evaluation of algorithms for analysis of ST and T-wave changes. This data contains 90 annotated excerpts of ambulatory ECG recordings from 79 subjects (70 men in the age group of 30 to 84, and 8 women in the age group of 55 to 71). One subject information is missing. The database includes ST segment and T-wave change having 367 and 401 episodes, respectively (duration: 30 s to several minutes and peak displacement: 100 μ V to more than one mV). Two cardiologists worked independently to annotate each record beat-by-beat for changes in ST segment and T-wave morphology, along with rhythm and signal quality.

PTB database contains 549 records from 290 subjects (aged between 17 to 87; 209 men, and 81 women). Minimum one and maximum five

Table 4

Commonly used ECG database.

Sl. No.	Database	Description	Disease	Data Origin
1	QT	105 records	Supraventricular Arrhythmia	MIT Laboratory for Computational Physiology
2	PTB	549 records from 290 subject	* Myocardial infarction * Bundle branch block	Cardiology of University Clinic Benjamin
3	MIT-BIH Arrhythmia	48 half-hour records obtained from 47 subjects	Ventricular ectopic beats	Boston's Beth Israel Hospital
4	St. Peterberg	17 men and 15 women, aged 18–80	Coronary angiography, Ischemia	St. Petersburg Institute of Cardiological Techniques
5	China Medical University Hospital (CMUH)	Warehousing based on the integration of all of the hospital's patients	CVDs	China Medical University Hospital
6	European ST-T	90 annotated collected ambulatory ECG recordings from 79 subjects	Myocardial ischemia	European Society of Cardiology
7	PhysioNet/CinC AF Classification Challenge 2017	8528 ECG recordings	Atrial fibrillation	AliveCor hand-held device
8	Physionet AFPDB	50 record sets from 48 different subjects	Atrial fibrillation	Steven Swiryn of Northwestern University
9	MIMIC-III waveform	67,830 ECG recording collected from 30,000 ICU patients	Diastolic blood pressure	MIMIC-III Clinical
10	MIT-BIH Noise Stress Test	12 ECG and 3 noises recordings of 30 min duration each	Arrhythmia detector	MIT Laboratory for Computational
11	Lobachevsky University Electrocardiography	200 ECG signals of 10 s duration	Sinus arrhythmia	Nizhny Novgorod City Hospital
12	PhysioNet/Computing in Cardiology Challenge 2017	10,000 ECG recordings	–	–
13	FANTASIA ECG	Healthy persons ECG records collected while watching movie Fantasia	Arrhythmia detection	–

ECG records have been obtained from each subject. There are no subjects with the numbers 124, 132, 134, or 161. Each record contains 15 simultaneously measured signals obtained from 12 traditional leads (such as, I, II, III, AVR, AVL, AVF, V1, V2, V3, V4, V5, and V6) and three Frank leads (V_x , V_y , V_z). Each signal contains 1000 samples/second, with 16-bit resolution over a 16.384 mV range. This database mainly consists of cardiac arrhythmia and grouped into four categories (normal, SVEB, VEB, and fusion).

St. Peterberg database consists of original ECG records obtained from patients (17 men aged between 18–80, and 15 women around the age 58) undergoing coronary artery disease testing. Majority of them had ventricular ectopic beats. Ischemia, coronary artery disease,

conduction abnormalities, and arrhythmias are all observed from recorded ECGs.

China Medical University Hospital (CMUH) database was recorded at the ECG laboratory China Medical University Hospital during the year 2009–2018, by a 12-lead ECG recorder (GE Medical Systems, Milwaukee, WI, USA) from 38,899 subjects. This contains 65,932 ECG waveforms having twelve types of heart rhythms (such as: AFIB, AFL, APB, BIGEMINY, CHB, EAR, FRAV, NSR, PSVT, SAV, ST, and VPB).

China Physiological Signal Challenge-2018 database contains 6877, 12 lead ECG signals (duration 6 to 60 s with a sampling frequency of 500Hz) for 8 different arrhythmia and NSR, collected from 11 various hospitals in China. The dataset contains N, AF, I-AVB, LBBB, RBBB, PAC,

Table 5

Performance evaluation metric for ECG signal classification/detection algorithms/ methodologies.

Sl. No.	Representation	Range	Remarks
1	$TPR = \text{Sensitivity} = \text{Recall} = \frac{TP}{TP + FN}$	[0-1]	Correctly classified positive class out of total actual positive class
2	$FNR = \frac{FN}{TP + FN}$	[0-1]	False rejection rate
3	$TNR = \text{Specificity} = \frac{TN}{TN + FP}$	[0-1]	Correctly excluded
4	$FPR = \frac{FP}{TN + FP}$	[0-1]	False acceptance rate
5	$\text{Precision} = \text{Positive predictive value} = \frac{TP}{TP + FP}$	[0-1]	Correctly classified positive class out of predicted positive class
6	$F1 \text{ score} = (1 + \beta) \frac{(Precision * Recall)}{\beta^2(Precision + Recall)}$	[0-1]	<ul style="list-style-type: none"> * $\beta = 1$: Balanced F1 score * Harmonic mean b/w precision & recall * Varies with class swapping or not symmetric * Not suitable for $TP = 0$, $FP > 0$, $FN > 0$
7	$\text{Accuracy} = \frac{TP + TN}{TP + TN + FP + FN}$	[0-1]	<ul style="list-style-type: none"> * Gold standard measure (i.e., positive test outcomes) * Not suitable for imbalance class * Over optimistic estimation
8	$G\text{-score} = \sqrt{\frac{TN}{TP + FN} \times \frac{TP}{TN + FP}}$	[0-1]	Inductive bias for imbalance class (i.e., based on predicted positive and negative accuracy)
9	$DSC = \frac{2 \times A \cap B }{ A + B } = \frac{TP + FP}{TP + TN + FP + FN}$	[0-1]	<ul style="list-style-type: none"> * Evaluation process metric during cardiac anatomical segmentation * A & B are data sets
10	$Kappa \text{ score (K)} = \frac{p_0 - p_e}{1 - p_e}$	[0-1]	<ul style="list-style-type: none"> * Measures inter-rater agreement for qualitative items * p_0 - Total accuracy * p_e - Random accuracy
11	$MCC = \frac{(TP \times TN - FP \times FN)}{\sqrt{(TP + FP)(TP + FN)(TN + FP)(TN + FN)}}$	[-1 to 1]	<ul style="list-style-type: none"> * Measure the difference between predicted values and actual values * Symmetric & overcomes class imbalance issues

PVC, STD, and STE types with records of 918, 1098, 704, 207, 1695, 556, 672, 825, and 202, respectively.

PhysioNet/CinC AF Classification Challenge-2017 database consists of 8528 (training) and 3658 (testing) recordings of duration 9 s to 61 s. These signals are collected using a single lead ECG instrument (named AliveCor hand-held device that automatically upload the recording on user's mobile). These signals are stored at 300 Hz, 16-bit files with a bandwidth 0.5–40 Hz and a ± 5 mV dynamic range. These ECG signals are grouped into four (such as: N-rhythm, AF-rhythm, other-rhythm, and noise) categories, by the experts.

PAF Prediction Challenge database consists of two-channel ECG recordings. This was created by "Computers in Cardiology Challenge (open competition aiming for developing automated methods for predicting PAF)" in the year 2001.

Medical Information Mart for Intensive Care (MIMIC)-III waveform database: For 10,282 different ICU patients, the matched subset contains 22,317 ECG records and 22,247 numeric records. The recordings usually contain digitized signals (ECG, ABP, breathing, and PPG) as well as periodic measurements (heart rate, saturation with oxygen, and systolic, mean, and median blood pressure). This collection of data is a subset of the MIMIC-III waveform database, comprising those recordings for which the patient has been identified and the associated clinical records can be found in the MIMIC-III clinical database. MIMIC-III data contains 840 (500-AF and 340-PAC/PVC) segments from 20 subjects (equal in number for AF and PAC/PVC).

Table 4 represents the commonly used ECG database for analysis of CVDs by various researchers. These databases consist of the ECG recordings during specific type of heart diseases (mainly arrhythmia, bundle branch block, and ischemia etc.). Highest number of ECG recordings are available in MIMIC-III database corresponding to diastolic blood pressure. Few of the data's are not annotated.

3.2. Evaluation criteria for ECG analysis and feature extraction

The ECG signal is mainly used by researchers for automatic classification/identification of various disease or heart related conditions, detection of parameters (such as: amplitude and duration) for rhythms, identification of diagnostic information, compression for robust transmission during telesurgery etc. Efficiency and reliability of models/techniques used for classification and feature extraction are evaluated by objective and subjective measures. Objective measures are mainly used by researches for effective comparison of the techniques. Few popularly used measures for ECG classification are accuracy, precision (pre), recall, F1 score, and weighted average etc. Table 5 represents various objective performance measures used by the researches for classification of ECG signals. These measures depend on the statistical measures (such as: true positive (TP), true negative (TN), false positive (FP), false negative (FN)) [84] obtained from confusion matrix or contingency table or error matrix in case of supervised learning. For unsupervised learning, the above mentioned matrix is called as matching matrix. TP, TN, FP, and FN represent normal class classified/detected as normal, abnormal class classified/detected as abnormal, abnormal class classified/detected as normal, and normal class classified/detected as abnormal, respectively. Precision, recall, F1 score, accuracy, sensitivity, specificity, and G-mean are derived from TP, TN, FP, and FN.

Recall/sensitivity measures the model's ability to detect positive samples. This is also known as hit rate, detection rate, and correctly classified positive class from actual positive class. False negative rate (FNR) represents rejection of abnormal samples. Specificity is represented as the ratio of correctly classified abnormal samples to the total number of abnormal samples. FPR is known as false acceptance rate or fall out. Precision/positive predictive value measures the degree to which estimates of different samples are similar. Precision refers to the number of true positives divided by the total number of positive predictions. F1 score measures the harmonic mean of precision and recall. In balanced F1 score, β is considered to be unity. Accuracy is a gold

Table 6
Performance evaluation metric for multi class ECG classification/detection.

	Predicted label by the model					$\sum(\text{All})$
	\hat{N}	\hat{S}	\hat{V}	\hat{F}	\hat{Q}	
Reference label	N	$C_{N,N}$	$C_{N,S}$	$C_{N,V}$	$C_{N,F}$	$C_{N,Q}$
	S	$C_{S,N}$	$C_{S,S}$	$C_{S,V}$	$C_{S,F}$	$C_{S,Q}$
	V	$C_{V,N}$	$C_{V,S}$	$C_{V,V}$	$C_{V,F}$	$C_{V,Q}$
	F	$C_{F,N}$	$C_{F,S}$	$C_{F,V}$	$C_{F,F}$	$C_{F,Q}$
	Q	$C_{Q,N}$	$C_{Q,S}$	$C_{Q,V}$	$C_{Q,F}$	$C_{Q,Q}$
		$P_r)_N$	$P_r)_S$	$P_r)_V$	$P_r)_F$	$P_r)_Q$

where, $C_{A,B}$: Total samples of Class-A predicated as Class-B, $\sum(A)$: Total samples of Class-A, $P_r)_A$: Total samples predicated as Class-A, $\sum(\text{All})$: Total samples in dataset.

standard measures for identifying correctly classified samples or diseases. G-score represents the degree of inductive bias in imbalance class. It is represented as $\sqrt{\text{specificity} \times \text{sensitivity}}$. Dice similarity coefficient (DSC) is used to calculate the parallelism between two sets of data (i.e., set A and set B). It measures spatial overlap index and validation parameter for reproducibility. DSC score ranges from 0 to 1 (with 0 indicating no spatial overlap and 1 indicating complete overlap between two sets of binary segmentation/classification data). The Kappa score is a unique measure used to assess the level of similarity between two human examiners or testers. The machine-learning community later adopted it to assess classification performance. The Matthews correlation coefficient (MCC) is a more dependable statistical rate that provides an excellent result only when the prediction performed adequately in all four confusion matrix categories (i.e., TP, TN, FP, FN).

Mathematical representation of these measures for two class are mentioned in Table 5 along with their ranges. For multi-class classification/detection system representation of these performance measures are provided in Table 6.

Several metrics are defined to describe the multi-class performance (such as: accuracy, sensitivity for any one class, and positive predictivity of any one class). Table 6 represents the symbols and variables for defining these metrics. Accuracy (Acc) is used to calculate the overall performance of all classes as shown in Eq. (1). Sensitivity of individual class is represented in Eq. (2). Probability of accurate classification in heartbeats/diseases is defined by positive predictivity of class A ($+P_A$) represented in Eq. (3).

$$Acc = \frac{(TP_N + TP_S + TP_V + TP_F + TP_Q)}{\sum \text{All}(total \text{ samples in database})} \quad (1)$$

$$Sen_A = \frac{TP_A}{\sum A} \quad (2)$$

$$+P_A = \frac{TP_A}{P_A} \quad (3)$$

3.3. ECG signal analysis

Researchers have used traditional based- and deep learning (DL) based- methods for analyzing various diagnostic features from the ECG signals for detecting CVDs. Analysis of ECG signal for these research papers presented in the literature are mainly grouped into three categories (such as: noise removal, feature extraction, and disease detection). In the following subsection, these works have been analyzed and compared.

3.4. Noise removal

This subsection discusses about various noise removal methods from ECG recordings which are added/mixed into ECG recording during

Table 7

Beat classification from ECG.

Sl. No.	Author & Year	Techniques used	Data	Classified beats	Performance Accuracy (%)	Remarks
1	Sannino et al. [88]	* Preprocessing (denoising, peak detection, signal segmentation, and temporal features extraction) * Classification by DNN (7-hidden layers, ReLU, and softmax)	MIT-BIH arrhythmia	N, A	* Training – 100 * Testing – 99.52	Limited data
2	Li et al. [54]	* Preprocessing, * Generation of 3D feature map, * Classification by CNN (residual, ASPP, GAP, and FC)	MIT-BIH arrhythmia	N, SVEB, F, VEB, Q	91.44	Poor performance
3	Nurmaini et al. [90]	* DAE (feature-extraction, -selection, and -reduction) * Classification by DNN (ReLU and softmax)	MIT-BIH arrhythmia	N, APC, PVC, RBBB, LBBB, P, VF, F, j	99.73	Limited data
4	Jiang et al. [93]	* MMNNs # Preprocessing # Imbalance problem processing (BLSM, CTFM, & 2PT) * CNN (feature extraction & classification)	MIT-BIH	N, S, V, F, Q	97.3	Limited class
5	Bidias et al. [94]	* PE, CEOP * Ordinal pattern based classification	ESC, MIT-BIH	L, R, N, e, j, A, V, P, a, S, F, U, f, E, J	ESC - 99.57	MIT-BIH accuracy was 93.67%
6	Wu et al. [95]	* Data preprocessing * Binarized 1D-CNN (convolution, pooling, dropout, normalization, ReLU, and softmax)	PhysioNet/ CinC AF classification challenge	N, AF, O, Noises	86	Poor performance
7	Pandey et al. [96]	* Preprocessing * Segmentation, FE * Classification (ensemble SVM, SVM, RF, KNN, LSTM)	MIT-BIH	N, S, V, F	94.40	Poor performance
8	Hannun et al. [97]	* Automatic preprocessing FE, selection, & classification by DNN	* MIT-BIH arrhythmia	Classes from Chang et al. [98]	-	Poor F1 score (0.83)
9	Zhai et al. [99]	* Coupling matrix * CNN (convolution, pooling, dropout, FC and softmax)	MIT-BIH	SVEB, VEB	-	Limited beats
10	Zhou et al. [100]	* ACE-GAN # GAN (G & D) # General classifier (CM) # Unsupervised classifier (STFT features)	MIT-BIH arrhythmia	N, SVEB, VEB, F, Q	99 (for SVEB & VEB beats)	Limited classes, Less no. of generated samples
11	Peimankar et al. [101]	* Preprocessing (noise reduction, segmentation, and dataset splitting) * DENs-ECG (CNN-LSTM) # 3-CNN networks # 2-BiLSTM networks # 1-Dense network	* Physionet QTDB # European ST-T # Sudden death MIT-BIH # NSR MIT-BIH # Supraventricular arrhythmia MIT-BIH	P, QRS, T, NW	* MITDB - 99.56 * QTDB - 96.78	Limited class
12	Patro et al. [102]	* Preprocessing (filtering, peak detection, segmentation) * 11-layers CNN	* MIT-BIH * Real-time data	N, SVE, VE, IVCD	* MITDB - 99.28 * Real-time-data-99.24 99.98	Limited class
13	Mirza et al. [106]	* Preprocessing (normalization, filtering, segmentation) * Classification by 1D-CNN	PTB	N, MInfra	99.98	Limited imbalance data

acquisition and provide misleading effect during classification. Almost all the researchers mainly used denoising as a preprocessing step for classification and disease detection. Authors have used various denoising steps for removal of noises. A few recently published papers on noise removal techniques are discussed below.

Chiang et al. [85] proposed 13 layer denoising auto encoder (DAE) with fully convolutional network (FCN) for removing the noises (BW, MA, and EM) from the ECG signals available in MIT-BIH Arrhythmia database. Authors have used the real noises associated with the ECG signals from the MIT-BIH noise stress test database (NSTDB). The noise samples were divided into training set (80%), validation set (10%), and testing set (10%). Performance of the algorithm was evaluated by improvement in signal-to-noise ratio (SNR_{imp}), percentage root mean square difference (PRD), and root mean square error (RMSE). Authors reported the PRD of 19.68% and RMSE of 0.063 for FCN based DAE. This method also helped in compressing the ECG signal in addition to denoising.

To analyze multichannel ECG, researchers mainly used QRS complex detection and QRS duration. Authors use a variety of techniques to detect QRS. A few papers on QRS complex detection techniques that have recently been published are discussed below.

Curtin et al. [86] developed an automated method for QRS detection and computation of QRS duration (QRSd) to analyze multichannel ECG (MECGs: i.e., ECG signal from 50 to 250 electrodes) acquired from cardiac re-synchronization therapy (CRT) patients. MECGs were collected at sampling rate of 1 kHz for 15–20 s duration and bit resolution of 24-bits. For loading and analysis of MECGs, authors implemented comprehensive stand alone software written in MATLAB and graphical user interface (GUI). The QRS complex detection was performed by five stages (i.e., channel grouping and averaging, peak detection, definition of QRS complex windows, identification of additional complexes, and classification of QRS complex morphologies). The QRS detection algorithm is designed using various stages (i.e., identification of significant peak in each channel, formation of array specific peak groups, delineation of channel-specific QRS complex border, delineation & measurement of array specific QRS complex border & duration, delineation & measurement of the global QRS complex & border & duration). The method was tested on the real data obtained from the CRT patients and achieved classification accuracy of 94.3%, sensitivity of 96%, and positive predictivity of 97.3%. The system performance was not validated due to the lack of other MECG system.

Dominguez et al. [87] proposed a q-lag unbiased finite impulse

response (UFIR) smoother techniques for denoising and feature extraction by retaining the properties of ECG signal. Here, N-number of ECG data points are optimally selected for minimizing MSE. In this work, authors used the above mentioned method for removing artifacts and identification of various features for classifying the ECG signal into AF or normal class. ECG features are extracted in five stages such as, detrending, QRS-complex detection, segmentation, adaptive iterative UFIR smoothing, and windowing of ECG waves. Authors used some silent points (such as: initial and final point of P-, Q-, S- and T- wave along with R- and T- peak) on ECG signal for feature extraction. This method has been tested on MIT-BIH arrhythmia database. This work was bench-marked with several Daubechies mother wavelets. The average time required for q-lag 1 and q-lag 2 are 6.81 s and 5.48 s for 21 parameters. UFIR method was found to be stable and provided good discrimination between the normal and arrhythmia features for classification. UFIR based classification provided an accuracy, sensitivity, and specificity of 99.3%, 99.6%, and 99.9%, respectively for AF classification.

ECG signals are mainly used for classification of diseases such as arrhythmia, various types of abnormal rhythms, myocardial ischemia, myocardial infarction etc,. The techniques for diseases classifications have been discussed in the below sections.

3.5. Beat classification

Some of the researchers have been used ECG signal for beat classification. Few techniques used in the literature for beat classification with different databases are discussed below and summarized in [Table 7](#)

Sannino et al. [88] proposed a DNN consists of seven hidden layers for ECG beat classification from MIT-BIH arrhythmia database. In this work, they divided cardiac arrhythmias into fatal and non-fatal (not life threatening). Authors performed preprocessing (i.e., denoising, peak detection, signal segmentation, and temporal feature extraction) prior to the classification of arrhythmia. Preprocessing stage removes PLI and baseline wanderings that occurred due to respiration or patient movements. Peak detection was followed by denoising to localize P-wave and T-wave. This helps in segmenting the beat from ECG signals. These segmented beats are used to find the temporal information (i.e., intervals of pre-RR, post-RR, local average-RR, and global average-RR) for classification by the DNN (consists of seven hidden layers along with rectified linear activation unit (ReLU) activation function and softmax layer). The DNN used 50-bit samples along with 4-temporal features (such as: pre-RR, post-RR, local average-RR, and global average-RR) for classifying them into normal- and abnormal-beats. Authors used MIT-BIH database having equal number of normal- and abnormal-beats (total 4576 beats). The model was trained by 60% of beats and tested by the rest 40% of beats. The performance of this method was studied by computing accuracy, sensitivity, and specificity. Authors reported 100% and 99.09% of training- and testing-accuracy, respectively. The training accuracy scores for Kstar and Random tree classifiers [89] were discovered to be the same as DNN classification network. They claimed that their method achieved a sensitivity value (i.e., 98.55%) close to the highest sensitivity value (i.e., 99.13%) obtained by Part classifier. The specificity value was found to be 99.52% (close to the highest value i.e., 99.80% obtained by KStar classifier).

Li et al. [54] determined 3-D data structure (contains the information about morphological characteristic, RR-interval, and beat-to-beat correlation feature) for classifying normal, SVEB, VEB, F, and unclassified beats by using CNN (consists of 10 convolution layer, one fully connected layer, and a softmax layer), from MIT-BIH arrhythmia database. This process was divided into three steps (preprocessing, generation of 3-D data structure, and classification by CNN). The preprocessing step normalized the ECG signal by utilizing the morphological features in three stages. Here, ECG signals are divided into segments (consist of one heartbeat having 128 samples without BW). Second step generated the 3-D data from all the channels of ECG signal by considering the common

features (such as: morphology, RR intervals, and beat-to-beat correlation of the segments). In third step, the 3-D data was fed to the CNN, which consists of two residual block, one atrous spatial pyramid pooling (ASPP) module, one global average pooling (GAP), and one fully connected (FC) layer. The framework aided in easy optimization and accuracy improvement. Four parallel blocks (consists of atrous convolution layers followed by batch normalization, and ReLU) were interconnected to form the ASPP module. This helped in retrieving specific and enormous heartbeat features from the signal in different resolutions (multi-scales). The output of ASPP module was fed to GAP layer. This layer was invariant to spatial translation and helped in reducing the number of parameters. This network was trained and tested by mini-batch gradient descent (MBGD) with a mini batch size of 128. Authors have computed each class performance along with model accuracy. This system achieved an overall accuracy of 91.44% for inter-patient practice. The method attained sensitivity of 89.05% and 95.15% for SVEB and VEB classes, respectively.

Nurmaini et al. [90] classified 10 types of ECG beats (such as: N, APC, PVC, RBBB, LBBB, paced (P), ventricular flutter wave, fusion of ventricular & normal (F), fusion of paced & normal (f), and nodal escape (j)) from freely available ECG at MIT repository by a DL technique, which consists of unsupervised deep auto-encoders (DAE) for pre-training and DNN for fine tuning. DAE helped in overcoming the drawbacks of DNN learning process (i.e., local minima due to random weight initialization and unlabeled data during the initialization of random requirement for labeled data) by learning the generic features using greedy layer wise training. This makes the network to perform faster for classification and prediction problems. In this case, DAE helped in data preprocessing (such as: robust feature-extraction, selection, and dimensional reduction) in a non-linear and unsupervised method. DAE reduced 232-features into 32-features with aggregate energy value of 99%. The output of DAE was fed to the DNN (consists of 32 nodes in the input layer and 10 nodes in the output layer). Authors used ReLU activation function, adam optimizer, learning rate (0.1 to 0.0001) as hyper-parameters. Softmax layer was used for classification. The model was trained and tested by 80% and 20% of the data, respectively. This system achieved an overall accuracy, sensitivity, precision, specificity, and F1 score of 99.73%, 91.20%, 93.60%, 99.80%, and 91.80%, respectively. Similar works were done by Swapna et al. [91] and Yildirim et al. [92]. In [91] authors have used CNN, recurrent structures (such as: RNN, LSTM, and gated recurrent unit (GRU)) and hybrid of CNN for classification of arrhythmia and obtained an accuracy of 83.4%. In [92] authors used convolutional auto-encoder (AE) for reducing signal dimension and LSTM classifiers to identify arrhythmias and recorded an accuracy of 99%.

Jiang et al. [93] developed multi-module neural network system (MMNNS) that consisted preprocessing, imbalance problem processing, feature extraction, and classification module for classifying the ECG heartbeats (such as: N, SVEB, VEB, F, and Q) from the MIT-BIH, European ST-T, and MIT-BIH ST change database. In the first stage of MMNNS, different duration of median filter was used to remove P-wave, QRS complex, T-wave to obtain the baseline corrected signal (by subtracting the filtered signal from the original ECG signal). This filtered signal was fed to a 12-tap low pass filter to eliminate high frequency noise and power-line interference. This followed the PAN-Tompkin algorithm for detection of R-peak and Z-score normalization to avoid offset & amplitude scaling. The pre-processed output followed the imbalance problem module (that consists of borderline-SMOTE (BLSM), context-feature module (CTFM), and two-phase training (2PT)) to overcome the variations of signals available in each class. BLSM module was responsible for oversampling the minority class by synthesizing linear interpolation of samples. This module followed CTFM and 2PT to expand the previously generated samples to double and avoid class imbalance. From each class DAE- and QRS-based features were extracted for classification by the CNN (which consists of input-, 3-convolution-, 3-maxpooling-, and fully connected layer). Authors have adopted leaky ReLU activation function, adam optimizer, and decaying learning

rate (decay-rate of 0.001) for faster training and eliminating vanishing gradient. Authors used 230,775 and 232,357 ECG beats for intra- and inter-patients, respectively for classifying four classes (such as: N, S, V, and F) and reported an accuracy, sensitivity, specificity, positive prediction rate, F-measure, and G-mean of 97.3%, 64.4%, 98.6%, 63.7%, 64%, and 79.7%, respectively for SVEB class. Whereas, the above-mentioned parameters were found to be 98.8%, 91.0%, 99.3%, 90.0%, 90.5%, and 95.1%, respectively for VEB class. The overall accuracy and multi-class area under curve (MAUC), were recorded to be 96.6% & 97.8%, 93.7% & 94.1%, & 94.3% & 93.2% for MIT-BIH, European ST-T, and MIT-BIH ST change database, respectively.

Bidias et al. [94] computed Shannon or permutation entropy (PE) and conditional entropy of ordinal patterns (CEOP) for analyzing normal and abnormal ECG beats from MIT-BIH arrhythmias and European society of cardiology (ESC) ST-T databases. In the normal beats, authors identified 5-beat types (such as: LBBB, RBBB, N, AEB, and NEB), whereas in abnormal group authors classified 10-beat types (i.e., APC, PVC, PB, AAPB, SPB, fusion of ventricle & N beat, unclassified beat, fusion of paced & N beat, VEB, and nodal premature beat). This method consists of segmentation (detection of RR interval and QRS complex) and classification (detection of normal and abnormal classes) based on signal dependent threshold value, which was computed based on fluctuation ratio (obtained by subtracting mean from ECG data and dividing it by standard deviation). Ordinal pattern based fluctuation ratio was used for classification. This system achieved an accuracy, sensitivity, and specificity of 93.67%, 55.57%, and 98.23%, respectively on MIT-BIH database. Authors recorded a classification accuracy of 99.57% for ESC database.

Wu et al. [95] proposed binarized 1D CNN for identifying four classes of rhythms (such as: N, AF, other rhythms (O), and noise) from the ECG signals, used in PhysioNet/CinC AF Classification Challenge 2017 database. Authors used data processing (consists of fixed duration slicing, full length padding, and bucket padding) followed by CNN for classification. The CNN model was composed of a block (which comprised 1D convolutional, average pooling, normalization, and ReLU) that was repeated 9 times, followed by global average pooling, dropout, dense layer, and softmax. The normalization layer helped in minimizing the internal covariant shift and improved the model convergence rate and performance. In this case, authors used L1- and L2-regularization, dropout, and data augmentation to minimize overfitting conditions in training data. Authors used binarized neural networks (BNNs) model to minimize computing resources. The method was experimented on 8528 single lead ECG signals recorded for a duration of 9 to 61 s. The database consists of 5154 normal, 771 AF, 2557 other, and 46 noisy rhythms. Authors have reported an average F1 score of 0.86. The number of AF and noisy rhythms included in this database was significantly lower than the number of normal rhythms. This model can be connected with other models in parallel to increase performance while elevating computational complexity.

Pandey et al. [96] proposed an ensemble of SVMs classifier for classifying four ECG heartbeats (such as: N, SVEB, VEB, and F) from MIT-BIH dataset. The method consist of preprocessing (noise removal and normalization), segmentation of heartbeats (estimation of 90 sample points on each side of 'R-peak'), and feature extraction (db1 mother wavelet, higher order cumulants, morphological descriptors, and R-R intervals), and classification (SVM, ensemble SVM, LSTM, RF, and KNN). Authors reported an overall accuracy, sensitivity, specificity, precision, and F1 score of 94.4%, 65.26%, 93.25%, 69.11%, and 66.24%, respectively for ensemble SVM classifier. In single classifier model, RF reported highest overall accuracy of 93.45%. The classification performance for the above discussed models were found to be low.

Hannun et al. [97] developed a DNN model to classify 12 rhythm classes (as mentioned by Chang et al. [98]) from the ECG signals available at MIT-BIH arrhythmia- and the recorded-databases obtained by a local hospital. This model consisted of signal processing, feature selection (reduction), and classification. The DNN network received the

raw ECG data as input and selected the feature automatically for classification. This DNN network consisted of 33-convolutional-, 18-ReLu-, 33-batch normalization-, and 16-dropout-layers followed by a softmax layer. Authors have used 91,232 single lead ECG signals recorded from 53,549 patients by Zio monitor at the rate of 200 Hz. The performance of this method was computed by AUC (0.97), average F1 score of (0.82), and sensitivity (94.1%) for MIT-BIH arrhythmia database. Authors applied the DNN to 2017 PhysioNet Challenge data to identify four rhythm classes (sinus rhythm, AF, noise, & others) and recorded an average F1 score of 0.83.

Zhai et al. [99] estimated dual-beat coupling matrix (CM) having dimension of 73×73 by considering three adjacent segmented R-R beats ($Beat_{i-1}$, $Beat_i$, and $Beat_{i+1}$) from the ECG signals for classification of SVEB and VEB by using a CNN classifier. CM converted 1D ECG signal to 2D image for classification by CNN. This matrix helped in capturing morphological and rhythmic information from the ECG recordings. CNN network consists of three convolution-, two pooling-, two dropout-, one fully connected-, and softmax-layers. This work was carried out in MatConvNet 1.0-beta23 toolbox. This model was experimented on MIT-BIH database [83] and reported F1 score of 72.5% and 89.2% for SVEB and VEB detection, respectively. This model was tested with SGDM optimizer (with weight initialization of 0.01 standard deviation), having batch size 64, epochs 100, dropout 50%, and learning rate $1e^{-3}$ (reduced by 2.3% for every epoch). Here, the common pool data for 'N' beats are misclassified as 'S' or 'V' beats. This problem was overcome by considering three adjacent beats for which the spectrograms were computed with a window size of 64, for the first and the last two betas. Computed spectrograms were used for calculating the correlation matrix for identifying the normal beats correctly.

Zhou et al. [100] developed generative adversarial network (GAN) with auxiliary classifier for ECG (ACE-GAN) to overcome the disadvantages/limitations of CNNs (such as: class imbalance problem and labeled ECG data deficiency). ACE-GAN system included data augmentation (by GAN), general ECG classifier (by CM), and a patient specific unsupervised classifier (based on short time FT (STFT) features). GAN network consists of a generator (G) and a discriminator (D) that works in adversarial manner. The 'G' generates fake data similar to the real one to mislead the 'D', whereas the 'D' tries to discriminate generated fake data by 'G'. The 'G' computed CM having dimension of 73×73 (using the embedded function, element wise multiplication, and vector multiplication) by considering a Gaussian noise (mean = 0, variance = 1) having dimension 100×1 vector. The generator used batch normalization and ReLU in all the hidden layers except the last layer. In this case, 400 beats of each class (N-, SVEB-, VEB-, F-, and unclassified-beats (Q)) were generated. Discriminator consists of three convolutional-, one max-pooling-, one average pooling-, and two fully connected-layers. The 'D' used ReLU activation functions in all hidden layers and 50% dropout in last two hidden layers. Softmax was the last layer of the discriminator for discriminating real training data from the generated fake data by the generator. The network was optimized by two objective functions, which were responsible for likelihood of correct source and likelihood of correct class. Here, authors used mean square error (MSE) loss for the above mentioned objective functions. This helped in stabilizing the GAN training process and aided in eliminating more collapse problem. The output of GAN was fed to the general ECG classifier, which work on the concept of CM. The last stage of ACE-GAN was an unsupervised classifier which computed 1024-point fast FT coefficients by a window duration of 64 and overlapping of 1. The model used adam optimizer, with a batch size of 128, dropout 50% and varying learning rate (0.0002, 0.5, and 0.999). The model was experimented on publicly available MIT-BIH arrhythmia database having five different heart beats (with a count of N = 20670, SVEB = 916, VEB = 1429, F = 690, and Q = 0). Authors showed that the sensitivity for classification of SVEB and VEB beats was 87% and 93%, respectively. Authors reported accuracy, sensitivity, specificity, precision and F1 score for SVEB to be $99\% \pm 0$, $87\% \pm 2$,

Table 8

Techniques for diseases detection / identification from ECG.

Sl. No.	Author & Year	Technique used	Data	Diseases identified	Performance accuracy (%)	Remarks
1	Bhoi et al. [109]	* LDA * QDA * DT * Naive Bayes	* MIT-BIH * EDB * Fantasia	Ischemia & arrhythmia	100	Limited episodes
2	Marinho et al. [110]	* FT * HOS * Goertzel * SCM	MIT-BIH	Cardiac arrhythmias	94.3	Poor performance
3	He et al. [111]	* DRN * DNN * BiLSTM	* CPSC * MIT-BIH arrhythmia	Arrhythmia	91.2	Poor performance
4	Bonab et al. [105]	CAD	MIT-BIH arrhythmia	Arrhythmia	98.33	Limited data
5	Chang et al. [98]	BiLSTM	CMUH	VPB, EAR	VPB - 100 EAR - 97.4	Limited diseases
6	Sharma et al. [113]	* Fourier-Bessel * LSTM	* MIT-BIH * Physionet challenge 2017 * Private data	Arrhythmia	90.07	Poor performance
7	Yao et al. [114]	ATL-CNN	China Physiological Signal Challenge 2018	Paroxysmal arrhythmias	81.2	Poor performance
8	Chen et al. [115]	* CNN * LSTM	* NSR MIT-BIH * Arrhythmia MIT-BIH * AF * PhysioNet/computing in cardiology challenge 2017	N & AFIB	97.15	Limited diseases
9	Ihsanto et al. [116]	* DSC NN * GS NN	MIT-BIH arrhythmia	Cardiac arrhythmia	99.88	Limited data
10	Mohonta et al. [118]	CWT	MIT-BIH arrhythmia	Arrhythmia	99.65	Limited data
11	Hasan and Bhattacharjee [103]	* EMD * IMF	* PTB * MIT-BIH * St. Peterberg	* BBB * Valvular heart disease * Myocarditis * Dysrhythmia * Myocardial infarction, * Cardiomyopathy, * Sinus bradycardia, * Atrial fibrillation, * Transient ischemic attack, * Sinus node dysfunction	98.24	Less data
12	Oktivasari et al. [119]	* DWT * EDB	European ST-T	Myocardial ischemia	90.3	Poor performance
13	Panganiban et al. [2]	* DL * EDSS	* PAF prediction * PTB diagnostic ECG * Challenge 2015 training set * Fantasia * PAF prediction challenge	* Atrial fibrillation * Bradycardia * Tachycardia * BBB	98.73	Less disease prediction

99%±0, 85%±1, and 86%±1, respectively. For VEB beats the above mentioned classification measure values were reported to be 99%±0, 93%±1, 99%±0, 94%±1, and 93%±0. The GAN model performance was computed by Frechet distance and reported to be 42, 58, 91, and 101 for N-, SVEB-, VEB-, and F-beats, respectively. Frechet distance was very high for the different classes.

Peimankar et al. [101] combined CNN and LSTM (renamed as DENS-ECG model) for identifying various delimiters from ECG waveforms (i.e., onset, peak, and offset of numerous waveforms such as: P, QRS, T, and No waves (NW)). Authors used preprocessing (noise reduction, segmentation, and dataset splitting) followed by classification network (consists of 3-CNN networks in cascade, 2-BiLSTM networks in cascade, and 1-dense network). Noise reduction was performed by a third order Butterworth band pass filter having frequency range of 0.5–40 Hz for eliminating baseline wander and high frequency noises. The filtered ECG was segmented to 1000 samples of signal. The pre-processed signals were fed into 3-stages of 1D-CNN. The CNN network provided feature maps by convolution process with different kernel sizes. In this case, the CNN took an advantages of creating local connections, shared weights, large number of layers, and minimizing the network complexity. Computational burden of 1D CNN depends upon number of filters, length of filters, and length of input signals. This work used BiLSTM network (which process the data in both the directions) to

predict the future values. BiLSTM network complexity depends on number of i/p-neurons, hidden-neurons, and constants based on cell-types. The network was trained by categorical-cross-entropy loss (CCEL) function, which consists of softmax-loss-function and cross-entropy-loss-function. The output of second BiLSTM network was fed into a time-distributed-dense-layer (consists of four neurons with softmax function). The model was trained with SGDM and adam optimizer along with dropout. Authors used four optimized hyper-parameters, such as learning rate, exponential decay rate for first & second moment, and numerical stability parameter. The work was experimented on 105-ECG records obtained from PhysioNet QT database (QTDB), which included the records from European ST-T, MIT-BIH sudden death, MIT-BIH normal sinus rhythm (NSR), and MIT-BIH supraventricular arrhythmia. Authors reported an average sensitivity and precision of 97.95% and 95.68%, respectively on 105-ECG records. For an unknown dataset, the model provided an average sensitivity and precision of 99.61% and 99.52%, respectively. DENS-ECG model recorded an average F1 score of 99.56% and 96.78% on MIT-DB and QTDB, respectively.

Patro et al. [102] proposed DL based classification model for classifying SVE, VE, intra-ventricular conduction disturbances (IVCD), and N beats from MIT-BIH and real-time ECG data/signals. The classification method consists of data acquisition, preprocessing, feature extraction,

and classification. Data acquisition was meant for the real time ECG data recorded by BPL-Digital-Holter-Trak-48 instrument (12-lead, 3-channel) available at Government General Hospital Guntur, India. Authors collected 5427 real time beats from various patients. The offline data obtained from MIT-BIH and real time data were subjected to pre-processing (i.e., filtering and R-peak detection). Filtering of the ECG signal was performed by a band pass filter having a frequency range of 0.05–100 Hz to suppress the high frequency components. From the filtered signal R-peak was detected and segmented. After the pre-processing, features are extracted from ECG signal (QRS complex, RR-, and heart rate-interval) automatically by convolution approach. The different features are concatenated and classified by 1D-CNN. In this case, the CNN model was made of 11 layers (3-convolutional-, 1-max-pooling-, 3-flatten-, and 3-dense-layers). The model was trained with two different learning rate (3×10^{-3} & 0.2) and two different epochs (50 & 300). The method obtained an overall accuracy and F1 score of 99.28% and 99.24%, respectively on MIT-BIH database. This model recorded an accuracy of 99.12% for real time database. Similar work were carried out by Hasan and Bhattacharjee [103], Wu et al. [104], Bonab et al. [105] on PTB-, Challenge-, and MIT-databases and recorded an accuracy of 98.24%, 93.20%, and 98.81%, respectively.

Mirza et al. [106] proposed a DL based automatic classification framework to detect 10 different myocardial infarction classes and one normal class from the ECG signals available in PTB database. This method consists of preprocessing (i.e., normalization, filtering by DWT, and segmentation) followed by 1D-CNN classification and performance evaluation. During the preprocessing stage, the raw ECG signals were subjected to normalization followed by noise & artifact removal by sym5 mother wavelet. The filtered signals were segmented to detect the R-peak, which provided the maximum coverage of QRS component. The preprocessed signals were fed to 1D-CNN classifier (consists of 2-convolutional-, 1-maxpooling-, 3-ReLU-, 2 dropout-, 1-flatten-, 1-dense-, and 1-softmax-layers). The model was trained by adam optimizer with 50 epochs. This network was trained, validated, and tested by 70%, 15%, and 15% of the ECG data recorded by 15-leads (12-standard and 3-frank leads), from 52-normal humans and 148-myocardial infarction persons. A total 672,907 ECG-beats (having 548,748 myocardial infarction beats) were used for the experiment. Authors reported an average accuracy, sensitivity, specificity, precision, and F1 score of 99.98%, 99.91%, 99.99%, 99.91%, and 99.91%, respectively. Similar work have been performed by Yadav et al. [107] in the year 2021 and recorded an accuracy of 99.82% with 12-leads ECG signals. Li et al. [108] detected myocardial infarction by single-lead convolutional generative adversarial network (SLC-GAN) classification method and reported an accuracy of 99.06%.

Some of the researchers have been used this ECG signal for identifying the arrhythmia conditions. Few techniques used in the literature for arrhythmia detection are discussed below and outlined in Table 8.

Bhoi et al. [109] classify ischemia and arrhythmia by analyzing the morphological changes occurred in the frequency domain of the QRS complex. It helps to identify the inflection points of QRS complex along with ischemic and arrhythmic condition. Authors have computed the ratio of average rise & fall amplitude along with the interval (ST-T segment) feature from the QRS complex and fed to linear discriminant analysis (LDA), quadratic discriminant analysis (QDA), Naive Bayes' classifier, and decision tree for classification. The representation for average rise amplitude ($R_{avg-amp}$) and average fall amplitude ($F_{avg-amp}$) are expressed in Eqs. (4) and (5), respectively.

$$R_{avg-amp} = \frac{\frac{1}{N} \sum_{i=1}^N R_i}{\frac{1}{M} \sum_{j=1}^M Q_j} \quad (4)$$

$$F_{avg-amp} = \frac{\frac{1}{L} \sum_{i=1}^L S_i}{\frac{1}{N} \sum_{j=1}^N R_j} \quad (5)$$

where, N , M , and L represent the number of 'R-wave', 'Q-wave', and 'S-wave' of the ECG signal, respectively. The performance of system was evaluated on Fantasia, MIT-BIH arrhythmia, and European ST-T databases [83]. The miss-classification error in decision tree was found to be the least compared to LDA and QDA.

Marinho et al. [110] proposed a system for detecting cardiac arrhythmias in ECG. The method had three main steps, such as: pre-processing, feature extraction, and classification. Initially, raw ECG signals were filtered (by lowpass adaptive filter) and QRS components were segmented. Features were extracted from pre-processed ECG signals by Fourier transform (for representing the signal by sinusoidal functions), Goertzel (for evaluating the coefficients of DFT), higher order statistics (HOS), and structural co-occurrence matrix (SCM) methods. These extracted features were used for classification by Naive-Bayes, SVM, multi-layer perception (MLP), and optimum path forest (OPF) classifiers. This method was tested on MIT-BIH heartbeat database on five different classes (such as: N, SVEB, VEB, F, and Q) as suggested by ANSI/AAMI. Among the various combination of feature extraction and classification techniques, HOS-Naive Bayes achieved an accuracy of 94.3%. From this study, HOS feature extraction method found better than other techniques.

He et al. [111] used a combination of deep-residual-network (learning of local features) and BiLSTM-network (global feature learning) for automatic classification of arrhythmias (such as: AF, I-AVB, LBBB, RBBB, PAC, PVC, ST-segment depression (STD), and ST-segment elevated (STE)) from the China Physiological Signal Challenge (CPSC) dataset [112]. This method perform the classification of variations present in ECG signals for common diseases. Also, this is resistant to interference. This work was carried out in three steps, such as: pr-processing, feature extraction, and classification. In preprocessing, authors have considered 30 s unprocessed 12-leads ECG recordings of same length, which were fed to DNN for learning local- and global-features, followed by the classification. Local features were extracted by residual modules (consist of 1D convolution, BN, ReLU, dropout, and max-pooling). These local features were fed to BiLSTM (composed of forward and backward LSTM) for summarization & finding the global features, which were used by the two dense layer & softmax for classification. The model was tuned with learning rate, dropout, kernel size, and LSTM etc. The model was trained and tested on 6877 and 2954 recordings, respectively. The model performance was compared with ResNet+Flatten, ResNet + GAP, ResNet + GMP, ResNet + LSTM, and CNN + BiLSTM structures. Authors claimed their model to be better than other five structures. Based on 450 test samples authors have computed F1 score of 74.8%, 92%, 88.2%, 88.9%, 78.7%, 85.1%, 78%, and 78% for N, I-AVB, LBBB, RBBB, PAC, PVC, STD, and STE, respectively.

Bonab et al. [105] developed computer-aided diagnostic (CAD) technique based on time-frequency analysis, for extracting the information from ECG signal to detect arrhythmia's. This method includes preprocessing, feature extraction from QRS complex, and classification of time-frequency features. ECG signal is mainly affected by environmental conditions, AC power, power-line noise (50 Hz–60 Hz), and baseline drift. Here, authors have used a lowpass Butterworth filter with a cut-off frequency of 0.1 rad/sample to suppress the effect of noise. This followed DWT-based approach to eliminate the low frequency baseline drift occurred due to breathing. The de-noised ECG was used for finding the features by analyzing the QRS complex from the spectral component. Due to the beat classes and white noise the spectral components were found to be similar. This redundant information were suppressed by signal compression. In this, author have used two-directional

Table 9

Techniques for AF classification from ECG signal.

Sl. No.	Author & Year	Techniques used	Data	Classification	Performance accuracy (%)	Remarks
1	Bashar et al. [61]	*KNN *SVM *RF	*MIMIC III *Wearable armband ECG *Physionet AFPDB	AF vs. PAC/PVC	87.89	Poor performance
2	Czabanski et al. [120]	LSVM	MIT-BIH AF	AF & non-AF	98.86	Limited data
3	Petmezas et al. [121]	*CNN *LSTM	MIT-BIH AF	N, AFIB, AFL, & J	97.87	Limited data
4	Hong et al. [122]	BiLSTM	MIT-BIH	AF, PVC, PAC	92	Poor performance
5	Tutuko et al. [123]	BiLSTM	*QT, Lobachevsky University *Cinc Challenge 2017 China *Physiological Signal Challenge *Local data	P-wave & RR	99.79	Minimum classification

two-dimensional PCA ($2D^2PCA$) for signal compression. The extracted compressed spectral features are classified by 16-layer CNN (main layers are convolution, normalization, ReLU, max-pooling, and softmax). This method has been tested on MIT-BIH arrhythmia dataset that consists of 48 two channel records, having duration of 30 min selected from 24 h recording, and collected from 47 subjects with a sampling rate of 350 Hz [83]. The dataset was recorded from 25 men (age: 32–89 years) and 22 women (age: 23–89 years). 80% (13200 beats) have been used for testing and rest 20% (3301 beats) have been used for training. The performance of this classification method was analyzed by accuracy, sensitivity, specificity, and precision. Authors reported an accuracy of 98.33% on time resolution of 0.05 sec and 18 frequency divisions. This performance can be further improved by using other optimization algorithms.

Chang et al. [98] proposed a four layer bidirectional long short-term memory (LSTM) network to detect 12 types of heart rhythms (such as: AFIB, AFL, APB, BIGEMINY, CHB, EAR, FRAV, NSR, PSVT, SAV, ST, and VPB) from ECG recordings collected from China Medical University Hospital (CMUH). The diagnostic performance of this model results highest accuracy for VPB (i.e., 100%) and lowest accuracy for EAR (i.e., 97.4%). The performance for classifying the diseases may be improved by introducing more layers and larger number of 12-lead ECG signals.

Sharma et al. [113] proposed a hybrid model (consist of Fourier-Bessel (FB) expansion and LSTM) for classifying cardiac arrhythmia from three different databases (such as: MIT-BIH arrhythmia, PhysioNet challenge 2017, and private data collected from Nakshatra Heart and Multi-specialty Hospital Indore, India). This method entails pre-processing (frequency normalization and signal denoising), QRS detection & extraction of RR interval, determination of FB sequences from RR interval, and classification by LSTM. The FB sequence-LSTM layer consist of total 41,301 parameters. The model classified ECG data into normal (N, NSR, LBBB, RBBB, pre-excitation (WPW), isolated QRS-like artifacts and unclassified beats) and arrhythmia (aberrated APB, atrial escape beat, ventricular escape beat, nodal escape beat, AFIB, atrial bigeminy, ventricular trigeminy, atrial flutter, SVT, ventricular flutter, second degree heart block, APB, NPB, PVC, SPB, and non-conducted P wave.). Authors have reported an accuracy of 90.07% for MIT-BIH database alone. The combined data achieved accuracy and F1 score of 80.53% and 79.60%, respectively. This method failed to detect the type of arrhythmias.

Yao et al. [114] proposed an attention-based time-incremental convolutional neural network (ATI-CNN) to exploit the temporal and spatial characteristics of ECG for multi-class arrhythmia (such as: N, AFIB, first-degree atrioventricular block (I-AVB), LBBB, RBBB, PAC, PVC, ST-segment depression (STD), and ST-segment elevation (STE)) detection from the 12-lead ECG signal available in China Physiological Signal Challenge 2018 database. Authors have used CNN (VGGNet) for extracting spatial information and LSTM for temporal information. The CNN consists of 13 convolutional layers and 5 pooling layers in connection with normalization layer and ReLU activation function. Here, two LSTM models are used. It helps in analyzing the varied length

ECG signal along with reduction in dimension. Researchers used two fully connected layers along with hyperbolic tangent function for ATI-CNN. This model can able to identify important segments along with the location of abnormality present in the ECG signal. Authors have trained and tested the model on a server with a Xeon E5 2650 CPU, 128GB memory, and four Titan Xp graphic cards in PyTorch 0.4.1 framework on Ubuntu 16.04 LTS system. This method achieved an average F1 score of 81.2% in classifying 8 types of arrhythmias and sinus rhythm. This approach classified 8 types of arrhythmias and sinus rhythms with an average F1 score of 81.2%.

Chen et al. [115] performed the classification of arrhythmia (such as: AFIB, ventricular bigeminy (B), AFL, pacing rhythm (P), and SBR) and NSR from the ECG recordings (obtained from MIT-BIH arrhythmia database, MIT-BIH NSR database (NSRDB), atrial fibrillation database (AFDB), and physioNet/computing in cardiology challenge 2017 database) by using the 15-layer (CNN with LSTM) network. CNN and LSTM extracts the spatial and time domain features, respectively. The CNN network has six pair of 1D-convolution and 1D-max pooling layers. The model has two LSTM networks. The ECG signal was pre-processed by Daubechies wavelet-6 to overcome baseline drift followed by the classification with CNN and LSTM network. The model was trained with parameters such as: adam optimizer, categorical cross-entropy loss, epoch 60, dropout 0.3, training 80%, and testing 20%. The results were tested with independent-testing-set developed by the authors. They reported accuracy, sensitivity, specificity, and positive predictive value of 99.32%, 97.75%, 99.51%, and 97.66%, respectively. For both N and AFIB, this system achieved an average accuracy of 97.15 %.

Ihsanto et al. [116] and Sanamdkar et al. [117] have used depth-wise separable convolutional (DSC) neural network and general sparsed neural network (GSNN), respectively for classifying sixteen classes cardiac arrhythmia (N, LBB, RBB, PVC, paced, APC, fusion of paced & N, fusion of ventricular & N, VF, nodal escape, non-conducted P-wave, AAP, ventricular escape, nodal premature, atrial escape, and unclassified) ECG beats from MIT-BIH database. In [116] authors have used four stages for ECG classification (such as: beat detection & segmentation, preprocessing, feature extraction, and classification). At first, beat and QRS are detected based on gradient amplitude, wavelet transform, and duration of ECG signal. The segmented beats are used for classification by the DSC neural network. Here, authors used three beat sizes (such as: 64, 128, and 256 samples) from the original sizes of 256. The output of different CNN's are ensembled using average method. The depth-wise separable CNN network consists of 21 layers (input, seven separable 1D convolution, four BN, four activation, three 1D convolution, one flattens and one dense) having 11,317 trainable parameters. Authors have considered 110,157 ECG beats (grouped into 16 classes) for the study, out of which 23,999 and 86,158 number of beats were used for training and testing, respectively. Authors have replicated 110,157 number of ECG beats by using zero padding. This system achieved the sensitivity, specificity, positive predictivity, and accuracy of 99.03%, 99.94%, 99.03%, and 99.88%, respectively. In [117] authors have used noise removal (by mean subtraction and 10-point moving low pass

filter), feature extraction/QRS recognition (by Pan and Tompkin's scheme for finding the diversion in QRS beat), and classification by GSNN. The cut-off frequency of the filter was set at 5–15 Hz. The filtered signal was used for finding the 9-time-domain, 9-frequency-domain, and 2-higher-level features (i.e., RR interval and wavelet energy). These extracted features were fed to the GSNN model, which used a quadratic loss function for classification. The model achieved an accuracy, precision, recall, F1 score, and time complexity of 98%, 98%, 98%, 98%, and 14.50 s, respectively on MIT-BIH arrhythmia dataset. This method performed better compared to ANN, SVM linear, and SVM-RBF.

Mohonta et al. [118] applied a deep learning model on the coefficients obtained by applying continuous wavelet transform (CWT) on ECG signals, for automatic arrhythmia detection. This method comprised of three parts such as: automatic beat segmentation, spectral transformation, and CNN based DL model for beat classification. The CWT identifies ECG beats by splitting the ECG signals into small duration consists of 81 samples. These segments are mapped into images (by using FFT, CWT gray-scale, STFT, and CWT RGB techniques) for classification. Here, authors classified the heart beats present in MIT-BIH database into five different types such as: normal, LBBB, RBBB, atrial premature, and PVC. This method achieved an average sensitivity, specificity, and accuracy of 98.87%, 99.85%, and 99.65%, respectively.

Some of the researchers have used the arrhythmia classification based on the features. Few researchers have detected the various diseases such as atrial fibrillation. A few of the techniques for AF have been discussed below and systematically outlined in Table 9.

Bashar et al. [61] used irregular information of the ECG signal to detect AF from PAC/PVC by using density Poincare plot (derived from difference of heart rate (DHR)) based ML (such as: KNN, SVM, and RF) techniques. This method consist of preprocessing & Poincare plot creation, extraction & selection of features, and classification. In preprocessing, ECG signals are segmented into 2-min non-overlapping segments for filtering and detection of QRS complex/R-peak by VERB algorithm [124]. From the enhanced R-peak density Poincare plot [125, 126] was generated by plotting next DHR beat vs. present DHR beat. The Poincare plot has a regular pattern (i.e., like a kite) for PAC and PVC. Whereas, the plot exhibit random behavior for AF or irregular variation of the heart rate (HR). From the Poincare plot features (such as: moment based, template correlation, Zernike moments, DWT, and Hough transform) were extracted. From the pool of raw features countable prominent-features were selected based on classification infinite latent feature selection (ILFS) algorithm [127]. In this approach, authors have calculated 79 (13-statistical moments, 14-correlation with templates, 14-Zernike moments, 24-DWT, and 14-standard Hough transform) features for performing the classification by KNN, SVM, and RF classifiers. These features classify AF vs. PAC/PVC for different segments and subjects. Out of 79 features 10 (1-Zernike moments, 5-wavelet, 4-correlation) features are ranked as per the assigned weight. This was performed by k(10)-fold cross validation. Out of next 10-ranked-features 9-features were common in 10 folds and was used for subject wise classification. Classification was performed by segment wise k-fold cross validation and subject wise cross validation. In segment wise classification KNN, linear-SVM, RBF-SVM, and RF obtained an accuracy of 87.89%, 93.09%, 95.27%, and 94.79%, respectively by considering 10-features. By using all 79-features, KNN, linear-SVM, RBF-SVM, and RF achieved an accuracy of 76.16%, 96.48%, 97.45%, and 97.09%, respectively. The overall accuracy was found to be the highest in SVM (10-features) and RF (79-features). This method was tested on MIMIC III waveform subset [128], wearable armband ECG database [129], and the Physionet AFPDB databases [130].

Czabanski et al. [120] used sixteen features by Lagrangian SVM (LSVM) for classification of heartbeats into AF and non-AF. Mainly, authors have used the heart irregularity features for assessment of AF. Those features were mean/median value of HR, standard deviation of instantaneous HR, RMSE of successive RR differences, Yeh's index, Zugaib's variability, Huey's index, and Haan's index etc. LSVM was used

for classification, which simultaneously improves the efficiency by reducing the complexity (due to the linear convergent algorithm instead of quadratic programming). This model was tested on 25 ECG signals obtained from MIT-BIH AF database. Authors reported sensitivity, positive predictive value, and classification accuracy of 98.94%, 98.39%, and 98.86%, respectively.

Atrial fibrillation (AFIB) classification from ECG signal was performed by various authors from MIT-BIH AFIB database using supervised, unsupervised, and reinforcement learning. Traditional Machine learning (ML) approaches were used by Kennedy et al. [49,131–134]. These documents have used RF [135–137], KNN [137–139], SVM [135, 137,138,140,141], multi-layer perceptron [142–145], and affine normalization. These methods reported low specificity. Xu et al. [146], Faust et al. [37], Andersen et al. [36], and Czabanski et al. [120] have used DL based approaches. Few of these techniques didn't perform well compared to traditional methods. It happened due to less number of annotated ECG data. The limitations of DL approaches were overcome by Petmezas et al. [121] using a novel hybrid neural model (combination of CNN and LSTM). Here, authors have classified AF into four ECG rhythm types (such as: N, AFIB, AFL, and AV junctional rhythm (J)). At first, noise from the data was removed by augmentation. This overcomes the data imbalance problem. The augmented data were fed to the CNN followed by the LSTM (consists of LSTM, flatten, fully connected, dropout, and o/p layer). Authors reported sensitivity and specificity of 97.87% and 99.29%, respectively.

Hong et al. [122] used deep learning model (consists of 1D convolution, followed by batch normalization, two BiLSTM networks for encoder, one BiLSTM for decoder, and softmax) layers for depicting the ECG features (P, QRS, T waves, and RR interval) for identifying AF, PVC, and PAC from the ECG signals. Authors used a sliding window with 3-RR intervals to determine the existence of P-wave for identifying AF and non-AF. Authors reported the highest sensitivity and specificity of 100%, 99% for QRS wave. Furthermore, this model can be applicable for different ECG's interpretations.

Tutuko et al. [123] identified AF based on P-wave and RR irregularities from the single lead ECG signal. This technique consists of preprocessing (noise removal, segmentation of ECG morphology, splitting the dataset), feature extraction (performed by 4 convolutional CNN without max-pooling layer), classification of normal condition by BiLSTM (based on ECG morphology, such as: P-wave, QRS complex, T-wave, and isoelectric line). Authors have detected the ECG to be arrhythmia based on P-wave (present/absent) and irregular rhythm. Authors have used five different databases (such as: QT, Lobachevsky University, Cinc Challenge 2017, China Physiological Signal Challenge 2018, ECG recordings from Mohammad Hoesin Indonesian Hospital) for analysis. Here, 90% and 10% of the collected signals have been used for training and testing process, respectively. This system achieved sensitivity, precision, specificity, accuracy, and F1 score of 98.91%, 99.01%, 99.79%, 99.79%, and 98.96%, respectively.

Some of the researchers identified various heart disease using different techniques. Few researchers have identified the heart diseases from ECG signal classification techniques are discussed below and important information are outlined in Table 8.

Hasan and Bhattacharjee [103] have used empirical mode decomposition (EMD) and intrinsic mode functions (IMFs) to obtain the modified ECG signal from the original ECG for classification of multiple heart diseases (such as: bundle branch block (BBB), valvular heart disease, myocarditis, dysrhythmia, myocardial infarction, cardiomyopathy, sinus bradycardia, AFIB, transient ischemic attack, and sinus node dysfunction etc). EMD in time domain provides intrinsic features by using IMFs that help in discarding the noise. EMD computes the IMF signal by subtracting the mean (i.e., obtained by considering the upper and lower envelope corresponding to the maxima and minima of the signal, respectively) from the original signal. Generation of IMFs were iterated till a threshold value was achieved. This value of IMF was subtracted from the original ECG signal to obtain the residual signal.

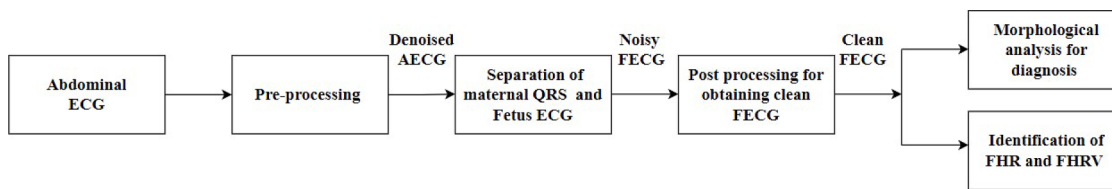


Fig. 6. Block diagram for obtaining fetal ECG.

This total process was repeated to get multiple number of IMFs. Authors have calculated six IMFs, out of which the first three IMFs were used to construct the modified ECG signal. This altered ECG was used by a 13 layers deep CNN network (consisted of input layer, five convolution layer, three fully connected layer, and softmax layer etc.) for classification. Here, authors have classified the ECG signals into 7, 4, and 9 classes for PTB, MIT-BIH, and St. Peterberg databases, respectively. Authors have reported an accuracy of 98.24% for PTB, 97.70% for MIT-BIH, and 99.71% in the St. Peterberg databases. The performance for some databases need to be improved.

Oktivasari et al. [119] developed a real-time system with three leads (LA, RA, and LL) to detect MI by analyzing the ST-interval and T wave. To remove the noises from the real time data authors used band-pass filter (cut off frequency: 0.01–120 Hz) and 8-level discrete wavelet transform (DWT) with Daubechies mother wavelet. Authors extracted various features such as: mean heart rate (HR), HR standard, mean QRS amplitude, standard QRS amplitude, mean QRS time, standard QRS time, mean PR interval, standard PR interval, mean QT interval, standard QT interval, mean ST level, standard ST level, T level onset, and T level offset for MI identification by fuzzy logic. The model was tested with EDB for improvisation. Authors have not validated their results for real time ECG recordings by the cardiologist.

Panganiban et al. [2] developed a DL based ECG diagnostic support

system (i.e., EDSS, which consists of wearable HealthyPiV3 biosensors, Raspberry Pi board, microcontroller, display, battery, Wi-Fi unit, and laptop etc.) for ECG arrhythmia classification to detect heart related disorders (such as: atrial fibrillation, bradycardia, tachycardia, and BBB). This approach pre-processed (removal of noise by splitting the signal to 10 s duration) the data prior to converting into spectrograms for analysis by deep CNN. The DL network was built by Inception v3 model that used cross-entropy loss function for optimization. Training and testing of the model was performed with 80% and 20% of the data (collected from PAF prediction challenge database for AF, PTB diagnostic ECG database for BBB, challenge 2015 training set for bradycardia, and Fantasia & PAF prediction challenge database for healthy signals), respectively. The weights are used by the diagnosis system for classifying the signal captured by the sensors. In this work, authors have performed the classification by two ways: i.e., binary (normal vs. abnormal classes) and quinary (normal and 4 types of arrhythmias). Quinary classification achieved an average accuracy, specificity, sensitivity, positive predictive value, and F1 score of 98.73%, 99.21%, 96.83%, 96.85%, and 96.83%, respectively. Whereas, in binary classification the above discussed performances were found to be 97.33%, 96.60%, 97.61%, 97.06%, and 97.33%.

By analyzing different databases, evaluation criteria for ECG and its feature extraction, noise removal, beat classification, identifying &

Table 10
Techniques for detecting fetal heart abnormalities from AECG.

S. No.	Author & Year [Reference]	Techniques used	Data	Purpose (or) Identification	Performance accuracy (%)	Remarks
1	Zhang et al. [158]	* ADT * ICA	* PhysioNet/Computing in Cardiology Challenge 2013 * Real-time data	* FHR * FECG	97.40	Testing was carried out on few subjects
2	Mohebbian et al. [147]	Cycle GAN	* A&D FECG, * NIFECG, * NI-FECG challenge * Simulated	* MECG * Scalp FECG	-	Invasive method was used
3	Ghonchi et al. [159]	* AE (dual attention module) * BiLSTM	* NIFECG1 * NIFECG2 * A&D FECG	* Fetal QRS * FECG extraction	* NIFECG1 - 97.83 * NIFECG2 - 93.53	Low SNR for weak FECG
4	Dhas et al. [160]	Adaptive FIR- filter	* Synthetic * Daisy	* MECG * Fetal R-peak	94.64	Low performance
5	Anisha et al. [161]	* SVM * SPWVD	* NIFECG * ADFECG * PhysioNet	Fetus cardiac abnormalities	97	Low accuracy for NIFECG
6	Barnova et al. [162]	* ICA * RLS * EEMD	* FECGDARHA * PhysioNet Challenge 2013	* Fetal QRS, * FECG * FHR * Fetal ST segment analysis	80	Less accuracy & more complex
7	Gurve et al. [163]	* NMF * ICA * PCA	* Silesia A&D FECG * PhysioNet challenge	* FECG * MECG * Noises	-	Fetal QRS detection can be improved in optimizing NMF
8	Yuan et al. [164]	* FastICA * SE	Daisy	* FECG * FHR * ST segment	-	* No real time data * Noisy ST segment
9	Yang et al. [165]	* SCG * GCG * fCTG * RMSE	Real time data	FHR	82.9	Less accuracy
10	Sengan et al. [166]	ARVNet	Local hospital	* FCT * FCRD	99	Less data

classifying arrhythmia, and heart disease detection, new approaches for analyzing ECG was developed and discussed in the following Section.

4. Recent strategies for analyzing ECG & identifying CVDs

By monitoring the ECG signal, researchers have developed various techniques and methods for identifying and classifying heart diseases. Despite this, there are some drawbacks in data usage, performance analysis, disease detection, and so on. To address this issues the models are improved. In few cases, other medical signals (fetus ECG, fundus image, and EEG) are analyzed to understand the diagnostic information available in ECG. This helps to identify the heart related diseases and the relation of heart signals with other medical signals or body parts (such as, eye, brain, and fetus). ECG signal also help in identifying the other related diseases such as sleep apnea, retinal related disease etc. Few of them are discussed below.

4.1. Fetus ECG

Complications during perinatal conditions leads to approximately 40% of perinatal and maternal death, worldwide. So monitoring the health condition of fetus from fetal heart rate (FHR) is a prime concern for the clinicians. Fetal ECG monitoring analysis provides crucial diagnostic information about fetus health (rhythmic, morphology, & fetal heart disease). This can be recorded by invasive- and non-invasive manner. In invasive procedure, electrodes are kept on fetus scalp for collecting fetal scalp ECG (SECG). SECG provides accurate heart rate and may cause infection. Non-invasive procedures are secure because the electrodes are placed on mothers abdomen [147]. This is called abdominal ECG (AECG). Clinicians have used Avalon and AN24 devices to capture AECG. This procedures for capturing AECG lags far behind in processing, monitoring, and analyzing compared to the standard ECG recording systems. The main disadvantages of this approach are lower SNR and greater interference with mother ECG (MECG).

Despite the rapid advancements in clinical ECG processing, monitoring and analysis systems, morphological analysis of fetal ECG (FECG) signals lags far behind and requires special attention. Extraction of FECG from MECG has numerous challenges (such as: 1. Low amplitude of FECG compared to MECG, 2. Overlapping of R-waves, 3. Maternal muscle-, uterine-, & fetal-movement, 4. Respiration activity, and 5. Numerous types of noises such as electro surgical, BW, & PLI). The primary challenge with this method leads to detection of FECG for producing less SNR due to the dominant nature of MECG, and the interference of this with MECG. Researchers in literature use a standard procedure (represented in Fig. 6) for detecting FECG from AECG. Because of the lower amplitude of the FECG, intersection of the R wave, and multiple sources of noise, makes extracting the FECG signal from MECG is time-consuming and inconvenient. Researchers have used adaptive filtering (linear, non-linear, and Kalman), signal decomposition (SVD, PCA, ICA, wavelet, non-negative-matrix factorization (NMF), EMD, tuning, adaptive filtration, alignment, and noise modeling), template subtraction, and hybrid-techniques for extraction of FECG signal from MECG. The non-linear approaches are ANN, ML, and DL. Many researchers in literature use a standard procedure (represented in Fig. 6) for detecting FECG from MECG. Few of the techniques for fetus ECG detection and identification have been discussed below and shown in Table 10. In literature, researchers used Daisy- [148], NIFECGC- [149, 150], ADFECG- [150,151], PhysioNet- [152,153], FECGSYN- [154, 155], NIFEA- [156], and NIMFEGCD- [157] databases.

Zhang et al. [158] developed a light weight personal FECG monitoring system (consists of bio-compatible electrode along with noise removal amplification, transmission and storage circuits) to record AECG of the pregnant woman along with MECG and FECG. This technique provided analyses of AECG signal along with localization of maternal QRS complex and fetal QRS complex. This device helps in capturing the AECG signal in different positions such as: supine, sitting,

and standing. The data acquisition module is the first block in the monitoring system which provides low noise, high input impedance, high CNRR, and high resolution digital output. This digital output was subjected to preprocessing (baseline wander cancellation and removal of power line interference) followed by elimination of maternal QRS complex (by ICA) and detection of FECG morphology (RR-interval and R-peak location). Authors combined adaptive dual threshold (ADT) and ICA algorithm to separate the FECG and MECG signals. The separated MECG signal was subtracted from AECG to obtain residual FECG. The noise associated with the residual signal was suppressed by wavelet adaptive thresholding technique. Here, authors used JADE algorithm to improve the quality of residual signal and to provide noticeable R-peaks. This module was tested on three different subjects in different postures at hospitals of NMU China and achieved an accuracy of 97.40%. Authors used Bland–Altman graph to predict the consistency of data.

Mohebbian et al. [147] used a sliding window on AECG for normalization, filtering, and feeding the proposed ECG to the cycle GAN network. In this case, FECG signal was extracted along with the fetal QRS and RR-interval. Authors used invasive (multi channel fetal scalp recordings obtained from A&D FECG database from PhysioNet) and non-invasive (NI) FECG, and NIFCEG challenge database along with simulated signals generated by FECGSYN toolbox. The recordings were preprocessed to eliminate the artifacts and noise by a band pass filter having the frequency range of (1100 Hz). Narrow bandpass filter loses the information so, Savitzky-Golay filter was used with a sliding window. This signal was normalized prior to applying to the attention based cycle GAN. This method performance was computed by extracted signal quality and QRS detection accuracy. Fetal QRS estimation attained F1 score of 99.6%, 99.7%, and 99.33% for the NIFECG, A&D FECG, and NIFECG challenge datasets, respectively. Similar work was carried out by Ghonchi et al. [159] by proposing auto-encoder (AE) equipped with dual attention mechanism made of squeeze & excitation and channel wise modules to obtain the exact FECG signal from a single channel AECG. The model consists of preprocessing (i.e., filtered by Butterworth band pass filter having frequency 1–100 Hz, segmented by non overlapping window of 200 samples), AE for signal compression followed by BiLSTM network for FECG extraction. The attention module aided learning to identify FECG hidden within AECG. This work was tested on three datasets (A&D FECG, NI-FECG1, and NI-FECG2) collected from PhysioNet. For the NIFECG1 database, this approach achieved an accuracy of $93.53 \pm 4.97\%$ with a window size of 100 for fetal-QRS detection. This accuracy was improved with a window size, and was reaching a maximum of $97.83 \pm 2.41\%$ for a window size of 500. When the window size went up from 100 to 500, the overall training time increased from 0.33 to 1.63 s. For NIFECG2 dataset, the recorded accuracy was $88.54 \pm 11.17\%$. This method failed to detect too weak fetal-QRS signal. The model must be optimized for real-time applications.

Dhas et al. [160] developed a module consists of adaptive FIR filter to extract the FECG from recorded AECG. In this case, the adaptive filter used past-samples (taken from MECG) and future-samples (taken from AECG) for improving FECG extraction. This technique composed of FIR filter & its weight updation, computation of error signal from AECG & thorax-ECG, and extraction of FECG. This was implemented on Virtex-VC707-FPGA board and evaluated the module performance by throughput, power consumption, and resource utilization. PRMS-difference, o/p-SNR, RMSE, and fetal-R-peak-detection-accuracy were used to evaluate the performance of adaptive FIR filter. The authors extracted FECG from simulated and Daisy datasets using varying filter lengths. The filtering approach reported PSNR-difference, SNR, and RMSE 83.04%, 8.52 db, and 0.0208, respectively for 38-taps having word length of 24. The aforementioned method used a maximum power of 1.287 W at 139.47 MHz clock frequency. On the Daisy dataset, the accuracy of this approach in detecting fetal R-peaks was calculated to be 94.64%.

Anisha et al. [161] detected fetus cardiac abnormalities from AECG

signals. This method consists of AECG acquisition, preprocessing, extraction of FECG, post processing, FE, and classification by SVM. Acquisition of AECG was made by a non-invasive procedure. The AECG signal was preprocessed to eliminate maternal interference, impulse in noise, PLI, and BW. The preprocessed signal was subjected to FECG extraction for MECG detection and its cancellation followed by post-processing. MECG detection consists of Fast-ICA followed by signal correspondence algorithm and smoothed Pseudo Wigner–Ville distribution (SPWVD). Fast-ICA separated MECG from FECG components. This followed signal correspondence technique to recognize various heart beats and fiducial locations. SPWVD was used to examine AECG in the time and frequency domains in order to uncover hidden information in the signal and interpret this diagnostic details. In frequency domain, AECG found maternal-R-peak, QRS-offset, and QRS-onset. AECG (excluding MECG) was enhanced in the post-processing stage by the FIR filter (consisting of a low pass filter followed by a high pass filter) to improve the FECG. From the enhanced FECG, FHR-, FECG-features were extracted and fed to the SVM classifier for detecting fetal cardiac abnormalities. This technique was experimented on NIFECG-, abdominal-and-direct (AD)-FECG-, and PhysioNet-databases and performance metrics were evaluated for maternal interference detection, FECG extraction, FHR estimation, FECG-FE, and classification. Authors reported the highest accuracy of 97% for detection of FHR and FECG from ADFECG database.

Barnova et al. [162] used ICA, recursive least squares (RLS), and ensemble EMD (EEMD) to extract NI-FECG signal from AECG. Authors used FastICA (base on kurtosis or maximum-likelihood or maximum-negentropy) to extract independent source components. ICA alone couldn't identify FECG, but enhanced MECG and AECG. The above drawback was eliminated by RLS (used adaptive approach to minimize the difference between true-o/p and real-o/p). This aided in the extraction of superior FECG in the presence of a small quantity of MECG, which were further smoothed by EEMD (used to decompose the non stationary ECG signal into intrinsic mode functions (IMF) for extracting the peaks and valleys to compute residual signals). This technique was experimented on FECG A&D with reference heartbeats annotations (FECGDARHA)- and PhysioNet Challenge 2013-databases for computation of fetal QRS, FECG, FHR, & fetal ST segment and obtained an overall accuracy of 80%.

Gurve et al. [163] separated MECG, FECG, and noises by using NMF, ICA, and PCA. At first, AECG signal was filtered using a high pass Butterworth filter (cutoff frequency of 2 KHz), followed by a notch filter. The filtered ECG was compressed using compressive sensing (CS) to improve resilience, reduce power consumption, and simplify hardware implementation. The compressed signal was decomposed to non negative matrices (basis-, activation-matrix) having rank R by NMF (using STFT). In this case, the rank of NMF matrices ranged from 3 to 6. Rank 4 matrices provided the highest QRS. Authors performed normalization to dominate the activation related to FECG. This followed the inverse-STFT to obtain FECG, MECG, and noises. This work was experimented on Silesia for A&D FECG-, and Physionet challenge-databases. Here, authors reported the highest average sensitivity, precision, and F1 score of 96.5%, 97%, and 96.75%, respectively for recovered signals by NMF decomposition with a compression ratio of 75%.

Yuan et al. [164] designed a wearable low power FECG monitoring system with Android smartphone to detect FECG and FHR in real time. This system consisted of AECG data acquisition, FECG extraction, transmission, and monitoring. AECG data was collected by three leads with four electrodes. The hardware for AECG collector consists of signal acquisition (by ADS1293), Cypress semiconductor processor (CY8C4247), Bluetooth module 4.1, and power supply unit. The AECG signal was fed for extraction of FHR. The extraction block consists of preprocessing (elimination of BW, mean subtraction, and whitening) followed by FastICA and computation of entropy (identify the randomness). The AECG collector transmitted the signals to smartphone through Bluetooth for separation & displaying of FECG and FHR. This

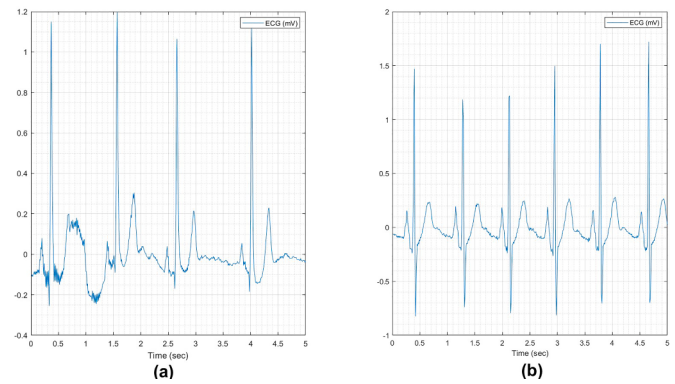


Fig. 7. ECG Signals: (a) normal, (b) during sleep apnea.

system helped in remote diagnosis about the fetus. Authors used Daisy database for validating the algorithm and reported an average entropy of 1.22, 0.29, and 0.73 for FECG, AECG, and MECG, respectively. Characteristics of the system were represented by input voltage (403mV), input resistance (500 MΩ), CMRR (95 dB), and minimum detectable signal (2 μV) etc.

Yang et al. [165] used 3-sensors (capable for measuring inertia units, such as accelerometer and gyroscopes) along with the fetal cardiotocography (FCTG) probe on the abdomen of the pregnant woman for detecting FHR from the signals of seismo- and gyro-cardiogram (SCG and GCG). Sensor-1 was placed upper part, whereas the other two (sensor-2 and sensor-3) were placed at the lower part of abdomen. Accelerometer and gyroscopes measure SCG and GCG, signals respectively. These signals were collected from 10-pregnant women for five minutes for each positions (supine, sitting, and standing) at the Department of Obstetrics and Gynecology, New York University (NYU). The methodology for FHR detection consisted of pre filtering (band pass and IIR filter), followed by signal fusion in frequency domain (by CWT using Morse mother wavelet), and FHR extraction (cepstrum approach). Cepstrum was applied to the spectrum of the fused signal. Cepstrum computed the inverse FT of real part of the logarithm of FT of the signal in time domain. FHR computed from the periodicity of the spectrum (i.e., from the peaks). Authors analyzed the performance of this approach by Bland–Altman analysis. Recorded FCTG were compared with the evaluated values of FHR by SCG & GCG by RMSE and absolute percentage error (APE). Highest RMSE value was recorded in supine position. This work provided satisfactory results for FCTG compared to FECG. This technique failed to eliminate motion artifacts of both the fetus and mother. The sensors need improvement for better contact and acquisition.

Like AECG, cardiac images are used to identify the diagnostics information of the fetal heart in clinic. Monitoring the fetus heart abnormalities by experienced sonographers is challenging. So, these images are used in computer vision to analyze the structure and function of fetal heart. Many researchers developed various conventional and AI strategies to analyze and forecast the growth of fetal heart and its function. In DL, researchers used 2D U-Net [167], 3D U-Net [168], 3D V-Net [169], and 2D segment [170] for segmentation of the heart and identifying structural heart diseases (chamber-size, valve mobility, pericardial effusion and fetal cardiac tumor (FCT)). Few of the techniques for identifying the structural disorders of heart are discussed in the following paragraph.

Sengan et al. [166] developed attention-residual V-Net architecture (ARVNet) to segment the fetal cardiac rhabdomyomas (FCRD) from the ultra sound images to study the abnormalities in LV, RA, LA, and tricuspid valve. The network used cross entropy loss function, dice optimization, and hybrid loss function. This work was experimented on the cardiac heart images collected from Selvam Hospital Melapalayam, Tirunelveli, Tamil Nadu, India and reported an overall accuracy of 99%

Table 11

Sleep apnea detection methods based on single-lead ECG signal.

Sl. No.	Authors & Year	Database	ECG used	Framework	Features	Methodology	Accuracy (%)	Remarks
1	Lin et al. [171]	* Physionet apnea * NCKU hospital	HRV, EDR	ML	* CWT * Bag-of- features	* Preprocessing * FE * Classification (SVM, EL, KNN) * Validation	* BoF features: # 90.5–10 s # 91.4–60 s	Poor performance
2	Qin et al. [172]	* Apnea ECG * Sun-yat-sen hospital	RR-interval by Christov algorithm	DL	Representation learning (RL)	* Preprocessing * Classification (RL based-1D -CNN, Bi-GRU)	91.9	Accuracy need to be improved
3	Yeh et al. [173]	MIT Physionet	Pre processed ECG	DL	-	* 15 subband decomposed signals * 1D-CNN	* 100/ recording * 85.8/minute	Limited data
4	Feng et al. [174]	Computers in Cardiology 2000 Challenge	Pre processed ECG	DL	* Frequential stack sparse auto-encoder (FSAE)	* Time dependent cost specific classification (HNN, metacost algorithm)	85.1/segment	Poor performance
5	Sheta et al. [175]	Physionet's CinC challenge -2000	Pre processed ECG	ML (SVM, LDC, decision tree, LDA, KNN, LR, Naive Bayes, boosted trees) & DL	Average HR, mean RR, RMSE of RR, number of R-peak, SD of RR & HR, PSD, pNN50	* Noise removal by noise filter * FE * Classification	86.25	DL performs better than ML
6	Chang et al. [98]	MIT PhysioNet Apnea-ECG	Pre processed ECG	DL	-	* Preprocessing (BP filtering, standardizing) * Classification (1D deep CNN)	* 87.9/minute * 97.1/ recording	Less data
7	Zarei et al. [176]	* Physionet apnea-ECG * Fantasia	ECG- derived respiration (EDR) HRV	ML (KNN, RUSBoost, gentleBoost, SubspaceKNN, ANN, & SVM)	* Alphabet entropy * Fuzzy * Sample entropy	* Preprocessing * FE & selection * Classification	* 93.26/ segment * 100/ recording	SA types not defined
8	Bozkurt et al. [177]	*Sakarya Hendek public hospital	HRV Pre processed ECG	Hybrid ML	* HRV * ECG * QRS	* Preprocessing (filtering by Notch, IIR, & MA filter) * FE (Fisher, PCA) * Classification (DT, KNN, SVM, Ensemble)	*82.11 for 3 features *85.12 for 13 features	Less Accuracy
9	Singh et al. [178]	* Apnea ECG * University college Dublin (UCD) * Physionet challenge	EDR Heartbeat interval (HBI)	DL	Statistical (mean, SD)	* Segmentation (EDR, HBI) * FE * Classification (Stack auto- encoder based DNN, SVM)	* Apnea ECG - 94.3 * UCD - 72	Poor performance
10	Zarei et al. [179]	* Physionet Apnea-ECG * UCD	Pre processed	ML	ApEn, FE, CCE, IQR, RP, and poincare plot	* Preprocessing * WT, FE * OSA Classification * Feature selection	Physionet ECG - 92.98 UCD - 93.70	Poor performance

approximately for different views.

4.2. Sleep apnea

Sleep apnea is a sleeping disorder characterized by intermittent or insufficient breathing while sleeping. Despite the fact that sleep apnea is very common with people in their early fifties. The majority of cases remain undiagnosed due to high medical costs. Sleep irregularities can be detected and subjectively classified using electroencephalography (EEG), electrooculography (EOG), electromyography (EMG), and polysomnography (PSG). Analyzing the asymmetrical RR intervals from the ECG signal can effectively identify sleep apnea. Deep neural networks based on LSTM and BiLSTM can detect sleep apnea from ECG signals. BiLSTM outperforms LSTM because it can determine optimal weights based on both forward and backward learning. The model's effectiveness is assessed using an ECG signal from the Physionet database. Classification accuracy is computed for various hyper parameters. This technique achieved an overall accuracy of 100% with rmsprop optimizer, 20 epoch, and learning rate of 0.01.

Appearance of R-wave magnitude during sleep apnea is shown in Fig. 7. By analyzing the R-wave from ECG signal, the sleep apnea can be predicted earlier. Setiawan and Lin [180] analyzed different sleep apnea detection methods and represented in Table 11. Author proposed a sleep

apnea detection algorithm that uses a DL framework based on 1D and 2D deep CNN with EMD for a preprocessed ECG signal to differentiate between normal and apnea happenings. The EMD is ideal for extracting essential components that are specific to the underlying biological or physiological processes. Authors validated their findings using night ECG recordings from 33 subjects with an average apnea-hypopnea index (AHI) of 30.23/h from the PhysioNet Apnea-ECG database (PAED). The raw ECG signal was normalized and filtered using the FIR band pass filter during preprocessing. To generate several features, the pre-processed ECG signal was degraded using EMD technique. Several important created features were chosen using neighborhood component analysis (NCA). This method with segment-level classification provided accuracy, sensitivity, and specificity of 93.8%, 94.9%, and 92.7%, respectively based on 5-fold cross-validation. Whereas subject-level classification provided accuracy, sensitivity, and specificity 83.5%, 75.9%, and 88.7%, respectively.

4.3. Real time data

Analyzing real time ECG data from the subjects can provide accurate and instant information about the heart conditions. In this approach, the original data are collected by wireless sensors and wearable battery-powered smart devices, which are integrated with mobile phones,

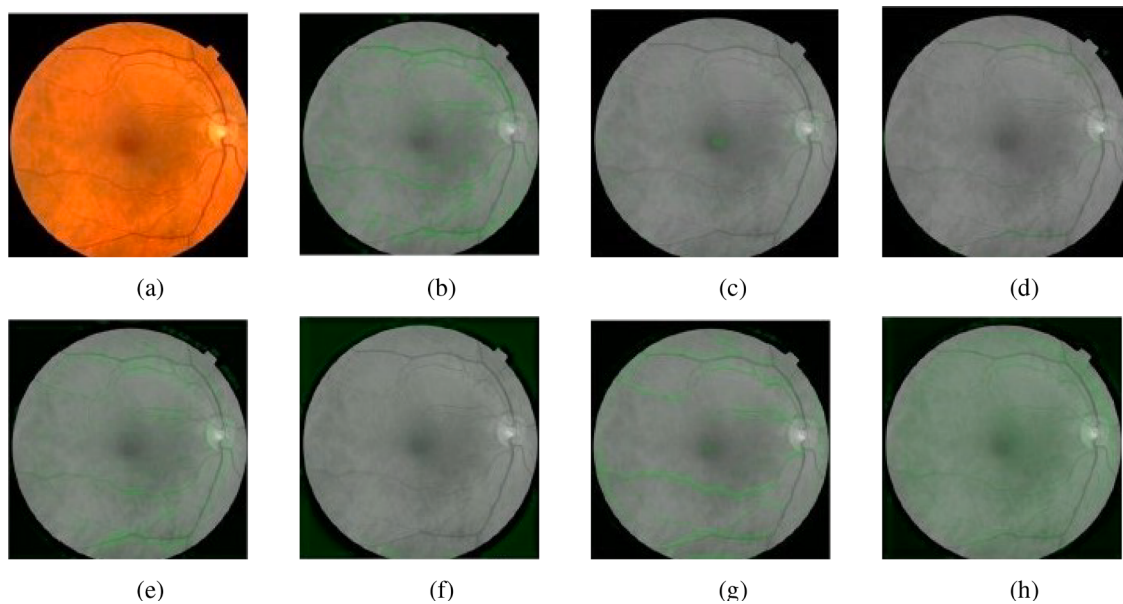


Fig. 8. Appearance of retina in different diseases conditions [189] : (a) Sample color retinal image taken from the UK Biobank dataset. The remaining images are black and white versions of the original retinal image. The soft attention heat map superimposed in green for every prediction as follows: (b) age, (c) gender, (d) smoker or not, (e) diabetic condition, (f) BMI, (g) systolic blood pressure (SBP), and (h) diastolic blood pressure (DBP) Attention maps for a single image of retinal fundus. (For interpretation of the references to color in this figure legend, the reader is referred to the web version of this article.)

smartwatches, ePatch, and wearable handheld monitoring devices. The interconnection of these devices provide continuous track on ECG signals by monitoring QRS complex and other ECG characteristics to improve real-time monitoring, detection, and treatment of various CVDs. Few of the devices used for ECG analysis are Holter monitor devices, relative energy based wearable R-peak detection (REWARD), and wearable sensors.

Wearable armband ECG monitoring system uses different channels (3 ECG channels, 1 EMG channel, and 1 tri-axial accelerometer signals) for recording heart signals for a long period of time to analyze the CVDs without any side effects (dry electrodes and skin irritation). This device produces noise during acquisition and can be minimized by PCA and NLMS. The noise free ECG signal fed into SVM classifier having radial basis function (RBF) for classification. Hanssen et al., used SVM-RBF classifier to compute HR along with classical parameters (such as: SDNN, RMSSD, and powers at low and high frequency bands) from the ECG recording obtained by a armband recorder placed over 16 volunteers. These parameters obtained by SVM-RBF and Holter method were found to be of same value.

Orlandic et al. [181] used REWARD algorithm to detect R-peak from the real-time ECG based on non linear filtering method (Relative-Energy (Rel-En)). Uchaipichat et al. [8] used a holter monitoring for identifying MI from the ST-episode. Authors used European ST-T database from Physionet and achieved the sensitivity of 91.37%. They have used a time frequency-based wavelet transform method to improve MI detection. Marston et al. [182] employed wearable stand-alone devices capable of measuring the electrical activity of the heart via ECG in order to detect cardiac arrhythmias associated with palpitations. Zenicor Medical Systems AB Sweden created the Zenicor mobile ECG device which consist of two electrodes for capturing ECG recordings for 30 s duration from the patient's thumb. This device works with a web-based service (that allows to analyze, interpret, present, process, and save ECG recordings) for identifying CVDs. Saadatnejad et al. [183] proposed a wearable device to capture the ECG and developed a wavelet transform based LSTM RNN algorithm for CVD diagnosis. Miao et al. [184] proposed a wearable, low-power perspective ECG monitoring system (consists of reaction sensors and self designed ECG sensors) housed in smartphone. The completely integrated analogue front-end (AFE), commercial

microcontrol unit (MCU), secure digital (SD) card, and Bluetooth module compose the wearable ECG sensor. This system identifies arrhythmia diagnosis from abnormal ECG patterns in various activities.

4.4. CVDs identified from retina

CVDs can also be identified from the two-dimensional pictorial representation of the rear part of the human eye i.e., the fundus image (which is captured non-invasively by a special camera known as a fundus camera). The retina consists of the macula and fovea (contain the highest concentration of cones and are responsible for bright vision), optic disc (known as blind spot and contains the retinal nerve fibres), and blood vessels (help in nourishing the retina) [185]. Retinal structures are affected due to the progression of diabetes and hypertension. Different features (such as: microaneurysms, exudate, and hemorrhage) appear/develop over the retina due to the complication of diabetics. These affect the vision [186]. An increase in intraocular pressure causes an alteration in the structure (i.e., increases cup size and reduces the rim) of the optic disc (OD). This leads to unrecoverable damage of retinal nerve fibres and causes peripheral vision loss (i.e., glaucoma) [187]. Hypertension, hyperglycemia, and dyslipidaemia occur due to an increase in blood pressure, fasting glucose level, and triglyceride levels, respectively. These disorders appear with each other during CVDs. CVDs cause structural changes (early micro circulation) in retinal blood vessels. These changes in the retina helps physicians to assess the patient's risk due to CVDs, diabetes, and hypertension. A couple of literature are available for accessing heart-related diseases from the retinal images. Poplin et al. [188] identified CVD risk factors (such as, age, gender, lifestyle data (smoking, drinking, and salty taste), BP, and body mass index (BMI)) from retinal images. Authors used DL to predict hypertension, hyperglycemia, and dyslipidaemia from the retinal fundus image obtained during the study of chronic diseases among the Chinese in central China.

As per the report published by Cordero [200], women and younger people experience a comparatively higher risk for hypertension, diabetes, hypertriglyceridemia, and systemic inflammation than men. The above-mentioned risks play a greater role in coronary heart disease (CHD). Coronary micro vascular dysfunction is reported to be an

Table 12

Techniques for identifying different diseases and its conditions from retinal fundus images.

S. No.	Author & Year	Model	Data	Purpose (or) Identification	Performance accuracy (%)	Remarks
1	Meedeniya et al. [191]	Attention U-Net with ResNet50	RIM-ONE	Glaucoma detection	* OD segment - 99.58 * Inception-v3 - 98.79	Less data
2	Rim et al. [192]	DL algorithm	* CMERC-HI * SEED * UK Biobank * Screening centers	RetiCAC	79	Less accuracy
3	Korot et al. [193]	DL	UK Biobank	Gender	86.5	Low performance
4	Cen et al. [194]	* DL platform * CNNs * Mask-RCNN	* PACS * LEDRS * EyePACS * IDRID * PALM * REFUGE	39 types fundus diseases	92.19	Less accuracy
5	Hsia et al. [195]	DL with mask R-CNN	Taichung Veterans General Hospital	OCT	* Choroidal thickness - 90 * Sub foveal choroidal thickness - 89.9	Less accuracy
6	Morona et al. [196]	SSCAV	RITE	* Retinal arteries * Vein segmentation	96.05	Less data
7	Son et al. [197]	DL	Heterogeneous	CAC score	-	Less data
8	Dai et al. [188]	DL	UK Biobank	Hypertension	60.94	Less accuracy
9	Zhang et al. [198]	NN	XMUHS	* Hypertension * Hyperglycemia * Dyslipidemia * Atherosclerosis	* Hypertension - 68.8 * Hyperglycemia - 78.7 * Dyslipidemia - 66.7 58.3	Less data
10	Chang et al. [98]	DL	HPC-SNUH	* DL-FAS		Low performance
11	Rim et al. [199]	DL	Beijing Eye Study	Systemic biomarkers	91	Less accuracy

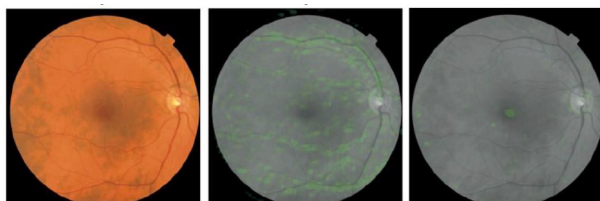


Fig. 9. Retinal characteristics that are related with risk factors for CVDs (as indicated in green) [190]. (For interpretation of the references to color in this figure legend, the reader is referred to the web version of this article.)

important contributor to CHD in women. Coronary artery and retinal vessels undergo similar kinds of physiological changes during hypertension [201,202]. Literature [203,204] documented the relationship between retinal arteriolar changes and CHDs. CHDs can be measured from the retinal images by arteriole to venule ratio (AVR), which represents the ratio of central retinal artery occlusion eye condition (CRAE) to central retinal vein occlusion eye condition (CRVE). Mainly, AVR measures the change in branching patterns during cardiac risk. It helps in identifying myocardial ischemia and CHDs. A few of the literature's are not clear about narrower arterioles or wider venules or both for lower AVR. An AVR of 1.0 represents equal arterioles and venules calibers in the eye. A lower value of AVR represents relatively the wider venules than the arterioles. Both the wider venules and the narrower arterioles represent an increased risk for CHDs.

Zhang et al. [198] used image preprocessing (subtractive normalization approach) followed by statistical analysis (risk factors analysis by receiver operating characteristics (ROC) curves and area under the ROC curve (AUC)) for predicting the CVDs from retinal images. Wang et al., used Cox regression model to identify the relation between the AVR, retinal arteriolar, venular calibers, and CHDs. Authors used the interaction between age, gender, and retinal vessel calibers for identifying the CHDs. They reported higher interaction between age and venular calibers. McGeechan et al. [205] predicted retinal vessel caliber and Framingham risk scores to access CHDs. The authors reported several

clinical implications (1. Gender difference in association with retinal vessel caliber with CHDs. This indicates that micro vascular dysfunction is more contributed to CHDs in women than men. 2. Arteriole narrowing occurs due to an increase in age, BP, and endothelial dysfunction. This further leads to an increase in CHDs, and 3. Wider retinal venules indicate increased CHDs. This is less clear in women. Retinal vessel changes reported a consistent change with inflammatory markers, endothelial dysfunction, increased aortic, and stiffness in atrial value).

Several population based clinical studies showed that the retinal micro vascular signs from retinal images are effectively made for predicting clinical stroke events, stroke death, and cerebral diseases [205–208]. Apart from this, people are affected by ocular fundus diseases such as: diabetic retinopathy (DR) [209], age-related macular degeneration (AMD) [210], retinal vein occlusion [211], glaucoma, retinal detachment [212], and fundus tumor [213,214]. The most common cause of vision impairment leads to DR, AMD, and glaucoma. Cen et al. [194] created a multi-disease automatic detection platform using CNNs to classify 39 different types of common fundus diseases and its conditions from color fundus images. They built a deep learning platform (DLP) that was trained, validated, and tested using 249,620 fundus images collected from three different datasets. It can predict the likelihood of each disease and display heat-maps with deep learning explainability in real-time.

Retinal vasculature such as branching angles, diameter, and curvature tortuosity help in identifying CVDs [215], coronary artery diseases [216], and diabetic mellitus [217]. Coronary artery calcium score (CACS) from retinal fundus images are evaluated with DL technologies [211]. Retinal images provides detail information about human vasculature and insights into heart related diseases. Rim et al. [192] proposed DL based algorithm to determine the CAC from retinal images. Authors proposed a cardiovascular disease risk stratification system based on the facts stated above. The results of this techniques were consistent with the results of conventional CAC from the cardiac CT scan.

Poplin et al. [189] proposed a DL based DNN model to predict the cardio vascular risk factor from retinal fundus image. Figure 8 represents the variation in fundus images due to different CVDs risk factors (such as: age, gender, smoker or not, diabetic condition, BMI, SBP, and

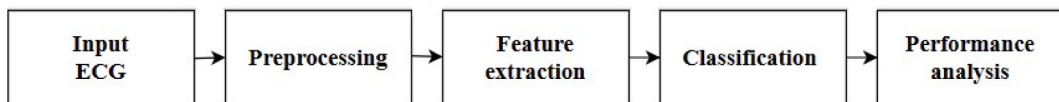


Fig. 10. Proposed schematic diagram for arrhythmia detection from ECG signal.

DBP). **Figure 8(a)** represents the original color fundus image obtained from UK Biobank dataset [108]. **Figure 8(b) to (h)** represent the gray scale retinal images for higher age person ($>= 58$ years), female person, non smoker, diabetic patient, and person having higher BMI, respectively. These fundus images were used to identify the CVDs.

Figure 8 (b) identified as the fundus image of a person aged 59.10. However, the person's true age is 57.60. The retinal fundus image for a female person is shown in **Fig. 8(c)** as same. Variation in fundus image of non smoker person is shown in **Fig. 8(d)**. The non-diabetic patient retinal fundus image is shown in **Fig. 8(e)**. This provided 6.7% prediction. **Figure 8(f)** shows the BMI of a person's retinal fundus image by predicting a person BMI as 24.1 kg/m^2 as compared to the actual value of 26.3 kg/m^2 . The systolic blood pressure (SBP) and diastolic blood pressure (DBP) of a person are shown in **Fig. 8(g) to (h)**.

Some researchers have used different models to identify/detect various human diseases and its conditions by using the retinal fundus images. Few of them have been discussed below and summarized in **Table 12**. Korot et al. [193], Rim et al. [192], Cen et al., [194], Hsia et al. [195], Son et al. [197], Dai et al. [188], Chang et al. [98], and Rim et al. [199] used DL based approaches to identify various diseases from retinal images with the help of different databases. Meedeniya et al. [191] proposed an attention U-Net-based Res-Net50 model to detect glaucoma, a condition of eye that can damage the optic nerve. Zhang et al. [198] used NN method to identify hypertension, hyperglycemia, and dyslipidaemia with an accuracy of 66.8%, 78.7%, and 66.7%, respectively. Some researchers predicted hypertension with an accuracy of 60.94% and an AUC of 0.6506 from retinal images. They used attention mapping to demonstrate the relationship between retinal anatomical regions and hypertension predictions from the customized CNN as shown in **Fig. 9**. Retinal abnormalities can be defined as a wide range of features with varying sizes, shapes, regions, distribution, and density making it difficult to extract relevant characteristics. Furthermore, colored retinal images have high dimensions, with attributes present in various regions of the retina. Inconsistent illumination, patient movement, image noises, low contrast, and irregular retinal pigmentation are contributed to fundus image distortion. Researchers addressed the constraint of current CNN architectures, which can only receive a single retinal picture with a single CVD label, by proposing a weakly-supervised framework that can accept two retinal images (both the left retina and the right retina) with a single CVD label as input.

Table 12 discusses the DL models as well as the identification of CVDs from fundus image. Different authors used various retinal databases (such as: RIM-ONE, UK Biobank, RITE, and HPC-SNUH etc.) for identifying various diseases (such as: glaucoma, hypertension, hyperglycemia, and dyslipidaemia etc.). Mainly hypertension is the commonly detected disease from the fundus images. These models are diseases specific. These methods were validated on a few labeled databases and reported accuracy $\leq 95\%$. As a result, a more accurate model for identifying multiple CVDs from fundus images is required.

5. Challenges and research gap

Major complexities associated with the ECG analysis are: necessity of handcrafted features, huge data requirements for training, over-fitting & under-fitting of the network, complexity in the architecture, requirement of more depth network to extract complex features, difficulty in hyper-parameter tuning, and poor performance.

The deep learning models used for disease classification from the ECG signal, require plenty of diverse data, which are hardly collected

from the various hospitals due to medical regulations. The ECG recordings obtained from modern ECG devices and cardiologist are not documented till now. Everyday a huge amount of ECG data are collected from different patients, which are difficult and time consuming for investigating by the heart specialist. Most of the researchers have classified maximum 4/5-classes of ECG abnormalities including normal ECG. These number of classes are very less for the detection of abnormality from the normal ECG. Also the data is hardly available for various heart disease patients. Classification performance is gradually reduces, when the number of classes increases. Real-time automatic analysis of ECG signal is under developed.

ECG recordings are found to be different in various physiological conditions and possess unique temporal & morphological features. These features may vary at different time slot for different group of people having same clinical/pathological symptoms. Also, for same symptom the ECG may have variations in morphology [16]. Sometimes, different cardiac problems may provide same morphological structures in ECG recording and leads to inter class similarity [218–220].

By analyzing the bottleneck in disease classification from ECG signals this work tries to develop an efficient deep network model for various disease classification. It also create the data for different diseases from the ECG signal with the consultation of cardiologist. The model will be implemented by FPGA for real-time data analysis. By considering these drawbacks and issues a future road-map is developed for detecting heart diseases and it is closely explained in the following Section.

6. Future road-map

By examining the ECG analyses techniques, the future road map is proposed for analyzing the ECG signal. **Figure 10** shows the suggested technical steps for analyzing the heart related diseases from the ECG signals. The important blocks are ECG acquisition, preprocessing, feature extraction, classification, performance analysis and disease detection.

The input ECG signals can be captured by offline and real time. Pre-recorded data from the local hospitals have been used for identifying the diseases. Whereas in real time, the input data are collected from the wearable devices for continuous analyses. Preparing raw data to be acceptable for analysis, preprocessing (which transforms or changes data through a sequence of procedures) performed by SVD, or PCA, or ICA, or by mean subtraction or noise removal or combination of more than one methods. SVD is a matrix factorization algorithm that divides any matrix into three generic and familiar matrices. It has some significant uses in image processing and machine learning. Understanding eigenvalues and eigenvectors is crucial to comprehending the idea of singular value decomposition. One of the most widely used unsupervised machine learning techniques is PCA, which has a wide range of uses, including data exploration, wavelet transform, data compression, and data de-noising etc., The main objective of PCA is to generate such principal components, which may characterize the data points with a set of principal components. ICA technique is used to improve decision trees and multi layer perceptron classification rates and helps to simplifies the structure of both classifiers, improving generalization properties. The proposed preprocessing is based on the hypothesis that an ICA analysis will convert the classification model into a space where the components are impartial and aligned to the axes, making it more suited to the way a decision tree is constructed. In addition, inference of a multi layer perceptron weights will be much simpler because the gradient exploration in the weight space will pursue individual trajectories. As a result,

classifiers are less complex, and error rates are lower in some databases.

The output from preprocessing step is fed to the feature extraction process. This technique turns the raw data into numerical features that can be handled while keeping the information in original dataset. Compared to machine learning on the raw data directly, it produces better outcomes. Researchers used DFT, DCT, DWT, STFT, DL, and Gabor filters techniques for feature extraction. It produces better outcomes than directly using machine learning to original data. DCT, divides the data into two stages. At first stage, DCT is applied to the whole signal to achieve the DCT coefficients, and then a portion of the coefficients are chosen to create relevant features in the second stage. DCT coefficient structure has the same aspects as the input signal. In DWT feature extraction, the approximation coefficient of DWT with some important features from high frequency coefficients are chosen. STFT is used to compute spectral response from a window that moves along the data in another window.

Data from feature extraction techniques are given to the classification step and subsequently into the performance analysis block (for computation of sensitivity, specificity, positive predictive value, F1 score, and accuracy) for calculation. In order to determine the most effective preprocessing and feature extraction method, the performance output of several data sets are compared. The best outcome that has been determined for validation will be given to the physicians for verification.

7. Conclusion

Analyzing ECG is an important method for identifying abnormalities in heart function. Early detection of heart diseases are still a challenging task for many researchers but with DL, ML, CAD, SVD, and PCA etc., methods, an automated detection of heart conditions with ECG analysis and classification become possible. This review paper provide an in-depth evaluation of various traditional and machine learning methods used in each stage of ECG signal analysis, with a focus on the ECG classification task. Many researchers used deep learning techniques which demonstrate more efficient detection and classification results compared to others. A wide range of hardware and software tools for this research area have also been described. Furthermore, the significant challenges and limitations have been discussed, and recommendations for future research have been made. The majority of researchers used MITDB to evaluate their methods of ECG analysis and classification based on one-dimensional ECG data. The main implication of this review paper is to analyze the heart conditions effectively. To analyze this ECG signal, the modern research approaches and future road map are formed to detect various diseases & abnormalities in the heart. Real-time data from wearable devices enables more effective intrusion of the limitations over ECG data analysis. Recently published literature based on beat classification, disease identification, noise removal, disease classification, and real-time ECG analysis by analyzing ECG waveform are summarized in a tabular form. The future scope of this review aims to develop a wearable device that can calculate the real time data of human/fetal for long-term remote monitoring applications. The study helps in identifying heart disorder from retinal fundus image and this can be further examined by physicians for better diagnosis.

Declaration of Competing Interest

The authors declare that they have no known competing financial interests or personal relationships that could have appeared to influence the work reported in this paper.

Data availability

No data was used for the research described in the article.

References

- [1] A.F. Hussein, A. N, M. Burbano-Fernandez, G. Ramrez-Gonzlez, E.W. Abdulhay, V.H.C. de Albuquerque, An automated remote cloud-based heart rate variability monitoring system, *IEEE Access* 6 (2018) 77055–77064, <https://doi.org/10.1109/ACCESS.2018.2831209>.
- [2] E.B. Panganiban, A.G. Paglinawan, W.Y. Chung, G.L.S. Paa, ECG diagnostic support system (EDSS): A deep learning neural network based classification system for detecting ECG abnormal rhythms from a low-powered wearable biosensors, *Sens. Bio-Sensing Res.* 31 (2021) 1–15, <https://doi.org/10.1016/j.sbsr.2021.100398>.
- [3] K.K. Patro, A.J. Prakash, S. Samantray, J. Pawia, R. Tadeusiewicz, P. Plawiak, A hybrid approach of a deep learning technique for real-time ECG beat detection 32 (3) (2022) 345–413, <https://doi.org/10.34768/amcs-2022-0033>.
- [4] M. Sarlija, F. Jurisic, S. Popovic, A convolutional neural network based approach to QRS detection. *Proceedings of the 10th International Symposium on Image and Signal Processing and Analysis*, 2017, pp. 121–125, <https://doi.org/10.1109/ISPA.2017.8073581>.
- [5] S. Kaplan Berkaya, A.K. Uysal, E. Sora Gunal, S. Ergin, S. Gunal, M. B. Gulmezoglu, A survey on ECG analysis, *Biomed. Signal Process. Control* 43 (2018) 216–235, <https://doi.org/10.1016/j.bspc.2018.03.003>.
- [6] C. Ye, B.V.K. Vijaya Kumar, M.T. Coimbra, Heartbeat classification using morphological and dynamic features of ECG signals, *IEEE Trans. Biomed. Eng.* 59 (10) (2012) 2930–2941, <https://doi.org/10.1109/TBME.2012.2213253>.
- [7] E.B. Mazomenos, T. Chen, A. Acharyya, A. Bhattacharya, J. Rosengarten, K. Maharatna, A time-domain morphology and gradient based algorithm for ECG feature extraction. *2012 IEEE International Conference on Industrial Technology*, 2012, pp. 117–122, <https://doi.org/10.1109/ICIT.2012.6209924>.
- [8] N. Uchaipichat, C. Thanawattano, A. Buakhamsri, The development of ST-episode detection in Holter monitoring for myocardial ischemia, *Procedia Comput. Sci.* 86 (2016) 188–191, <https://doi.org/10.1016/j.procs.2016.05.059>.
- [9] I. Romero, L. Serrano, ECG frequency domain features extraction: a new characteristic for arrhythmias classification. *2001 Conference Proceedings of the 23rd Annual International Conference of the IEEE Engineering in Medicine and Biology Society* vol. 2, 2001, pp. 2006–2008, <https://doi.org/10.1109/EMBS.2001.1020624>.
- [10] I. Guler, E.D. Ubeyleli, ECG beat classifier designed by combined neural network model, *Pattern Recognit.* 38 (2) (2005) 199–208, <https://doi.org/10.1016/j.patcog.2004.06.009>.
- [11] M. Song, J. Lee, S. Cho, K.-J. Lee, S.K. Yoo, Support vector machine based arrhythmia classification using reduced features, *Int. J. Control. Autom. Syst.* 3 (2005) 571–579, <https://doi.org/10.1016/j.ijartmed.2008.04.007>.
- [12] S.-N. Yu, C. Hsiang, Electrocardiogram beat classification based wavelet and probabilistic neural network, *Pattern Recognit. Lett.* 28 (2007) 1142–1150, <https://doi.org/10.1016/j.patrec.2007.01.017>.
- [13] S.-N. Yu, K.-T. Chou, Integration of independent component analysis and neural networks for ECG beat classification, *Expert Syst. Appl.* 34 (4) (2008) 2841–2846, <https://doi.org/10.1016/j.eswa.2007.05.006>.
- [14] C. Ye, M.T. Coimbra, B.V.K.V. Kumar, Arrhythmia detection and classification using morphological and dynamic features of ECG signals. *2010 Annual International Conference of the IEEE Engineering in Medicine and Biology*, 2010, pp. 1918–1921, <https://doi.org/10.1109/EMBS.2010.5627645>.
- [15] H. Khorrami, M. Moavenian, A comparative study of DWT, CWT and DCT transformations in ECG arrhythmias classification, *Expert Syst. Appl.* 37 (2010) 5751–5757, <https://doi.org/10.1016/j.eswa.2010.02.033>.
- [16] S. Banerjee, M. Mitra, Application of cross wavelet transform for ECG pattern analysis and classification, *IEEE Trans. Instrum. Meas.* 63 (2014) 326–333, <https://doi.org/10.1109/TIM.2013.2279001>.
- [17] R. Arvanaghi, S. Daneshvar, H. Seyedarabi, A. Goshvarpour, Classification of cardiac arrhythmias using arterial blood pressure based on discrete wavelet transform. *Biomedical Engineering: Applications, Basis and Communications*, 2017, pp. 1918–1921, <https://doi.org/10.4015/S101623721750034X>.
- [18] U. Satija, B. Ramkumar, M.S. Manikandan, A new automated signal quality-aware ECG beat classification method for unsupervised ECG diagnosis environments, *IEEE Sens. J.* 19 (2019) 277–286, <https://doi.org/10.1109/JSEN.2018.2877055>.
- [19] C. Venkatesan, P. Karthigaikumar, A. Paul, S. Satheeskumaran, R. Kumar, ECG signal preprocessing and SVM classifier-based abnormality detection in remote healthcare applications, 2018, <https://doi.org/10.1109/ACCESS.2018.2794346>.
- [20] M. Hammad, A. Maher, K. Wang, F. Jiang, M. Amran, Detection of abnormal heart conditions based on characteristics of ECG signals, *Measurement* 125 (2018) 634–644, <https://doi.org/10.1016/j.measurement.2018.05.033>.
- [21] R.J. Martis, U.R. Acharya, C.M. Lim, J.S. Suri, Characterization of ECG beats from cardiac arrhythmia using discrete cosine transform in PCA framework, *Knowledge-Based Syst.* 45 (2013) 76–82, <https://doi.org/10.1016/j.knosys.2013.02.007>.
- [22] H. Kaur, Rajin, On the detection of cardiac arrhythmia with principal component analysis, *Wirel. Pers. Commun.* 97 (2017) 5495–5509, <https://doi.org/10.1007/s11277-017-4791-1>.
- [23] R. Martinek, R. Kahankova, J. Jezewski, R. Jaros, J. Mohylova, M. Fajkus, J. Nedoma, P. Janku, H. Nazeran, Comparative effectiveness of ICA and PCA in extraction of fetal ECG from abdominal signals: Toward non-invasive fetal monitoring, *Front. Physiol.* 9 (2018) 1–25, <https://doi.org/10.3389/fphys.2018.00648>.
- [24] R. Martin-Clemente, J. Camargo-Olivares, S. Hornillo-Mellado, M. Elena, I. Román, Fast technique for noninvasive fetal ECG extraction, *IEEE Trans.*

- Biomed. Eng. 58 (2011) 227–230, <https://doi.org/10.1109/TBME.2010.2059703>.
- [25] R. Martis, U.R. Acharya, H. Prasad, K. Chua, C. Lim, J. Suri, Application of higher order statistics for atrial arrhythmia classification, Biomed. Signal Process. Control 8 (2013) 888–900, <https://doi.org/10.1016/j.bspc.2013.08.008>.
- [26] R.R. Jorge, A. Mexicano, J. Bila, S. Cervantes, R. Ponce, Feature extraction of electrocardiogram signals by applying adaptive threshold and principal component analysis, J. Appl. Res. Technol. 13 (2015) 261–269, <https://doi.org/10.1016/j.jart.2015.06.008>.
- [27] R. Gopal, V. Ranganathan, Evaluation of effect of unsupervised dimensionality reduction techniques on automated arrhythmia classification, Biomed. Signal Process. Control 34 (2017) 1–8, <https://doi.org/10.1016/j.bspc.2016.12.017>.
- [28] P. de Chazal, M. O'Dwyer, R. Reilly, Automatic classification of heartbeats using ECG morphology and heartbeat interval features, IEEE Trans. Biomed. Eng. 51 (7) (2004) 1196–1206, <https://doi.org/10.1109/TBME.2004.827359>.
- [29] V. Krasteva, I. Jekova, R. Schmid, Perspectives of human verification via binary QRS template matching of single-lead and 12-lead electrocardiogram, Natl. Libr. Med. 13 (2018) 1–25, <https://doi.org/10.1371/journal.pone.0197240>.
- [30] L. Gerencser, G. Kozmann, Z. Vago, K. Haraszti, The use of the SPA method in ECG analysis, IEEE Trans. Biomed. Eng. 49 (10) (2002) 1094–1101, <https://doi.org/10.1109/TBME.2002.802007>.
- [31] P. Shimpi, S. Shah, M. Shroff, A. Godbole, A machine learning approach for the classification of cardiac arrhythmia, 2017 International Conference on Computing Methodologies and Communication (ICCMC), 2017, pp. 603–607, <https://doi.org/10.1109/ICCMC.2017.8282537>.
- [32] S. Kiranyaz, T. Ince, M. Gabbouj, Real-time patient-specific ECG classification by 1-D convolutional neural networks, IEEE Trans. Biomed. Eng. 63 (3) (2016) 664–675, <https://doi.org/10.1109/TBME.2015.2468589>.
- [33] W. Yin, X. Yang, L. Li, L. Zhang, N. Kitsuwani, R. Shinkuma, E. Oki, Self-adjustable domain adaptation in personalized ECG monitoring integrated with IR-UWB radar, Biomed. Signal Process. Control 47 (2019) 75–87, <https://doi.org/10.1016/j.bspc.2018.08.002>.
- [34] J. Huang, B. Chen, B. Yao, W. He, ECG arrhythmia classification using STFT-based spectrogram and convolutional neural network, IEEE Access 7 (2019) 92871–92880, <https://doi.org/10.1109/ACCESS.2019.2928017>.
- [35] X. Zhai, C. Tin, Automated ECG classification using dual heartbeat coupling based on convolutional neural network, IEEE Access 6 (2018) 27465–27472, <https://doi.org/10.1109/ACCESS.2018.2833841>.
- [36] R.S. Andersen, A. Peimankar, S. Puthusserypady, A deep learning approach for real-time detection of atrial fibrillation, Expert Syst. Appl. 115 (2019) 465–473, <https://doi.org/10.1016/j.eswa.2018.08.011>.
- [37] Faust, Oliver, Automated detection of atrial fibrillation using long short-term memory network with RR interval signals, Comput. Biol. Med. 102 (2018) 327–335, <https://doi.org/10.1016/j.combiom.2018.07.001>.
- [38] D. Yoon, H.S. Lim, K. Jung, T.Y. Kim, S. Lee, Deep learning-based electrocardiogram signal noise detection and screening model, Healthc. Inform. Res. 25 (2019) 201–211, <https://doi.org/10.4258/hir.2019.25.3.201>.
- [39] R. Sinha, An Approach for Classifying ECG Arrhythmia based on Features Extracted from EMD and Wavelet Packet Domains, 2012, Ph.D Thesis.
- [40] B. Hwang, J. You, T. Vaessen, I. Myin-Germeys, B.-T.Z. Cheolsoo Park, Deep ECGNet: An optimal deep learning framework for monitoring mental stress using ultra short-term ECG signals, Telemed. e-Health 24 (2018) 753–772, <https://doi.org/10.1089/tmj.2017.0250>.
- [41] S.A. Alshebeili, T.N. Alotaiby, L.M. Aljafar, W.M. Alsabhan, ECG-based subject identification using common spatial pattern and SVM, J. Sens. (2019) 1–9, <https://doi.org/10.1155/2019/8934905>.
- [42] H. Khamis, R. Weiss, Y. Xie, C.-W. Chang, N.H. Lovell, S.J. Redmond, QRS detection algorithm for telehealth electrocardiogram recordings, IEEE Trans. Biomed. Eng. 63 (7) (2016) 1377–1388, <https://doi.org/10.1109/TBME.2016.2549060>.
- [43] M. Jia, F. Li, Z. Chen, X. Xiang, X. Yan, High noise tolerant R-peak detection method based on deep convolution neural network, IEICE Trans. Inf. Syst. 102 (11) (2019) 2272–2275, <https://doi.org/10.1587/transinf.2019EDL8097>.
- [44] C. Lin, C. Mailhes, J.-Y. Tourneret, P- and T-wave delineation in ECG signals using a Bayesian approach and a partially collapsed Gibbs sampler, IEEE Trans. Biomed. Eng. 57 (12) (2010) 2840–2849, <https://doi.org/10.1109/TBME.2010.2076809>.
- [45] C.-C. Lin, C.-M. Yang, Heartbeat classification using normalized RR intervals and morphological features, 2014 International Symposium on Computer, Consumer and Control (2014) 1–11, <https://doi.org/10.1155/2014/712474>.
- [46] M.R. Arefin, K. Tavakolian, R. Fazel-Rezai, QRS complex detection in ECG signal for wearable devices. 2015 37th Annual International Conference of the IEEE Engineering in Medicine and Biology Society (EMBC), 2015, pp. 5940–5943, <https://doi.org/10.1109/EMBC.2015.7319744>.
- [47] D.V. Madeiro, L. Marques, T. Han, Roberto, Evaluation of mathematical models for QRS feature extraction and QRS morphology classification in ECG signals, Measurement 156 (2020) 1–29, <https://doi.org/10.1016/j.measurement.2020.107580>.
- [48] F. Zhang, J. Tan, Y. Lian, An effective QRS detection algorithm for wearable ECG in body area network, 2007 IEEE Biomedical Circuits and Systems Conference, 2007, pp. 195–198, <https://doi.org/10.1109/BIOCAS.2007.4463342>.
- [49] A. Kennedy, D.D. Finlay, D. Guldenring, R.R. Bond, K. Moran, J. McLaughlin, Automated detection of atrial fibrillation using R-R intervals and multivariate-based classification, J. Electrocardiol. 49 (6) (2016) 871–876, <https://doi.org/10.1016/j.jelectrocard.2016.07.033>.
- [50] S. Ioffe, C. Szegedy, Batch normalization: Accelerating deep network training by reducing internal covariate shift, In Proceedings of the 32nd International Conference on International Conference on Machine Learning (ICML'15), 2015, 448–456, <https://doi.org/10.48550/arXiv.1502.03167>.
- [51] D. Silva, Fabio, The Role of R-Spondin3 in Coronary Artery Formation and Novel Roles for Retinoic Acid signaling in Cardiac Development and Repair, 2017, Ph.D. thesis.
- [52] D. Cooley, Categories of Arrhythmias, The Texas Heart Institute, 2018, pp. 1–8, <http://www.texasheartinstitute.org/HIC/Topics/Cond/arrhyat.cfm>.
- [53] S. Naik, S. Debnath, V. Justin, A review of arrhythmia classification with artificial intelligence techniques: Deep vs. machine learning, 2021 2nd International Conference for Emerging Technology (INSET), 2021, pp. 1–14, <https://doi.org/10.1109/INSET51464.2021.9456394>.
- [54] F. Li, Y. Xu, Z. Chen, Z. Liu, Automated heartbeat classification using 3-inputs based on convolutional neural network with multi-fields of view, IEEE Access 7 (2019) 76295–76304, <https://doi.org/10.1109/ACCESS.2019.2921991>.
- [55] S. Sahoo, M. Dash, S. Behera, S. Sabut, Machine learning approach to detect cardiac arrhythmias in ECG signals: a survey, IRBM 41 (4) (2020) 185–194, <https://doi.org/10.1016/j.irbm.2019.12.001>.
- [56] A. Prakash, S. Samantray, C. Bala, Y. Narayana, An automated diagnosis system for cardiac arrhythmia classification, 2021, pp. 301–312, <https://doi.org/10.1201/9781003146810-13>.
- [57] Z. Cai, C. Liu, G. Hongxian, X. Wang, L. Zhao, Q. Shen, E. Ng, J. Li, An open-access long-term wearable ECG database for premature ventricular contractions and supraventricular premature beat detection, J. Med. Imaging Health Inform. 10 (2020) 2663–2667, <https://doi.org/10.1166/jmhi.2020.32892663>.
- [58] M. Alrahalhal, N. Ajlan, Y. Bazi, H. Alhichri, T. Rabczuk, Automatic premature ventricular contractions detection for multi-lead electrocardiogram signal, 2018, pp. 0169–0173, <https://doi.org/10.1109/EIT.2018.8500197>.
- [59] M. Abdelazeez, F.F. Firouzeh, S. Rajan, A.D.C. Chan, Multi-stage detection of atrial fibrillation in compressively sensed electrocardiogram. 2020 IEEE International Instrumentation and Measurement Technology Conference (I2MTC), 2020, pp. 1–6, <https://doi.org/10.1109/I2MTC43012.2020.9128396>.
- [60] G. Luongo, S. Schuler, A. Luik, T. Almeida, D. Soriano, O. Doessel, A. Loewe, Non-invasive characterization of atrial flutter mechanisms using recurrence quantification analysis on the ECG: A computational study, IEEE Trans. Biomed. Eng. 68 (3) (2021) 914–925, <https://doi.org/10.1109/TBME.2020.2990655>.
- [61] S.K. Bashar, D. Han, Z. Fearass, E. Ding, T. Fitzgibbons, A. Walkley, D. McManus, B. Javid, K. Chon, Novel density poincaré plot based machine learning method to detect atrial fibrillation from premature atrial/ventricular contractions, IEEE Trans. Biomed. Eng. 99 (2020) 1–13, <https://doi.org/10.1109/TBME.2020.3004310>.
- [62] A.M.A. Zaidi, M.J. Ahmed, A. Bakibillah, Feature extraction and characterization of cardiovascular arrhythmia and normal sinus rhythm from ECG signals using LabVIEW (2017) 1–6, <https://doi.org/10.1109/ICIVPR.2017.7890871>.
- [63] S. Mitra, A.K. Saha, S. Sardar, A. Singh, Remission of congenital complete heart block without anti-Ro/La antibodies: A case report, Ann. Pediatr. Cardiol 6 (2013) 182–194, <https://doi.org/10.4103/0974-2069.115278>.
- [64] Y. Feng, C. Roney, M. Hocini, S. Niederer, E. Vigmond, Robust atrial ectopic beat classification from surface ECG using second-order blind source separation, 2020, pp. 1–4, <https://doi.org/10.22489/CinC.2020.473>.
- [65] D. Somwanshi, R. Tiwari, H. Saini, S. Gupta, ECG feature extraction and detection of first degree atrioventricular block, 2018, <https://doi.org/10.1109/ICRAIE.2018.8710343>.
- [66] D.S.B. Sundaram, R. Balasubramani, S. Shivaram, A. Muthyalu, S. Arunachalam, Single lead ECG discrimination between normal sinus rhythm and sleep apnea with intrinsic mode function complexity index using empirical mode decomposition, 2020 Computing in Cardiology, 2018, pp. 0719–0722, <https://doi.org/10.1109/EIT.2018.8500188>.
- [67] H. Mayala, G. Hrkeshsingh, D. Shire, P. Pallangyo, K. Bakari, S. Kilonzo, W. Kara, W. Hu, A review on pharmacological management of paroxysmal supraventricular tachycardia, IOSR J. Dent. Med. Sci. 16 (2017) 84–86, <https://doi.org/10.9790/0853-1606048486>.
- [68] P. Mahanty, A. Chatterjee, D. Sanjay, R. Shukla, Self-resolving mobitz type II second-degree heart block (atypical Wenckebach block) after cesarean section under subarachnoid block: A case report, Cureus 12 (2020) 1–18, <https://doi.org/10.7759/cureus.10704>.
- [69] R. Martinek, R. Kahankova, R. Jaros, K. Barnová, A. Matonia, M. Jezewski, R. Czabanski, K. Horoba, J. Jezewski, Non-invasive fetal electrocardiogram extraction based on novel hybrid method for intrapartum ST segment analysis, IEEE Access (2021) 1, <https://doi.org/10.1109/ACCESS.2021.3058733>.
- [70] N. Perera, C. Daluwatte, Detecting strict left bundle branch block from 12-lead electrocardiogram using support vector machine classification and derivative analysis 41 (2018) 1–4, <https://doi.org/10.22489/CinC.2018.030>.
- [71] R. Mahmud, S. Jamal, Effect of his bundle pacing on right bundle branch block located distal to site of pacing, J. Electrocardiol. 64 (2020) 58–65, <https://doi.org/10.1016/j.jelectrocard.2020.11.009>.
- [72] J. Yu, X. Wang, X. Chen, J. Guo, Automatic premature ventricular contraction detection using deep metric learning and KNN, Biosensors 11 (2021) 1–22, <https://doi.org/10.3390/bios11030069>.
- [73] D. Han, S.K. Bashar, F. Mohagheghian, E. Ding, C. Whitcomb, D.D. McManus, K. H. Chon, Premature atrial and ventricular contraction detection using photoplethysmographic data from a smartwatch 20 (2020) 3–25, <https://doi.org/10.3390/s20195683>.
- [74] Y. Chang, S.-H. Wu, L. Tseng, H.-L. Chao, C. Ko, AF detection by exploiting the spectral and temporal characteristics of ECG signals with the LSTM model. Computing in Cardiology Conference, CinC 2018, in: Computing in Cardiology,

- IEEE Computer Society, United States, 2018, pp. 1–4, <https://doi.org/10.22489/CinC.2018.266>.
- [75] K. Thygesen, J.S. Alpert, A.S. Jaffe, M.L. Simoons, B.R. Chaitman, H.D. White, Third universal definition of myocardial infarction, *AHA J.* 126 (2012), <https://doi.org/10.1161/CIR.0b013e31826e1058>.
- [76] A. Krizhevsky, I. Sutskever, G.E. Hinton, ImageNet classification with deep convolutional neural networks, *Commun. ACM* 60 (2012) 84–90, <https://doi.org/10.1145/3065386>.
- [77] G.T. Lines, B.L. de Oliveira, O. Skavhaug, M.M. Maleckar, Simple T-wave metrics may better predict early ischemia as compared to ST segment, *IEEE Trans. Biomed. Eng.* 64 (6) (2017) 1305–1309, <https://doi.org/10.1109/TBME.2016.2600198>.
- [78] K. Jafarian, V. Vahdat, S. Salehi, M. Mobin, Automating detection and localization of myocardial infarction using shallow and end-to-end deep neural networks, *Appl. Soft Comput.* 93 (2020) 1–14, <https://doi.org/10.1016/j.asoc.2020.106383>.
- [79] P. Nag, S. Mondal, F. Ahmed, A. More, M. Raihan, A simple acute myocardial infarction (heart attack) prediction system using clinical data and data mining techniques, 2017 20th International Conference of Computer and Information Technology (ICCIT), 2017, pp. 1–6, <https://doi.org/10.1109/ICCITECHN.2017.8281809>.
- [80] M. Jia, F. Li, J. Wu, Z. Chen, Y. Pu, Robust QRS detection using high-resolution wavelet packet decomposition and time-attention convolutional neural network, *IEEE Access* 8 (2020) 16979–16988, <https://doi.org/10.1109/ACCESS.2020.2967775>.
- [81] D. Cooley, Bundle Branch Block, Texas Heart Institute, 2019, <https://www.texasheart.org/heart-health/heart-information-center/topics/bundle-branch-block/>.
- [82] L.J. Christiano, T.J. Fitzgerald, The band pass filter, *Int. Econ. Rev.* 12 (2003) 435–465, <https://doi.org/10.1111/1468-2354.t01-1-00076>.
- [83] A.L. Goldberger, L.A.N. Amaral, L. Glass, J.M. Hausdorff, P.C. Ivanov, R.G. Mark, J.E. Mietus, G.B. Moody, C.-K. Peng, H.E. Stanley, Components of a new research resource for complex physiologic signals, *Am. Heart Assoc.* 101 (2000) 215–220, <https://doi.org/10.1161/01.CIR.101.23.e215>.
- [84] M. Jia, F. Li, Y. Pu, Z. Chen, A lossless electrocardiogram compression system based on dual-mode prediction and error modeling, *IEEE Access* 8 (2020) 101153–101162, <https://doi.org/10.1109/ACCESS.2020.2998608>.
- [85] H.-T. Chiang, Y.-Y. Hsieh, S.-W. Fu, K.-H. Hung, Y. Tsao, S.-Y. Chien, Noise reduction in ECG signals using fully convolutional denoising autoencoders, *IEEE Access* 7 (2019) 60806–60813, <https://doi.org/10.1109/ACCESS.2019.2912036>.
- [86] A.E. Curtin, K.V. Burns, A.J. Bank, T.I. Netoff, QRS complex detection and measurement algorithms for multichannel ECGs in cardiac resynchronization therapy patients, *IEEE J. Transl. Eng. Health Med.* 6 (2018) 1–11, <https://doi.org/10.1109/JTEHM.2018.2844195>.
- [87] C. Lastre-Domínguez, Y.S. Shmaliy, O. Ibarra-Manzano, M. Vazquez-Olguín, Denoising and features extraction of ECG signals in state space using unbiased FIR smoothing, *IEEE Access* 7 (2019) 152166–152178, <https://doi.org/10.1109/ACCESS.2019.2948067>.
- [88] G. Sannino, G.D. Pietro, A deep learning approach for ECG-based heartbeat classification for arrhythmia detection, *Future Gener. Comput. Syst.* 86 (2018) 446–455, <https://doi.org/10.1016/j.future.2018.03.057>.
- [89] J.G. Cleary, L.E. Trigg, K*: an instance-based learner using and entropic distance measure 5 (1995) 108–114, <https://doi.org/10.1016/b978-1-55860-377-6.50022-0>.
- [90] S. Nurmaini, R. Partan, W. Caesarendra, T. Dewi, M. Rahmatullah, A. Darmawahyuni, V. Bhayu, F. Firdaus, An automated ECG beat classification system using deep neural networks with an unsupervised feature extraction technique, *Appl. Sci.* 9 (2019) 1–17, <https://doi.org/10.3390/app9142921>.
- [91] S. G, S. K P, V. R, Automated detection of cardiac arrhythmia using deep learning techniques, International Conference on Computational Intelligence and Data Science (ICCIIDS), *Procedia Comput. Sci.* 132 (2018) 1192–1201, <https://doi.org/10.1016/j.procs.2018.05.034>.
- [92] O. Yildirim, U.B. Baloglu, R.-S. Tan, E.J. Ciaccio, U.R. Acharya, A new approach for arrhythmia classification using deep coded features and LSTM networks, *Comput. Methods Programs Biomed.* 176 (2019) 121–133, <https://doi.org/10.1016/j.cmpb.2019.05.004>.
- [93] J. Jiang, H. Zhang, D. Pi, C. Dai, A novel multi-module neural network system for imbalanced heartbeats classification, *Expert Syst. Appl.* 1 (2019) 1–15, <https://doi.org/10.1016/j.eswa.2019.100003>.
- [94] J.B. Bidias á Mougonfan, J.A. Eyebe Fouda, M. Tchuenté, W. Koepf, Adaptive ECG beat classification by ordinal pattern based entropies, *Commun. Nonlinear Sci. Numer. Simul.* 84 (2020) 1–9, <https://doi.org/10.1016/j.cnsns.2019.105156>.
- [95] Q. Wu, Y. Sun, H. Yan, X. Wu, ECG signal classification with binarized convolutional neural network, *Comput. Biol. Med.* 121 (2020) 1–9, <https://doi.org/10.1016/j.combiomed.2020.103800>.
- [96] S.K. Pandey, R.R. Janghel, V. Vani, Patient specific machine learning models for ECG signal classification, International Conference on Computational Intelligence and Data Science (ICCIIDS), *Procedia Comput. Sci.* 167 (2020) 2181–2190, <https://doi.org/10.1016/j.procs.2020.03.269>.
- [97] A.Y. Hannun, P. Rajpurkar, M. Haghpanahi, G.H. Tison, C. Bourn, M.P. Turakhia, A.Y. Ng, Cardiologist-level arrhythmia detection and classification in ambulatory electrocardiograms using a deep neural network, *Nat. Med.* (2019) 65–69, <https://doi.org/10.1038/s41591-018-0268-3>.
- [98] K.-C. Chang, P.-H. Hsieh, M.-Y. Wu, Y.-C. Wang, J.-Y. Chen, F.-J. Tsai, E.S. Shih, M.-J. Hwang, T.-C. Huang, Usefulness of machine learning-based detection and classification of cardiac arrhythmias with 12-lead electrocardiograms, *Can. J. Cardiol.* 37 (1) (2021) 94–104, <https://doi.org/10.1016/j.cjca.2020.02.096>.
- [99] X. Zhai, Z. Zhou, C. Tin, Semi-supervised learning for ECG classification without patient-specific labeled data, *Expert Syst. Appl.* 158 (2020) 1–10, <https://doi.org/10.1016/j.eswa.2020.113411>.
- [100] Z. Zhou, X. Zhai, C. Tin, Fully automatic electrocardiogram classification system based on generative adversarial network with auxiliary classifier, *Expert Syst. Appl.* 174 (2021) 1–13, <https://doi.org/10.1016/j.eswa.2021.114809>.
- [101] A. Peimankar, S. Puthusserpady, DENS-ECG: a deep learning approach for ECG signal delineation, *Expert Syst. Appl.* 165 (2021) 1–11, <https://doi.org/10.1016/j.eswa.2020.113911>.
- [102] K. Patro, A. Prakash, S. Samantray, J. Plawiak, R. Tadeusiewicz, P. Plawiak, A hybrid approach of a deep learning technique for real-time ECG beat detection, *Int. J. Appl. Math. Comput. Sci.* 32 (2022) 455–465, <https://doi.org/10.34768/amcs-2022-0033>.
- [103] N.I. Hasan, A. Bhattacharjee, Deep learning approach to cardiovascular disease classification employing modified ECG signal from empirical mode decomposition, *Biomed. Signal Process. Control* 52 (2019) 128–140, <https://doi.org/10.1016/j.bspc.2019.04.005>.
- [104] Q. Wu, Y. Sun, H. Yan, X. Wu, ECG signal classification with binarized convolutional neural network, *Comput. Biol. Med.* 121 (2020) 456–465, <https://doi.org/10.1016/j.combiomed.2020.103800>.
- [105] A. Asgharzadeh-Bonab, M.C. Amirani, A. Mehrizi, Spectral entropy and deep convolutional neural network for ECG beat classification, *Biocybern. Biomed. Eng.* 40 (2020) 691–700, <https://doi.org/10.1016/j.bb.2020.02.004>.
- [106] A.H. Mirza, S. Nurmaini, R. Partan, Automatic classification of 15 leads ECG signal of myocardial infarction using one dimension convolutional neural network, *Appl. Sci.* 12 (2022) 1–13, <https://doi.org/10.3390/app12115603>.
- [107] S.S. Yadav, S.B. More, S.M. Jadhav, S.R. Sutar, Convolutional neural networks based diagnosis of myocardial infarction in electrocardiograms. 2021 International Conference on Computing, Communication, and Intelligent Systems (ICCCIS), 2021, pp. 581–586, <https://doi.org/10.1109/ICCCIS51004.2021.9>.
- [108] W. Li, Y.M. Tang, K.M. Yu, S. To, SLC-GAN: An automated myocardial infarction detection model based on generative adversarial networks and convolutional neural networks with single-lead electrocardiogram synthesis, *Inf. Sci.* 589 (2022) 738–750, <https://doi.org/10.1016/j.ins.2021.12.083>.
- [109] A.K. Bhoi, K.S. Sherpa, B. Khandelwal, Ischemia and arrhythmia classification using time-frequency domain features of QRS complex, *Procedia Comput. Sci.* 132 (2018) 606–613, <https://doi.org/10.1016/j.procs.2018.05.01>.
- [110] L.B. Marinho, N.de M.M. Nascimento, J.W.M. Souza, M.V. Gürelp, P.P. Rebouças Filho, V.H.C. de Albuquerque, A novel electrocardiogram feature extraction approach for cardiac arrhythmia classification, *Future Gener. Comput. Syst.* 97 (2019) 564–577, <https://doi.org/10.1016/j.future.2019.03.025>.
- [111] R. He, Y. Liu, K. Wang, N. Zhao, Y. Yuan, Q. Li, H. Zhang, Automatic cardiac arrhythmia classification using combination of deep residual network and bidirectional LSTM, *IEEE Access* 7 (2019) 102119–102135, <https://doi.org/10.1109/ACCESS.2019.2931500>.
- [112] F. Liu, C. Liu, L. Zhao, X. Zhang, X. Wu, X. Xu, Y. Liu, C. Ma, S. Wei, Z. He, J. Li, E. Ng, An open access database for evaluating the algorithms of electrocardiogram rhythm and morphology abnormality detection, *J. Med. Imaging Health Inform.* 8 (2018) 1368–1373, <https://doi.org/10.1166/jmih.2018.2442>.
- [113] A. Sharma, N. Garg, S. Patidar, R. San Tan, U.R. Acharya, Automated pre-screening of arrhythmia using hybrid combination of Fourier-Bessel expansion and LSTM, *Comput. Biol. Med.* 120 (2020) 1–11, <https://doi.org/10.1016/j.combiomed.2020.103753>.
- [114] Q. Yao, R. Wang, X. Fan, J. Liu, Y. Li, Multi-class arrhythmia detection from 12-lead varied-length ECG using attention-based time-incremental convolutional neural network, *Inf. Fusion* 53 (2020) 174–182, <https://doi.org/10.1016/j.inffus.2019.06.024>.
- [115] H. Chen, F. Li, Z. Zhang, A bucket-stream rBRIEF extraction architecture for SLAM applications on embedded platforms. 2020 International Conference on Field-Programmable Technology (ICFPT), IEEE, 2020, pp. 277–280, <https://doi.org/10.1109/ICFPT51103.2020.900047>.
- [116] E. Ihsanto, K. Ramli, D. Sudiana, T.S. Gunawan, An efficient algorithm for cardiac arrhythmia classification using ensemble of depthwise separable convolutional neural networks, *Appl. Sci.* 10 (2) (2020) 1–16, <https://doi.org/10.3390/app10020483>.
- [117] S. Sanamidkar, S. Hamde, V. Asutkar, Analysis and classification of cardiac arrhythmia based on general sparsed neural network of ECG signals, *SN Appl. Sci.* 2 (2020) 1–9, <https://doi.org/10.1007/s42452-020-3058-8>.
- [118] S.C. Mohonta, M.A. Motin, D.K. Kumar, Electrocardiogram based arrhythmia classification using wavelet transform with deep learning model, *Sens. Bio-Sensing Res.* 37 (2022) 1–8, <https://doi.org/10.1016/j.sbsr.2022.100502>.
- [119] P. Oktivasarı, M. Hasyim, H.S. Amy, H. Freddy, Suprijadi, A simple real-time system for detection of normal and myocardial ischemia in the ST segment and T wave ECG signal (2019) 327–331, <https://doi.org/10.1109/ICOIAC74670.2019.8938461>.
- [120] R. Czabanski, Horoba, Wrobel, A. Matonia, Martinek, Kupka, J. Jezewski, R. Kahankova, J. Leski, Detection of atrial fibrillation episodes in long-term heart rhythm signals using a support vector machine, *Sensors* 20 (2020) 65–74, <https://doi.org/10.3390/s20030765>.
- [121] G. Petmezas, K. Haris, L. Stefanopoulos, V. Kilintzis, A. Tzavelis, J.A. Rogers, A. Katsaggelos, N. Maglavera, Automated atrial fibrillation detection using a hybrid CNN-LSTM network on imbalanced ECG datasets, *Biomed. Signal Process. Control* 63 (2021) 1–12, <https://doi.org/10.1016/j.bspc.2020.102194>.
- [122] J. Hong, H.-J. Li, C. chi Yang, C.-L. Han, J. chien Hsieh, A clinical study on atrial fibrillation, premature ventricular contraction, and premature atrial contraction

- screening based on an ECG deep learning model, *Appl. Soft Comput.* 126 (2022) 1–13, <https://doi.org/10.1016/j.asoc.2022.109213>.
- [123] B. Tutuko, M.N. Rachmatullah, A. Darmawahyuni, S. Nurmaini, A.E. Tondas, R. Passarella, R.U. Partan, A. Rifai, A.I. Sapitri, F. Firdaus, Short single-lead ECG signal delineation-based deep learning: implementation in automatic atrial fibrillation identification, *Sensors* 22 (2022) 1–9, <https://doi.org/10.3390/s22062329>.
- [124] S.K. Bashar, M.B. Hossain, A.J.W. Eric Ding, D.D. McManus, K.H. Chon, Atrial fibrillation detection during Sepsis: Study on MIMIC III ICU data, *IEEE J. Biomed. Health Inform.* 24 (11) (2020) 3124–3135, <https://doi.org/10.1109/JBHI.2020.2995139>.
- [125] J.W. Chong, N. Esa, D.D. McManus, K.H. Chon, Arrhythmia discrimination using a smart phone, *IEEE J. Biomed. Health Inform.* 19 (3) (2015) 815–824, <https://doi.org/10.1109/JBHI.2015.2418195>.
- [126] D. Han, S.K. Bashar, J. Lazaro, E. Ding, C. Whitcomb, D. Mcmanus, K. Chon, Smartwatch PPG peak detection method for sinus rhythm and cardiac arrhythmia, vol. 2019, 2019, pp. 4310–4313, <https://doi.org/10.1109/EMBC.2019.8857325>.
- [127] G. Roffo, S. Melzi, U. Castellani, A. Vinciarelli, M. Cristani, Infinite feature selection: A graph-based feature filtering approach, *IEEE Trans. Pattern Anal. Mach. Intell.* 43 (12) (2021) 4396–4410, <https://doi.org/10.1109/TPAMI.2020.3002843>.
- [128] A.L. Goldberger, L.A.N. Amaral, L. Glass, J.M. Hausdorff, P.C. Ivanov, R.G. Mark, J.E. Mietus, G.B. Moody, C.-K. Peng, H.E. Stanley, Components of a new research resource for complex physiologic signals, *PhysioNet* 101 (2000) 215–220, <https://doi.org/10.1161/01.cir.101.23.e215>.
- [129] J. Lazaro, M.B. Hossain, Y. Noh, P.L. Ki, H. Chon, N. Reljin, Wearable armband device for daily life electrocardiogram monitoring, *IEEE Trans. Biomed. Eng.* 67 (12) (2020) 3464–3473, <https://doi.org/10.1109/TBME.2020.2987759>.
- [130] A. Johnson, T. Pollard, L. Shen, L.-W. Lehman, M. Feng, M. Ghassemi, B. Moody, P. Szolovits, L. Celi, R. Mark, MIMIC-III, a freely accessible critical care database, *Sci. Data* 3 (2016) 1–9, <https://doi.org/10.1038/sdata.2016.35>.
- [131] R. Andersen, E. Poulsen, S. Puthusserypady, Novel approach for automatic detection of atrial fibrillation based on inter beat intervals and support vector machine. Proceedings of 39th Annual International Conference of the IEEE Engineering in Medicine and Biology Society, IEEE, 2017, pp. 2039–2042, <https://doi.org/10.1109/EMBC.2017.8037253>.
- [132] M. Kumar, R.B. Pachori, U. Rajendra Acharya, Automated diagnosis of atrial fibrillation ECG signals using entropy features extracted from flexible analytic wavelet transform, *Biocybern. Biomed. Eng.* 38 (3) (2018) 564–573, <https://doi.org/10.1016/j.bbe.2018.04.004>.
- [133] X. Cui, E. Chang, W.-H. Yang, B.C. Jiang, A.C. Yang, C.-K. Peng, Automated detection of paroxysmal atrial fibrillation using an information-based similarity approach, *Entropy* 19 (12) (2017) 1–14, <https://doi.org/10.3390/e19120677>.
- [134] M.S. Islam, N. Ammour, N. Alajlan, H. Aboalsamh, Rhythm-based heartbeat duration normalization for atrial fibrillation detection, *Comput. Biol. Med.* 72 (2016) 160–169, <https://doi.org/10.1016/j.combiomed.2016.03.015>.
- [135] Q. Rahman, L. Tereshchenko, M. Kongkatong, T. Abraham, M. Roselle Abraham, H. Shatkay, Utilizing ECG-based heartbeat classification for hypertrophic cardiomyopathy identification, *IEEE Trans. Nanobiosci.* 14 (2015) 505–512, <https://doi.org/10.1109/TNB.2015.2426213>.
- [136] D. Sopic, A. Aminifar, A. Aminifar, D.A. Alonso, Real-time event-driven classification technique for early detection and prevention of myocardial infarction on wearable systems, *IEEE Trans. Biomed. Circuits Syst.* 12 (2018) 982–992, <https://doi.org/10.1109/TBCAS.2017.8325140>.
- [137] D. Lai, Y. Zhang, X. Zhang, Y. Su, M.B.B. Heyat, An automated strategy for early risk identification of sudden cardiac death by using machine learning approach on measurable arrhythmic risk markers, *IEEE Access* 7 (2019) 94701–94716, <https://doi.org/10.1109/ACCESS.2019.2925847>.
- [138] F. Melgani, Y. Bazi, Classification of electrocardiogram signals with support vector machines and particle swarm optimization, *Inf. Technol. Biomed.*, *IEEE Trans.* 12 (2008) 667–677, <https://doi.org/10.1109/ITB.2008.923147>.
- [139] A. Rad, T. Eftestol, K. Engan, U. Irusta, J. Kvaloy, J. Kramer-Johansen, L. Wik, A. Katsaggelos, B. Ali, ECG-based classification of resuscitation cardiac rhythms for retrospective data analysis, *IEEE Trans. Biomed. Eng.* 64 (10) (2017) 2411–2418, <https://doi.org/10.1109/TBME.2017.2688380>.
- [140] S. Raj, K.C. Ray, ECG signal analysis using DCT-based DOST and PSO optimized SVM, *IEEE Trans. Instrum. Meas.* 66 (2017) 470–478, <https://doi.org/10.1109/TIM.2016.2642758>.
- [141] C.K. Jha, M.H. Kolekar, Cardiac arrhythmia classification using tunable Q-wavelet transform based features and support vector machine classifier, *Biomed. Signal Process. Control* 59 (2020) 74–88, <https://doi.org/10.1016/j.bspc.2020.101875>.
- [142] C.M. Fira, L. Goras, An ECG signals compression method and its validation using NNs, *IEEE Trans. Biomed. Eng.* 55 (4) (2008) 1319–1326, <https://doi.org/10.1109/TBME.2008.918465>.
- [143] T. Mar, S. Zaunseder, J.P. Martínez, M. Llamedo, R. Poll, Optimization of ECG classification by means of feature selection, *IEEE Trans. Biomed. Eng.* 58 (8) (2011) 2168–2177, <https://doi.org/10.1109/TBME.2011.2113395>.
- [144] B. Fatih, H. Oulhadj, D. Boutana, S. Patrick, Automatic ECG arrhythmias classification scheme based on the conjoint use of the multi-layer perceptron neural network and a new improved metaheuristic approach, *IET Signal Proc.* 13 (2019) 140–149, <https://doi.org/10.1049/iet-spr.2018.5465>.
- [145] V. Mai, I. Khalil, C. Meli, ECG biometric using multilayer perceptron and radial basis function neural networks. 2011 Annual International Conference of the IEEE Engineering in Medicine and Biology Society, 2011, pp. 2745–2748, <https://doi.org/10.1109/IEMBS.2011.6090752>.
- [146] X. Xu, S. Wei, C. Ma, K. Luo, L. Zhang, C. Liu, Atrial fibrillation beat identification using the combination of modified frequency slice wavelet transform and convolutional neural networks, *Hindawi J. Healthc. Eng.* 23 (2018) 1–8, <https://doi.org/10.1155/2018/2102918>.
- [147] M.R. Mohebbian, S.S. Vedaei, K.A. Wahid, A. Dinh, H.R. Marateb, K. Tavakolian, Fetal ECG extraction from maternal ECG using attention-based cycleGAN, *IEEE J. Biomed. Health Inform.* 26 (2) (2022) 515–526, <https://doi.org/10.1109/JBHI.2021.3111873>.
- [148] K. Leuven, B. De Moor, P. Gersem, B. De Schutter, W. Favoreel, B. De, M. Peter, D. Gersem, W. Favoreel, DAISY: A database for identification of systems, *Journal A* 38 (1997) 4–5, https://pub.deschutter.info/abs/97_70.html.
- [149] A. Goldberger, L. Amaral, L. Glass, J. Hausdorff, P. Ivanov, R. Mark, J. Mietus, G. Moody, C. Peng, H. Stanley, Physiobank, physiotoolkit, and physionet: components of a new research resource for complex physiologic signals, *Circulation* 101 (23) (2000) 15–20, <https://doi.org/10.1161/01.cir.101.23.e215>.
- [150] M. Hasan, M.B.I. Reaz, M. Ibrahimy, M. Hussain, J. Uddin, Detection and processing techniques of FECG signal for fetal monitoring, *Biol. Proced. Online*, 11 (2009) 263–295, <https://doi.org/10.1007/s12575-009-9006-z>.
- [151] J. Jezewski, A. Matonia, T. Kupka, D. Roj, R. Czabanski, Determination of fetal heart rate from abdominal signals: evaluation of beat-to-beat accuracy in relation to the direct fetal electrocardiogram, *Biomed. Tech./Biomed. Eng.* 57 (2012), <https://doi.org/10.1515/bmt-2011-0130>.
- [152] R. Sameni, G. Clifford, A review of fetal ECG signal processing issues and promising directions, *Open Pacing Electrophysiol. Ther.* 3 (2010) 4–20, <https://doi.org/10.2174/1876536X01003010004>.
- [153] I. Silva, J. Behar, R. Sameni, T. Zhu, J. Oster, G. Clifford, G. Moody, Noninvasive fetal ECG: The PhysioNet/Computing in Cardiology Challenge 2013, *Comput. Cardiol.* (2010), vol. 40, 2013, pp. 149–152, <https://www.ncbi.nlm.nih.gov/pmc/articles/PMC4230703/>.
- [154] F. Andreotti, J. Behar, S. Zaunseder, J. Oster, G. Clifford, An open-source framework for stress-testing non-invasive foetal ECG extraction algorithms, *Physiol. Meas.* 37 (2016) 627–648, <https://doi.org/10.1088/0967-3334/37/5/627>.
- [155] J. Behar, F. Andreotti, S. Zaunseder, J. Oster, G. Clifford, A practical guide to non-invasive fetal electrocardiogram extraction and analysis, *Inst. Phys. Eng. Med.* 37 (5) (2016) 1–35, <https://doi.org/10.1088/0967-3334/37/5/R1>.
- [156] J. Behar, F. Andreotti, S. Zaunseder, J. Oster, G. Clifford, An ECG simulator for generating maternal-fetal activity mixtures on abdominal ECG recordings, *Physiol. Meas.* 35 (2014) 1537–1550, <https://doi.org/10.1088/0967-3334/35/8/1537>.
- [157] E. Stulas, M. Urru, R. Tumbarello, L. Raffo, R. Sameni, D. Pani, A non-invasive multimodal fetal ECG-doppler dataset for antenatal cardiology research, *Sci. Data* 8 (2021) 1–30, <https://doi.org/10.1038/s41597-021-00811-3>.
- [158] Y. Zhang, Z. Xiao, Y. Xing, C. Yang, J. Li, C. Liu, A. Gu, Wearable fetal ECG monitoring system from abdominal electrocardiography recording, *Biosensors (Basel)* 12 (2022) 475–491, <https://doi.org/10.3390/bios12070475>.
- [159] H. Ghonchi, V. Abolghasemi, A dual attention-based autoencoder model for fetal ECG extraction from abdominal signals, *IEEE Sens. J.* 22 (23) (2022) 22908–22918, <https://doi.org/10.1109/JSEN.2022.3213586>.
- [160] E. Dhas S, D. S, M. Extraction of fetal ECG from abdominal and thorax ECG using a non-causal adaptive filter architecture, *IEEE Trans. Biomed. Circuits Syst.* 16 (2022) 981–990, <https://doi.org/10.1109/TBCAS.2022.3204993>.
- [161] M. Anisha, S.S. Kumar, E.E. Nithila, M. Benisha, Detection of fetal cardiac anomaly from composite abdominal electrocardiogram, *Biomed. Signal Process. Control* 65 (2021) 1–12, <https://doi.org/10.1016/j.bspc.2020.102308>.
- [162] K. Barnova, R. Jaros, R. Kahankova, A. Matonia, M. Jezewski, R. Czabanski, K. Horoba, J. Jezewski, R. Martinek, A novel algorithm based on ensemble empirical mode decomposition for non-invasive fetal ECG extraction, *PLoS One* 16 (2021) 1–49, <https://doi.org/10.1371/journal.pone.0256154>.
- [163] D. Gurve, S. Krishnan, Separation of fetal-ECG from single channel abdominal ECG using activation scaled non-negative matrix factorization, *IEEE J. Biomed. Health Inform.* 24 (2020) 1–12, <https://doi.org/10.1109/JBHI.2019.2920356>.
- [164] L. Yuan, Y. Yuan, Z. Zhou, Y. Bai, S. Wu, A fetal ECG monitoring system based on the android smartphone, *Sensors* 19 (2019) 446–460, <https://doi.org/10.3390/s19030446>.
- [165] C. Yang, C. Antoine, B. Young, N. Tavassolian, A pilot study on fetal heart rate extraction from wearable abdominal inertial sensors, *IEEE Sens. J.* 19 (2019) 1–9, <https://doi.org/10.1109/JSEN.2019.2930886>.
- [166] S. Sengan, A. Mehboodiya, S. Bhatia, S.S. Saranya, M. Alharbi, S. Basheer, V. Subramanyawamy, Echocardiographic image segmentation for diagnosing fetal cardiac rhabdomyoma during pregnancy using deep learning, *IEEE Access* 10 (2022) 114077–114091, <https://doi.org/10.1109/ACCESS.2022.3215973>.
- [167] O. Ronneberger, P. Fischer, T. Brox, U-Net: Convolutional networks for biomedical image segmentation, *LNCs* 9351 (10) (2015) 234–241, https://doi.org/10.1007/978-3-319-24574-4_28.
- [168] O. Cicek, A. Abdulkadir, S. Lienkamp, T. Brox, O. Ronneberger, 3D U-Net: Learning Dense Volumetric Segmentation from Sparse Annotation, *International Conference on Medical Image Computing and Computer-Assisted Intervention*, 50, 2016, doi: https://doi.org/10.1007/978-3-319-46723-8_49.
- [169] F. Milletari, N. Navab, S.A. Ahmadi, V-Net: Fully convolutional neural networks for volumetric medical image segmentation, *Fourth International Conference on 3D Vision (3DV)* (2016) 565–571, <https://doi.org/10.1109/3DV.2016.79>.
- [170] V. Badrinarayanan, A. Kendall, R. Cipolla, SegNet: a deep convolutional encoder-decoder architecture for image segmentation, *IEEE Trans. Pattern Anal. Mach. Intell.* 39 (12) (2017) 2481–2495, <https://doi.org/10.1109/TPAMI.2016.2644615>.

- [171] C.-Y. Lin, Y.-W. Wang, F. Setiawan, N.T.H. Trang, C.-W. Lin, Sleep apnea classification algorithm development using a machine-learning framework and bag-of-features derived from electrocardiogram spectrograms, *J. Clin. Med.* 11 (1) (2022) 1–19, <https://doi.org/10.3390/jcm11010192>, <https://www.mdpi.com/2077-0383/11/1/192>
- [172] H. Qin, G. Liu, A dual-model deep learning method for sleep apnea detection based on representation learning and temporal dependence, *Neurocomputing* 473 (2022) 24–36, <https://doi.org/10.1016/j.neucom.2021.12.001>.
- [173] C.-Y. Yeh, H.-Y. Chang, J.-Y. Hu, C.-C. Lin, Contribution of different subbands of ECG in sleep apnea detection evaluated using filter bank decomposition and a convolutional neural network, *Sensors*, 22 (2022) 1–16, <https://doi.org/10.3390/s22020510>.
- [174] K. Feng, H. Qin, S. Wu, P. Weifeng, G.-Z. Liu, A sleep apnea detection method based on unsupervised feature learning and single-lead electrocardiogram, *IEEE Trans. Instrum. Meas.* 70 (2021) 1–13, <https://doi.org/10.1109/TIM.2020.3017246>.
- [175] A. Sheta, H. Turabieh, T. Thaher, J. Too, M. Mafarja, M. Hossain, S. Surani, K. Ho, Y.-H. Hu, Diagnosis of obstructive sleep apnea from ECG signals using machine learning and deep learning classifiers (2021) 1–20, <https://doi.org/10.3390/app11146622>.
- [176] A. Zarei, B.M. Asl, Automatic classification of apnea and normal subjects using new features extracted from HRV and ECG-derived respiration signals, *Biomed. Signal Process. Control* 59 (2020) 1–11, <https://doi.org/10.1016/j.bspc.2020.101927>.
- [177] F. Bozkurt, M. Uçar, M. Bozkurt, C. Bilgin, Detection of abnormal respiratory events with single channel ECG and hybrid machine learning model in patients with obstructive sleep apnea, *IRBM* 41 (5) (2020) 241–251, <https://doi.org/10.1016/j.irbm.2020.05.006>.
- [178] H. Singh, R.K. Tripathy, R.B. Pachori, Detection of sleep apnea from heart beat interval and ECG derived respiration signals using sliding mode singular spectrum analysis, *Digit. Signal Process.* 104 (2020) 102–796, <https://doi.org/10.1016/j.dsp.2020.102796>.
- [179] A. Zarei, B.M. Asl, Automatic detection of obstructive sleep apnea using wavelet transform and entropy-based features from single-lead ECG signal, *IEEE J. Biomed. Health Inform.* 23 (2019) 1011–1021, <https://doi.org/10.1109/JBHI.2018.2842919>.
- [180] F. Setiawan, C.-W. Lin, A deep learning framework for automatic sleep apnea classification based on empirical mode decomposition derived from single-lead electrocardiogram, *Life (Basel)* 12 (2022) 1–26, <https://doi.org/10.3390/life12101509>.
- [181] L. Orlando, E. De Giovanni, A. Valdés, S. Yazdani, J.-M. Vesin, D. Atienza, REWARD: design, optimization, and evaluation of a real-time relative-energy wearable R-peak detection algorithm, 2019 41st Annual International Conference of the IEEE Engineering in Medicine and Biology Society (EMBC), 2019, pp. 3341–3347, <https://doi.org/10.1109/EMBC.2019.8857226>.
- [182] H.R. Marston, R. Hadley, D. Banks, M.D.C. Miranda Duro, Mobile self-monitoring ECG devices to diagnose arrhythmia that coincide with palpitations: A scoping review, *Healthcare (Basel)* 7 (2019), <https://doi.org/10.3390/healthcare7030096>.
- [183] S. Saadatnejad, M. Oveis, M. Hashemi, LSTM-based ECG classification for continuous monitoring on personal wearable devices, *IEEE J. Biomed. Health Inform.* 24 (2) (2020) 515–523, <https://doi.org/10.1109/JBHI.2019.2911367>.
- [184] F. Miao, Y. Cheng, Y. He, Q. He, Y. Li, A wearable context-aware ECG monitoring system integrated with built-in kinematic sensors of the smartphone, *Sensors* 15 (2015) 11465–11484, <https://doi.org/10.3390/s150511465>.
- [185] P. Elangovan, M.K. Nath, En-convNet: a novel approach for glaucoma detection from color fundus images using ensemble of deep convolutional neural networks, *Int. J. Imaging Syst. Technol.* 32 (2022) 2034–2048, <https://doi.org/10.1002/ima.22761>.
- [186] M.K. Kar, M.K. Nath, M. Mishra, Retinal vessel segmentation and disc detection from color fundus images using inception module and residual connection, *Artificial Intelligence and Technologies*, Springer Singapore, 2022, pp. 603–616, <https://doi.org/10.1016/j.neucom.2018.05.011>.
- [187] P. Elangovan, M.K. Nath, Glaucoma assessment from color fundus images using convolutional neural network, *Int. J. Imaging Syst. Technol.* 31 (2022) 955–971, <https://doi.org/10.1002/ima.22494>.
- [188] G. Dai, W. He, L. Xu, E. Pazo, T. Lin, S. Liu, C. Zhang, Exploring the effect of hypertension on retinal microvasculature using deep learning on east asian population, *PLoS One* 15 (2020) 1–13, <https://doi.org/10.1371/journal.pone.0230111>.
- [189] R. Poplin, A. Varadarajan, K. Blumer, Y. Liu, M. McConnell, G. Corrado, L. Peng, D. Webster, Predicting cardiovascular risk factors from retinal fundus photographs using deep learning, *Nat. Biomed. Eng.* 2 (2018) 158–164, <https://doi.org/10.1038/s41551-018-0195-0>.
- [190] H.R.H. Al-Absi, M.T. Islam, M.A. Refaei, M.E.H. Chowdhury, T. Alam, Cardiovascular disease diagnosis from DXA scan and retinal images using deep learning, *Sensors* 22 (12) (2022) 1–12, <https://doi.org/10.3390/s22124310>.
- [191] M.D.T. Shyamalee, Glaucoma detection with retinal fundus images using segmentation and classification, *Mach. Intell. Res.* 19 (2022) 563–580, <https://doi.org/10.1007/s11633-022-1354-z>.
- [192] T.H. Rim, C.J. Lee, Y.-C. Tham, N. Cheung, M. Yu, Deep-learning-based cardiovascular risk stratification using coronary artery calcium scores predicted from retinal photographs, *Lancet Digit. Health* 3 (2021) 306–316, <https://doi.org/10.1016/j.diaph.2020.100043>.
- [193] E. Korot, N. Pontikos, X. Liu, S. Wagner, L. Faes, J. Huemer, K. Balaskas, A. Denniston, A. Khawaja, P. Keane, Predicting sex from retinal fundus photographs using automated deep learning, *Sci. Rep.* 11 (2021) 1–8, <https://doi.org/10.1038/s41598-021-89743-x>.
- [194] L.-P. Cen, J. Ji, J.-W. Lin, S. Ju, H.-J. Lin, T.-P. Li, Y. Wang, J.-F. Yang, Y.-F. Liu, S. Tan, L. Tan, D. Li, Y. Wang, D. Zheng, Y. Xiong, H. Wu, J. Jiang, Z. Wu, D. Huang, M. Zhang, Automatic detection of 39 fundus diseases and conditions in retinal photographs using deep neural networks, *Nat. Commun.* 12 (2021) 1–13, <https://doi.org/10.1038/s41467-021-25138-w>.
- [195] W. Hsia, S. Tse, C. Chang, Y. Huang, Automatic segmentation of choroid layer using deep learning on spectral domain optical coherence tomography, *Appl. Sci.* 11 (2021) 54–88, <https://doi.org/10.3390/app11125488>.
- [196] J. Morano, A.S. Hervella, J. Novo, J. Rouco, Simultaneous segmentation and classification of the retinal arteries and veins from color fundus images, *Artif. Intell. Med.* 118 (2021) 102–116, <https://doi.org/10.1016/j.artmed.2021.102116>.
- [197] J. Son, J. Shin, E. Chun, K.-H. Jung, K. Park, S.J. Park, Predicting high coronary artery calcium score from retinal fundus images with deep learning algorithms, *Transl. Vis. Sci. Technol.* 9 (2020) 28–35, <https://doi.org/10.1167/tvst.9.2.28>.
- [198] L. Zhang, Z. An, X. Zhao, H. Wu, H. Li, Y. Wang, B. Sun, H. Li, S. Ding, X. Zeng, L. Chao, P. Li, W. Wu, M. Yuan, Prediction of hypertension, hyperglycemia and dyslipidemia from retinal fundus photographs via deep learning: Across-sectional study of chronic diseases in Central China, *PLoS One* 12 (2020) 1–11, <https://doi.org/10.1371/journal.pone.0233166>.
- [199] T. Rim, G. Lee, Y. Kim, Y.-C. Tham, C. Lee, S. Baik, Y. Kim, M. Yu, M. Deshmukh, B. Lee, S. Park, C. Sabanayagam, D. Ting, Y.X. Wang, J. Jonas, S.S. Kim, T. Y. Wong, C.-y. Cheng, Prediction of systemic biomarkers from retinal photographs: Development and validation of deep-learning algorithms, *Lancet Digit. Health* 2 (2020) 526–536, [https://doi.org/10.1016/S2589-7500\(20\)30216-8](https://doi.org/10.1016/S2589-7500(20)30216-8).
- [200] A. Cordero, E. Alegria, Sex differences and cardiovascular risk, *Heart (British Cardiac Society)* 92 (2006) 145–153, <https://doi.org/10.1167/hrt.2005.069187>.
- [201] M. Tanaka, H. Fujiwara, T. Onodera, D.J. Wu, M. Matsuda, Y. Hamashima, C. Kawai, Quantitative analysis of narrowings of intramyocardial small arteries in normal hearts, hypertensive hearts, and hearts with hypertrophic cardiomyopathy, *Circulation* 75 (1987) 1130–1139, <https://doi.org/10.1161/01.cir.75.6.1130>.
- [202] M.O. Tso, L.M. Jampol, Pathophysiology of hypertensive retinopathy, 1982, pp. 32–45, [https://doi.org/10.1016/s0161-6420\(82\)34663-1](https://doi.org/10.1016/s0161-6420(82)34663-1).
- [203] E. Tedeschi-Reiner, M. Strozzì, B. Skoric, Z. Reiner, Relation of atherosclerotic changes in retinal arteries to the extent of coronary artery disease, *Am. J. Cardiol.* 96 (2005) 1107–1116, <https://doi.org/10.1016/j.amjcard.2005.05.070>.
- [204] T.Y. Wong, Retinal arteriolar narrowing and risk of coronary heart disease in men and women, *Atheroscler. Risk Commun. Study* 287 (2002) 1153–1162, <https://doi.org/10.1001/jama.287.9.1153>.
- [205] K. McGeehan, Meta-analysis: retinal vessel caliber and risk for coronary heart disease, *Ann. Intern. Med.* 151 (2009) 404–414, <https://doi.org/10.7326/0003-4819-151-6-200909150-00005>.
- [206] P. Mitchell, J.J. Wang, T.Y. Wong, W. Smith, R. Klein, S.R. Leeder, Retinal microvascular signs and risk of stroke and stroke mortality 65(7) (2005) 1005–1009, <https://doi.org/10.1212/01.wnl.0000179177.15900.ca>.
- [207] H. Yatsuya, A. Folsom, T.-Y. Wong, R. Klein, B. Klein, A. Sharrett, Retinal microvascular abnormalities and risk of lacunar stroke atherosclerosis risk in communities study, *Stroke* 41 (2010) 1349–1355, <https://doi.org/10.1161/STROKEAHA.110.580837>.
- [208] M. Ikram, F.J. Jong, M. Bos, J. Vingerling, A. Hofman, P. Koudstaal, P. Jong, M. Breteler, Retinal vessel diameters and risk of stroke - the rotterdam study, *Neurology* 66 (2006) 1339–1343, <https://doi.org/10.1212/01.wnl.0000210533.24338.ea>.
- [209] D. Ting, C.M.G. Cheung, T. Wong, Diabetic retinopathy: global prevalence, major risk factors, screening practices and public health challenges: a review, *Clin. Exp. Ophthalmol.* 44 (2015) 124–132, <https://doi.org/10.1111/ceo.12696>.
- [210] W. Wong, X. Su, X. Li, C.M.G. Cheung, R. Klein, C.-y. Cheng, T.-Y. Wong, Global prevalence of age-related macular degeneration and disease burden projection for 2020 and 2040: A systematic review and meta-analysis, *Lancet Glob. Health* 2 (2014) 106–116, [https://doi.org/10.1016/S2214-109X\(13\)70145-1](https://doi.org/10.1016/S2214-109X(13)70145-1).
- [211] P. Song, Y. Xu, M. Zha, Y. Zhang, I. Rudan, Global epidemiology of retinal vein occlusion: a systematic review and meta-analysis of prevalence, incidence, and risk factors, *J. Glob. Health* 9 (2019) 1–9, <https://doi.org/10.7189/jogh.09.010427>.
- [212] D. Ardila, A. Kiraly, S. Bharadwaj, B. Choi, J. Reicher, L. Peng, D. Tse, M. Etemadi, W. Ye, G. Corrado, D. Naidich, S. Shetty, End-to-end lung cancer screening with three-dimensional deep learning on low-dose chest computed tomography, *Nat. Med.* 25 (2019) 954–961, <https://doi.org/10.1038/s41591-019-0447-x>.
- [213] M. Baskaran, R. Foo, C.-y. Cheng, A. Narayanasamy, Y.-F. Zheng, R. Wu, S.-M. Saw, P. Foster, T.-Y. Wong, T. Aung, The prevalence and types of glaucoma in an urban Chinese population: the Singapore Chinese eye study, *JAMA Ophthalmol.* 133 (2015) 1–13, <https://doi.org/10.1001/jamaophthalmol.2015.1110>.
- [214] M.T. Andreoli, F.Y. Chau, M.J. Shapiro, Y.I. Leiderman, Epidemiological trends in 1452 cases of retinoblastoma from the surveillance, epidemiology, and end results (SEER) registry, *Can. J. Ophthalmol.* 52 (6) (2017) 592–598, <https://doi.org/10.1016/j.jcjo.2017.05.012>.
- [215] S.B. Wang, P. Mitchell, G. Liew, T.Y. Wong, K. Phan, A. Thiagalingam, N. Joachim, G. Burlutsky, B. Gopinath, A spectrum of retinal vasculature

- measures and coronary artery disease, *Atherosclerosis* 268 (2018) 215–224, <https://doi.org/10.1016/j.atherosclerosis.2017.10.008>.
- [216] S. Seidelmann, B. Claggett, P. Bravo, A. Gupta, H. Farhad, B. Klein, R. Klein, M. Di Carli, S. Solomon, Retinal vessel calibers in predicting long-term cardiovascular outcomes: The atherosclerosis risk in communities study, *Circulation* 134 (2016) 1–32, <https://doi.org/10.1161/CIRCULATIONAHA.116.023425>.
- [217] K. McGeelchan, G. Liew, P. Macaskill, L. Irwig, R. Klein, A.R. Sharrett, B.E. Klein, J.J. Wang, L.E. Chambliss, T.Y. Wong, Risk prediction of coronary heart disease based on retinal vascular caliber (from the atherosclerosis risk in communities [ARIC] study), *Am. J. Cardiol.* 102 (1) (2008) 58–63, <https://doi.org/10.1016/j.amjcard.2008.02.094>.
- [218] S. Dilmac, M. Korurek, ECG heart beat classification method based on modified ABC algorithm, *Appl. Soft Comput.* 36 (2015) 641–655, <https://doi.org/10.1016/j.asoc.2015.07.010>.
- [219] S. Shadmand, B. Mashoufi, A new personalized ECG signal classification algorithm using block-based neural network and particle swarm optimization, *Biomed. Signal Process. Control* 25 (2016) 12–23, <https://doi.org/10.1016/j.bspc.2015.10.008>.
- [220] J. Mateo, A.M. Torres, A. Aparicio, J.L. Santos, An efficient method for ECG beat classification and correction of ectopic beats, *Comput. Electr. Eng.* 53 (2016) 219–229, <https://doi.org/10.1016/j.compeleceng.2015.12.015>.



Thivya Anbalagan completed B. Tech in Electronics and Communication Engineering from Sri Manakula Vinayagar Engineering College Puducherry, India, and M.Tech. in VLSI & Embedded Systems from Sri Manakula Vinayagar Engineering College Puducherry, India, in 2020. She is pursuing her Ph.D. in the Department of ECE, National Institute of Technology Puducherry, Karaikal, India. Her area of research is medical signal processing.



Malaya Kumar Nath completed B. E. in Electronics and Telecommunication Engineering from BPUT Odisha, India, and M. Tech in Electronics and Communication Engineering (Signal Processing) from Indian Institute of Technology Guwahati, India. He completed his Ph.D. from the Indian Institute of Technology Guwahati on Signal Processing. He joined National Institute of Technology Puducherry, Karaikal in July 2013, where he currently holds Assistant Professor position in the Department of Electronics and Communication Engineering. His area of research is machine learning and image processing.



Vijayalakshmi Dhurairajan completed B. E. in Electronics and Communication Engineering from Madurai Kamaraj University India, and M.E. in Communication Systems from Anna University Chennai, India, in 2008. She completed her Ph.D. in the Department of ECE, National Institute of Technology Puducherry, Karaikal, India, in 2022. She is working as an Assistant Professor in the Department of ECE, Vignan..s Institute of Engineering for Women, Visakhapatnam, India. Her area of research is image enhancement and image processing.



Archana Anbalagan completed her Bachelor of Medicine and Bachelor of Surgery (MBBS) from Sri Lakshmi Narayana Institute of Medical Sciences Puducherry, India.